



Volume 3
Impacts of Connected and Autonomous
Vehicles on Freight, Energy Use and
Emissions

2021 Report

Department of
**Civil,
Construction, &
Environmental
ENGINEERING**



Impacts of Connected and Autonomous Vehicles on Freight, Energy Use and Emissions

Faculty:

Chris Frey and George List

North Carolina State University

Research Assistants:

Soumya Sharma, Shioab Samandar, and Weichang Yuan

North Carolina State University



Table of Contents

Chapter 1: Impacts of Connected and Autonomous Trucks on Urban Network Performance	4
<i>Introduction</i>	5
<i>Literature Review</i>	8
<i>Level 4 Analysis</i>	14
<i>Level 5 Analysis</i>	32
<i>Summary and Conclusion</i>	36
<i>References</i>	40
Chapter 2: Impacts of Connected and Autonomous Trucks on Freeway Operations	42
<i>Introduction</i>	43
<i>Literature Review</i>	45
<i>Methodology</i>	48
<i>Results and Discussion</i>	54
<i>Conclusions</i>	57
<i>References</i>	58

Table of Contents

Chapter 3: Fuel Use and Emission Rates Reduction Potential for Light-Duty Gasoline Vehicle Eco-Driving	61
<i>Introduction</i>	62
<i>Materials and Methods</i>	64
<i>Results and Discussion</i>	70
<i>Conclusions</i>	80
<i>Recommendations for Future Work</i>	82
<i>References</i>	83



Chapter 1

Impacts of Connected and Autonomous Trucks on Urban Network Performance

George List, Professor
North Carolina State University

Soumya Sharma, Graduate Research Assistant
North Carolina State University

Leta Huntsinger, Director of Research,
Systems Planning, and Analysis
Institute of Transportation Research and Education (ITRE)
North Carolina State University

Shoaib Samandar, Research Associate
North Carolina State University





1.1 Introduction

In the coming decades, autonomous vehicles (AVs) are likely to grow in visibility on our highway networks. Although drastic changes are not expected, the fleet will begin to shift from being exclusively human-driven to a mix of traditional vehicles and AVs. Moreover, while our current fascination is with AVs for personal trips, commercial vehicles may be the actual early adaptors. Cost savings, productivity gains, and increased flexibility will pressure carriers to push forward with experimentation and deployment.

The introduction of connected-autonomous vehicles (CAVs), AVs, and connected vehicles (CVs) mixed with human-driven/ traditional vehicles (TVs) is expected to bring some mobility benefits for both freeway and arterial facilities. Nonetheless, the different operating characteristics of these vehicles have rendered these impacts highly variable. Furthermore, most mobility studies are simulation-based since field observations of CAVs, AVs, or CVs mixed with TVs are very limited. Thus, the modeling assumptions play a significant role in reporting the impacts.

This report discusses the impact of CAVs, AVs, CVs, and TVs on freeway network operation. Also, since the study focuses on the freight-related impacts of these technologies, the following nomenclature is followed in the rest of the text:

1. The term AVs is used to denote connected-autonomous trucks (i.e. all autos in the study are considered human-driven)
2. The term TVs is used to denote human-driven/ traditional trucks

This nomenclature is not at odds with typical terms in use today, but it is slightly different from what might be seen in other documents. So, the reader needs to keep these “definitions” in mind when reading the report.

It does not seem likely that truck AVs will simply be variants of existing trucks, as would be the case for hybrid or all-electric models. Instead, they may operate differently and have new infrastructure requirements. In many cases the driver cab is gone. The “tractor” looks more like a sports car than a truck. They may not have a driver on-board; they may be more conservative in their use of highway space; and

they may need special facilities so they can transition between manned and unmanned operation.

Because of these differences, drivers of traditional autos, trucks, etc. may be uncomfortable having AVs interspersed in the traffic stream. A push toward dedicated lanes may emerge. But even if this happens, the AVs will have to weave across traffic to enter and leave those lanes. That might present policy and operational challenges. Industry players, like Waymo, have acknowledged that abnormal situations like construction zones and adverse weather may be challenging. AVs may also find it necessary to cross double yellow lines to enter driveways or multiple lanes to complete turns. Waymo says it is tackling these issues by designing trucks with more sensors and reduced occlusions (1).

We study autonomy levels 4 and 5 as specified by the Society of Automotive Engineers (SAE) (2). level 4 allows autonomous driving "under certain conditions" while in level 5 AVs can go anywhere. For level 4, we assume the AVs can operate autonomously on controlled access facilities like freeways; they will be more amenable to AV operation than "lower class" facilities. For level 5, we assume they can use any link although we encourage them, through preferential weights, to use "higher-type" facilities where possible. We do not distinguish between AVs with and without communication/connection capabilities. We assume all of the AVs are connected as well as autonomous.

In level 4, we use the notion of a Mode Change Lot (MCL) to allow the trucks to transition between traditional truck (TV) and autonomous truck (AV) modes. These MCLs

are much like the "Transfer Hubs" suggested by Waymo and Uber as part of their "vision" for the future of AV trucks (1, 3). With these MCLs, the level 4 AV trips become blends of automated and manual driving segments. A trip might begin in TV mode, transition to AV mode, and then transition back to TV mode. For example, a truck making a local pickup and delivery trip might pick up the load and travel in TV mode to an MCL; transition to AV mode while on the freeway; and then transition back to TV mode at a second MCL so it can deliver the shipment to the receiver. We call these TAV trips because they involve operation both manually and autonomously.

Our focus is on peak period operation where capacity is scarce and congestion, common. Extension of our findings to other time periods seems reasonable. The three main questions we address are: 1) to what extent can AVs reduce the peak period levels of congestion, 2) what operational changes will be needed, and 3) what if any special facilities might be needed to accommodate these flows.

Our case study setting is the metropolitan area of Raleigh, NC. Moreover, we use the Triangle Regional Model (TRM), the planning model employed by the Capital Area Metropolitan Planning Organization (CAMPO), as the analysis tool. We do two separate analyses for autonomy levels 4 and 5. In the case of level 4, we assume a probability that traditional truck (TV) trips will be converted to blended conventional-automated trips (TAVs); and for level 5 we assume a likelihood that all TV trips will become AV trips. Moreover, in the case of level 4, we impose a circuitry restriction: that is, an eligible TV-to-AV conversion will only become a TAV trip if the extra distance traveled

An aerial photograph of a city street intersection, overlaid with a semi-transparent green filter. The image shows multiple lanes of traffic, crosswalks with white stripes, and a few vehicles. A large building is visible in the upper right quadrant. The overall scene is a typical urban street layout.

by the TAV trip is at or below a maximum “extra distance” threshold.

We use 2045 as the analysis year for the study because the TRM is presently validated for that horizon year. CAMPO is using 2045 for demand forecasting purposes. We are not suggesting that 2045 is a year in which AVs will become common, under either level 4 or 5 operations. Hence our analysis should be seen more as a with-without analysis than a forecast of conditions that might arise.

This report is organized as follows. A review of the technical literature focused on travel demand modeling of autonomous and connected vehicles in urban areas followed by a description of the Triangle Regional Model (TRM) that was used to conduct the analyses. Next is a description of the SAE level 4 analysis we conducted followed by a discussion about the level 5 analysis. Finally, we present conclusions and recommendations.



1.2 Literature Review

The existing literature on AVs is sparse, at least insofar as planning-level network impact studies are concerned. This is true even though the incorporation of trucks into the planning process has a long history. The studies that do exist have examined the likelihood of “modal” diversions from TVs to AVs.

Initially, and to some degree, even today, planning models used expansion factors to convert auto-only flows into mixed mode flows, including trucks. For a mixed flow rate of f , if the truck percentage p , and the passenger car equivalency (PCE) for the trucks was two autos, then the adjusted all-auto flow rate, f_a , was $f_a = f \cdot [(1-p) + 2 \cdot p]$ to be consistent with the BPR formula and the Highway Capacity Manual. It appears that the interest in explicitly accounting for truck flows began emerging in the 1980's as illustrated by Zattero and Weseman and Southworth (4, 5). Zattero and Weseman in 1981 developed a commercial vehicle trip generation model for the Chicago region using regression analysis. Truck travel data, land use and employment data were used to derive relations between the truck trips

generated to subareas of the Chicago region are estimated based on the land use characteristics of the area. Trucks are typically categorized into three sizes viz. (a) light for pickup and panel trucks, (b) medium for other single-unit vehicles, and (c) heavy for tractor-trailer units. Land use types were categorized as: residential, manufacturing, commercial, public building, public open space, transportation-communications-utilities (TCU), and other developed land. Land area and employment were used as measures of activity. Truck trips to each subarea were classified by vehicle size and land use of the subarea.

In response to the Intermodal Surface Transportation Efficiency Act of 1991 (ISTEA), urban areas and states developed and improved their freight modeling efforts (6). Progress continued into the next decade as more sophisticated methods were developed. The Quick Response Model and its freight enhancements encouraged these developments because of its ease of use; see Cohen et al. (7). Ruitter developed an urban truck travel model for the Phoenix metropolitan area in 1992

for which data was collected by conducting a truck travel survey of commercial vehicles operating in the area. The model was designed to be incorporated into the Maricopa Association of Governments Transportation and Planning Office's (MAGTPO's) travel model. A standard gravity model structure was used for the commercial vehicle trips distribution similar to the Phoenix person trip model (8). Fischer worked with the Monterey Bay region metropolitan planning organization (MPO) in 1996, to provide solutions to their agricultural freight transportation problems. The study inventoried existing freight facilities and movements in order to project future demand for freight transportation. The study worked with limited data and proposed three projects: a regional freight logistics center, a transportation service center, and a rail-truck intermodal terminal as solutions to the regions freight transportation issues (9). List et al. describe the first instance of a freight transportation model being used for the New York City metropolitan region. Truck flows were explicitly considered in the "Best Practice Model" used by the New York Metropolitan Transportation Council (NYMTC). Flow estimation was based on List and Turnquist (10, 11). Prem and Yu conducted a study in 1996 for the Quad County Regional Transportation Organization in Washington State. This is a large agro-based non-urban area and hence the model's main focus was on agricultural truck trips (but vehicle trips were also modeled). External survey data and data from a similar rural highway projects in the Washington-Oregon and some other states was used to inform the trip making between communities in the area. The authors suggested that such areas have unique data requirements

for freight transportation modeling, owing to their farm-to-market and roadway condition issues as opposed to the usual capacity-related issues in urban regions (12). Marker and Goulias used the Quick Response Freight Manual (QRFM) to model truck flows in the Centre County, Pennsylvania. The three-step process of trip generation, trip distribution, and trip assignment were employed as suggested in the QRFM. Trip generation was performed by four business employment types and the households were aggregated to traffic analysis zones (TAZs). Three truck types (consistent with the QRFM) were identified: 1) four-tire trucks, 2) one-unit trucks with six or more tires, and 3) combination trucks. Trip generation rates were determined for each truck type separately. Trip distribution was done using a doubly constrained gravity model along with travel-time based friction factors. Traffic assignment utilized the user equilibrium method. The model was calibrated by comparing total vehicle miles traveled as obtained from the model results against the observed data. The study tested the model by altering the TAZ sizes, one model used census tracts as TAZs while the other used census blocks as TAZs for the same network. No major loss of accuracy was found when comparing results from the two models even though the QRFM methods were originally designed for regional truck modeling using TAZs of tracts or larger (13). Slavin reviewed models for intra-urban trips and provided an improved framework to model truck trips in an urban environment. He also discussed how to use data more efficiently when estimating truck trips and using new data sources and tools for better modeling practices (14). Faris and Ismart developed a low-cost modeling

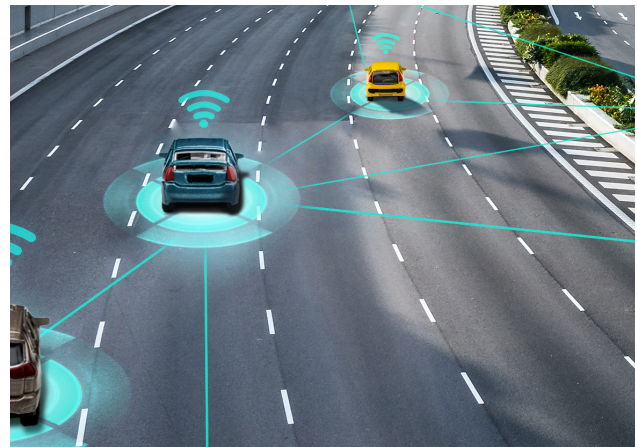
technique to model freight traffic for small to medium sized urban areas where limited local data is available. The purpose of their study was to provide freight modeling techniques that can be integrated easily with existing transportation demand models (like a traditional four-step model). Default QRFM trip generation rates and trucks classifications were used to evaluate truck trips and authors suggested conducting regional surveys in the future to replace the default values with local updated parameters (15).

The advent of AVs has brought a new facet to these efforts. Although the focus is heavily on auto-like AVs, researchers are endeavoring to ascertain how these vehicles will be utilized, to what extent, and how they might be accommodated. A good example is Hasnat et al. who focused on the impacts of auto-like AVs in the context of urban traffic patterns (16).

For AVs, "mode choice" has been the topic more heavily considered. Huang and Kockelman examine shipper's choice between autonomous trucks and conventional or human-driven trucks using a random-utility-based multi-regional input-output model, driven by foreign export demands (17). They simulated the impacts to freight traffic among 3109 U.S. counties and 117 export zones, via a nested-logit model for shipment or input origin and mode. They found that the adoption of autonomous trucks works in favor of longer truck trips, but rail's competitive prices hamper autonomous truck trips for trade distances over 3000 miles. Human driven trucks are found to dominate in shorter-distance freight movements, while Autonomous trucks dominate at distances of over 500 miles. Cantarella and Febraro review

the existing the existing methods for predicting truck trips and conclude that modeling user mode choice behavior with autonomous vehicles might require a hierarchically structured model (18).

The literature on network impacts of AVs is sparser. Smith examines the impacts of AVs on freight corridor planning (19). Nasri, Bektas, and Laporte explore the issues of route and speed optimization for AVs from a logistics network perspective (20). However, neither of



these studies examine the impact of AVs on urban network operation and performance.

The Triangle Regional Model

The Triangle Regional Model (TRM) is the planning tool used by the Capital Area Metropolitan Planning Organization (CAMPO) to examine network performance in future years for proposed capital investment plans and new operating strategies.

Geographically, the TRM captures the combined statistical area (CSA) of Raleigh-Durham-Chapel Hill. Dubbed the "Triangle Region", this CSA has a population of slightly more than two million people and covers 3380

square miles. It includes all of Orange, Wake and Durham counties, and parts of Chatham, Person, Granville, Franklin, Nash, Johnston, and Harnett Counties. Within it, Raleigh, Durham and Chapel Hill are the major employment and population centers. The TRM has 2956 traffic analysis zones (TAZs). 2857 of them are internal (I) and the remaining 99 are external (E), associated with highway entry/exit points. Figure 1.1 shows the TAZs, superimposed on the county boundaries.

As is typically the case, the TRM has trip tables that are a combination of II, IE, EI, and EE trips. The "I" stands for "internal" and the "E" for external. Thus, an IE trip originates with the TRM region and exits the region to go to an external destination. The vehicle types are single occupant autos (SOVs), high-occupant vehicles (HOVs), light duty trucks (LCVs), single unit trucks (SUTs) and multiunit trucks (MUTs).

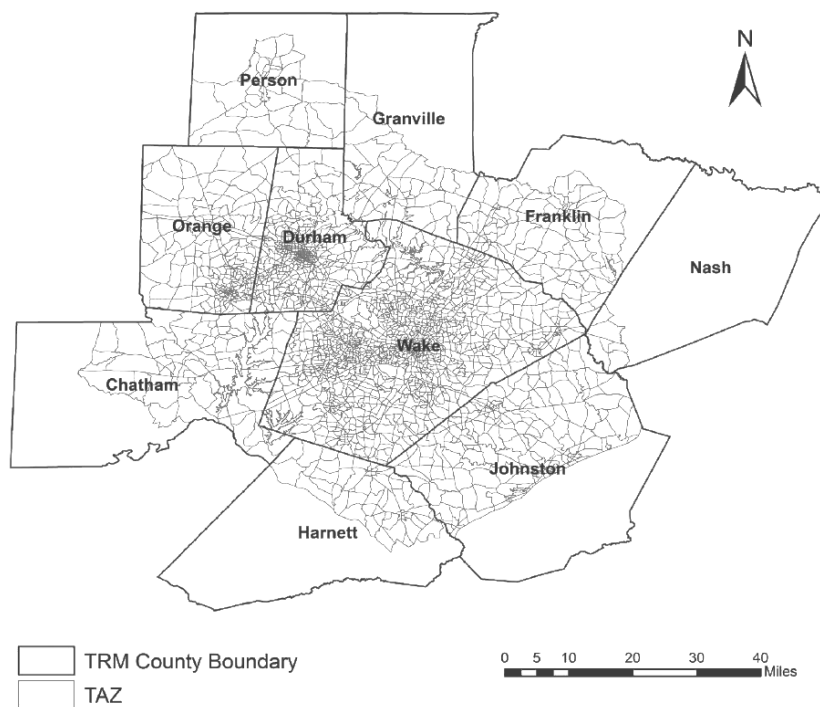


Fig. 1.1 The TRM, its geographic extent, and TAZs

The TRM uses four main time periods to model a typical weekday: AM peak (6:00-10:00 am), midday (10:00 am - 3:30 pm), PM peak (3:30-7:30 pm), and nighttime (7:30 pm to 6:00 am). Moreover, the AM and PM peaks are further subdivided into a peak hour and pre- and post-peak shoulders that are 1.5 hours long. For the AM peak, the pre-shoulder is 6:00-7:30 am; the peak hour is 7:30-8:30 am; and the post-shoulder is 8:30-10:00 am. For the PM peak, those same time intervals are 3:30-5:00 pm, 5:00-6:00 pm, and 6:00-7:30 pm respectively. This means the TRM has eight (8) time periods altogether: the AM peak (3 time periods), midday, the PM peak (3 time periods), and overnight.

The TRM is the currently in version 6 (TRMv6). This version is calibrated to regional socio-economic conditions for 2013. Future years, like 2045 that we are using, are derived from this base. TRMv6 is also the first version to have a separate submodel for commercial vehicle trip generation and distribution.

The TRM uses a traditional four-step process to assess network performance: trip generation, trip distribution, mode choice, and trip assignment. Figure 1.2 presents an overview of the TRM analysis procedure.

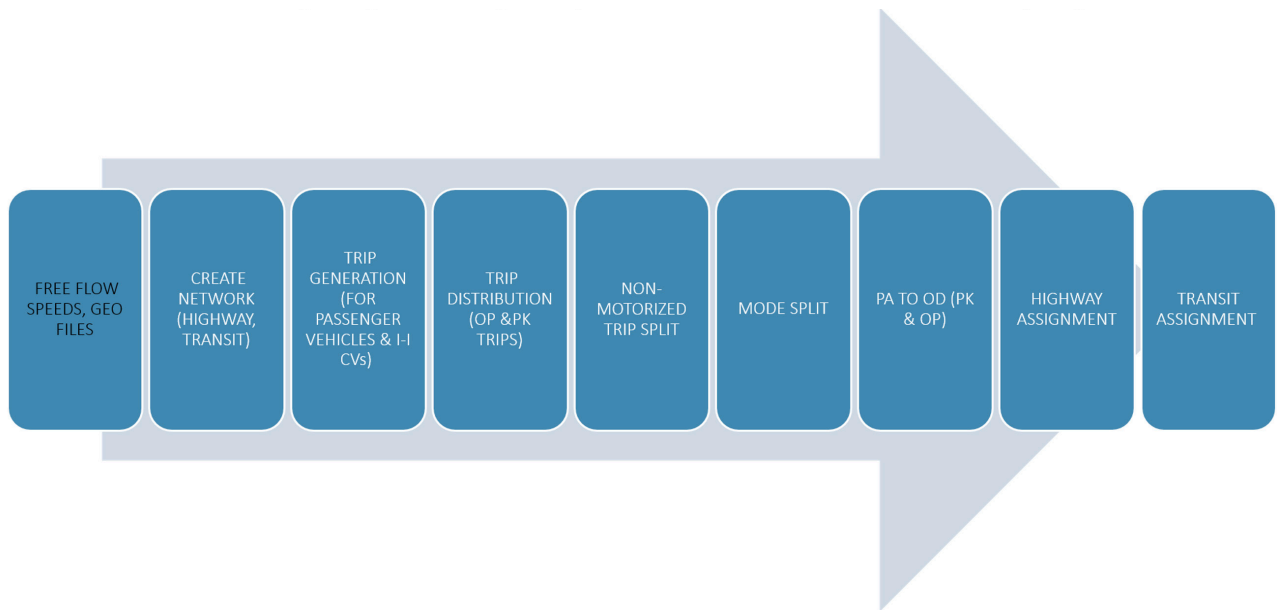


Fig. 1.2 Overview of the TRM process

Trip matrices are generated for five vehicle classes: single occupancy vehicles (SOVs), high-occupancy vehicles (HOVs), light commercial vehicles (LCVs), single unit trucks (SUTs), and multiple unit trucks (MUTs). However, only four of these are passed forward to traffic assignment. The LCVs are merged with auto trips to form SOVs and HOVs. The SUTs can be thought of as box trucks (two-axle, six tire), and the MUTs as tractor trailers (the typical 18-wheeler). Since these two truck types are explicitly considered in traffic assignment, the impacts of converting them to AV trips is the principle focus of our analyses.

A process called “PA to OD” (productions and attractions to origin-destination trip matrices) transforms the person trips into “vehicle trip matrices.” The person trips encompass a rich variety of trip types, “complicated” by the fact that the region has several large universities and community colleges, which means student, staff and faculty trips are treated as special cases. The “PA to OD” process is not described in detail here because it is not germane to the AV assessment. Briefly, trips are generated by purpose, time period, and zone and then the congested travel times from the AM peak equilibrium assignment are fed back to trip distribution as network impedances using “skims.” For the truck trips, generation and distribution are handled by a stand-alone procedure. There are two trip categories: “goods” and “service”; they both pertain to the LCV, SUT, and MUT vehicle types.

However, the “goods” trips pertain principally to the SUT and MUT truck types; and the “service” trips mainly pertain to the LCV and SUT truck types.

Again, for the truck trips, the EE, EI, and IE trips are imported from the North Carolina Statewide Travel Model (NCSTM). Only SUT and MUT trip tables exist in the statewide model. The NCSTM uses nationwide and more economy-sensitive Freight Analysis Framework (FAF) data to forecast freight-related truck trips throughout the state of North Carolina. The TRMv6 disaggregates the trips from the statewide model's zonal structure to that of the TRM. Again, see (21). TAZs in the statewide model that are inside the TRM's geographic boundary are matched to corresponding zones in the TRM. TAZs in the statewide model that are outside that boundary are mapped to entry/exit nodes on the TRM's periphery.

The II trip matrices are created separately. Daily LCV, SUT, and MUT trip matrices are created based on data obtained from a 2010 triangle region commercial vehicle travel survey. A cross-classification trip rate method is used. Inter-zonal travel impedances from the AM Peak equilibrium assignment are employed, as is the case for auto trips. The daily II trip matrices are then apportioned among the eight time periods using diurnal factors based on the 2010 survey results. These factors sum to unity (21).

Trip (traffic) assignment is done using a multiclass user equilibrium process. Solutions are obtained independently for each of the eight time periods. For each, capacities, by direction and link, are pre-multiplied by adjustment factors to account for the length of the time period and the extent to which peaking occurs. Truck trips are converted to “vehicle trips” using

“passenger car equivalent” values by truck type. The IE, EI, and EE truck trips, which exist only for SUTs and MUTs, are then pre-loaded based on an all-or-nothing assignment. After this is done, capacities are downward adjusted to account for these flows. A single-class equilibrium assignment follows. The results are presented in summary and detail for the PM peak.





1.3 Level 4 Analysis

As previously explained, we examined the impacts of the autonomous trucks for both SAE level 4 and level 5. Level 4 assumes the trucks can operate autonomously on portions of the highway network. Level 5 assumes they can operate anywhere.

A “big picture” of the analysis, for both level 4 and 5, can be seen in Figure 1.3. “Normally”, the TRMv6 proceeds with two parallel processes, one on the top for trucks (SUTs, MUTs, and LCVs) and another on the bottom for SOVs and HOVs. In normal use, the dotted line with the scissors indicates that the SOV and HOV trip tables are augmented by the LCV trip table, a portion goes to each, and then assigned as part of the trip tables for vehicles for those two vehicle types. In our case, we modified that “scissors” process so that changes were made to the SUT and MUT trip tables as well before highway assignment occurred.

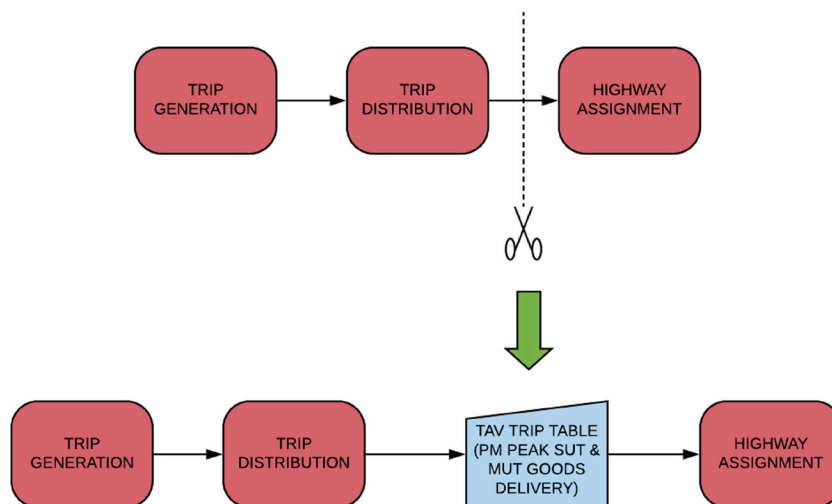


Fig. 1.3 Overview of the TRM process

In the level 4 analysis, the LCV trips were untouched (the LCV treatment is explained in detail later in the text). Changes were made only to the SUT and MUT trip tables. In the level 5 analysis, changes were made to the LCV trip matrices as well (again, more details given later in the text). Moreover, consistent with the SAE level 4 definition, we assumed that the trucks would only be able to operate autonomously on some portions of the highway network. We further assumed that these facilities would be the limited access freeways.

Trip Type Focus

In the level 4 analysis, we focused on the “goods” and “service” trips carried by the SUTs and MUTs. We did not include examination of the LCV trips in the level 4 analysis since LCV trips only comprise of “service” trips that might not be as amenable to AV conversion. This is because LCVs would traverse “lower level” facilities like arterials and the service person can be expected to provide a customized/expertise based service which might not be as easy to automate in the near future (examples are cleaning/ plumbing based services offered in LCVs).

AV Truck Routing

Since it was assumed that the AV trucks would operate autonomously only in some locations, we needed to decide 1) how the mode transitions would occur and 3) where they would happen.

For the first decision, we determined that safe “mode transitions” would need to occur. The truck should be standing still in a safe place. We invented the name “mode change lots” (MCLs) to designate these locations. Our notion of a

MCL may be the same as the “Transfer Hubs” described by Waymo and Uber; although we developed the idea independently. For our MCLs, a TV would enter the MCL, shift from TV to AV mode, let the driver disembark (if deemed appropriate), and then move on (the driver also might stay with the vehicle). At the end of the AV segment of the trip, the truck would enter a second MCL and undergo a similar mode change, in reverse. The AV would enter the MCL, stop, a driver would board (or resume control), and then continue.

For the second decision, we determined that a limited number of MCLs should be created. Ideally, they would be at every interchange; but with more than 40 interchanges in the TRM network, that seemed unreasonable. We examined numbers of MCLs ranging from one (1) to forty two (42) and determined that about 8-10 was reasonable. More will be said about this analysis shortly.

To revisit the blended TV/AV trips, some illustrations are useful. As was said, every “AV” trip was a combination of TV and AV segments. We called these TAV trips. To illustrate, an II trip that became a TAV trip had three segments: TV, AV, and TV. The first TV segment took the truck from the uncontrolled origin to a MCL. The AV segment took it from the MCL where it transitioned to AV operation to the one where it transitioned back to TV operation. This pattern pertained not only to II trips but also IE, EI, and EE trips where the “E” end of the trip was on an uncontrolled facility such as a rural arterial. In contrast, an EE trip that went to and from entry/exit nodes on controlled facilities would only have an AV segment. Finally, for an IE or EI trip where the E node was on a controlled facility, two segments existed: TV and AV in

the first case, AV and TV in the second. The same pertained to EE trips where one of the end nodes, but not both, were on a controlled facility.

This differentiation of the E nodes between “controlled” and “uncontrolled” facilities meant we had to create a new type of node on the periphery of the network. The E nodes had to be separated into those that were on controlled facilities (C) and those that were not (U). This differentiation meant that instead of four trip types (II, IE, EI, and EE), we had nine

(II, IU, IC, UI, UU, UC, CI, CU, and CC).

Figure 1.4 provides a graphical illustration of these ideas. Using a slightly more complex notation for the nodes in the trip, a trip from I_i to I_j would have three segments in its TAV trip: I_iM_1 , M_1M_2 and M_2I_j , using the subscripts “1” and “2” to differentiate between the first and second MCLs. An IU trip would become I_iM_1 , M_1M_2 , M_2U_j and an IC trip would become I_iM_1 and M_1C_j . CC trips would have only one segment: C_iC_j ; no intermediate MCLs would be involved.

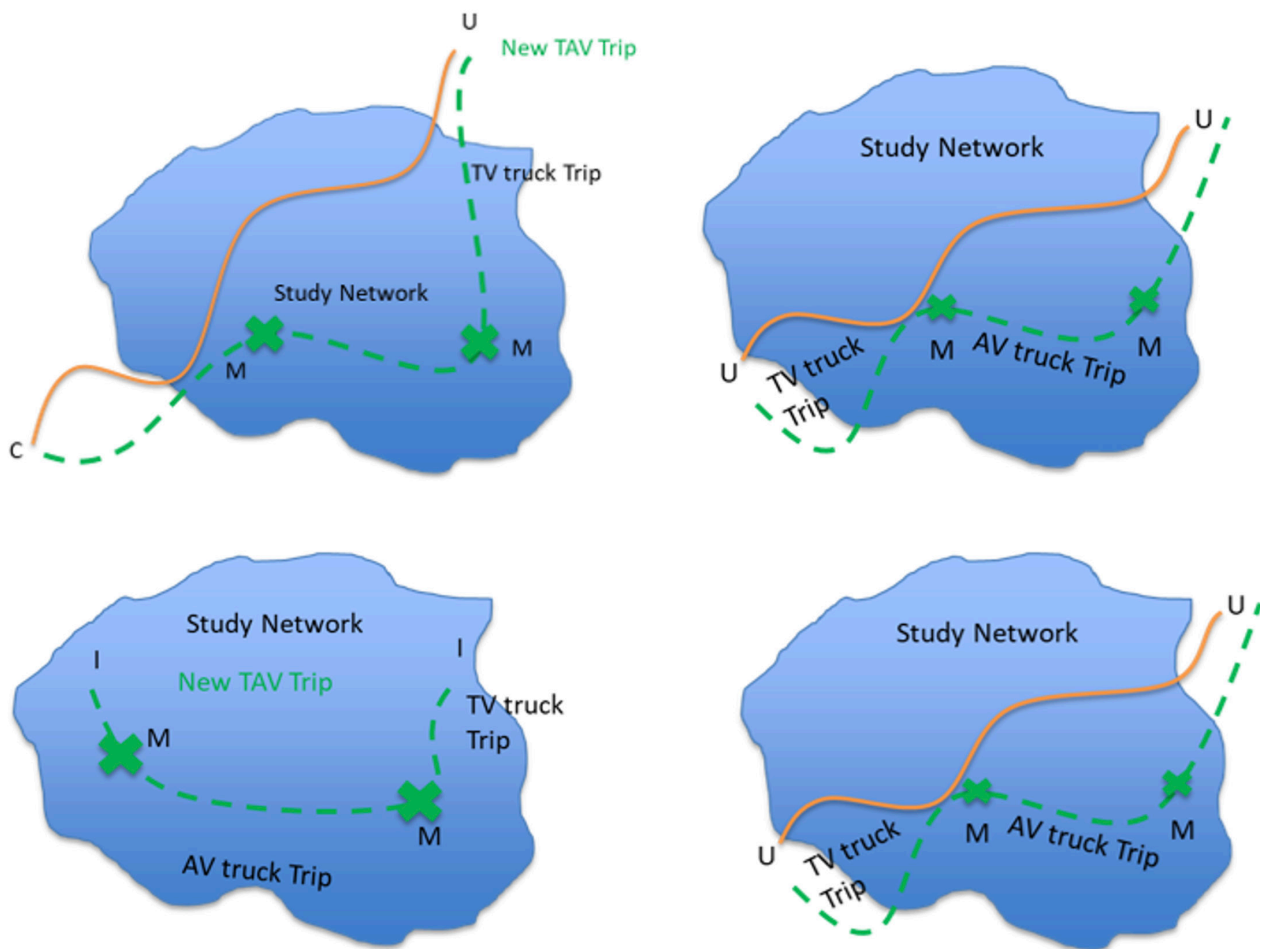


Fig. 1.4 Multi-segment trips involving mode change lots

Mode Change Lot Locations

Given these assumptions, our next task was to identify locations for the MCLs. If cost were no object, and land was available, there would be one MCL at every interchange. This would maximize the use of AV segments. Instead, we perceived that a few would be built, near places where high trip productions and attractions occurred.

A bi-objective p-Median / p-Center problem was formulated to identify the “best” locations for the MCLs. The best value for p was identified parametrically.

We started by identifying candidate locations. We computed the total truck trips originating and terminating in each of the internal TAZs. This originating-terminating (OT) value was obtained by adding the total originations (the row total in the trip matrix) to the total terminations (the column total) for both the SUT and MUT goods movement trips. The distribution of these OT values in the TRM region is shown in Figure 1.5. We then clustered TAZs with the greatest OT values and marked these clusters on the TRM network. Then, we identified interchanges near these clusters where creation of an MCL seemed feasible. This was done manually because it seemed that automating this selection would be complex, time consuming, and unlikely to yield a practical result. (Certainly, this process could in the future be automated.)

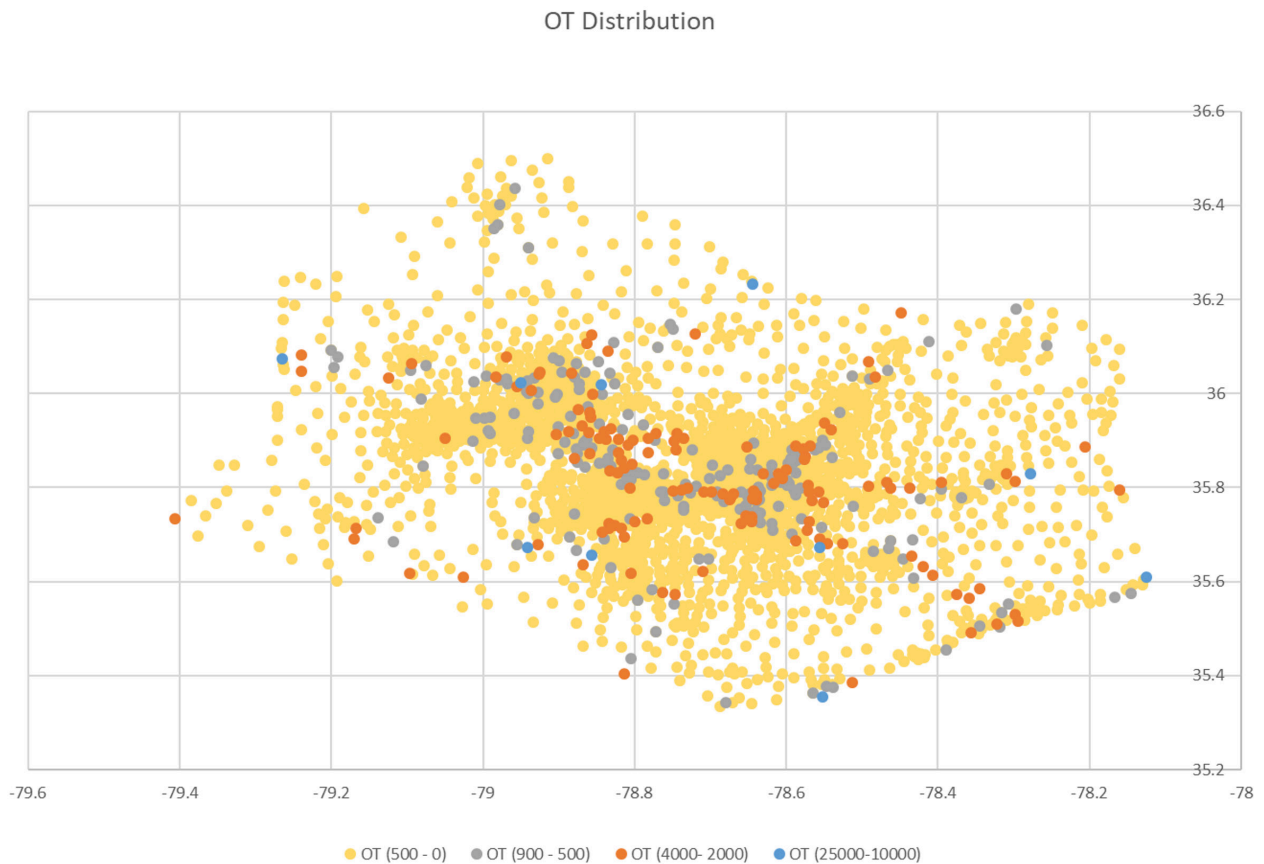


Fig. 1.5 Distribution of the Originating-Terminating (OT) Values in the TRM Region

Third, we identified TAZs within each cluster that could serve as surrogate MCLs. Originally, we wanted to add new “MCL” nodes to the TRM, but this proved to be an intractable idea because of the way the highway network was structured and the TRM processing code was written. Hence, technically, the AV trips are routed to and from these “off-freeway” TAZs. We perceived that this was a tolerable expedience. Where more than one TAZ might have been a logical one to select, we chose the one with the largest number of originating-terminating trips.

To identify the best sets of MCLs, we formulated a bi-objective p-Median / p-Center integer programming problem. It was as follows:

$$Z = w_a * d_{avg} + w_d * d_{max} \quad (1)$$

Subject to:

$$d_{avg} = \frac{1}{M} * \sum_i^N OT_i * D_i \quad (2)$$

$$d_{max} = \max_i D_i \quad (3)$$

$$\sum_{k=1}^K y_k \leq p \quad (4)$$

$$\sum_{k=1}^K x_{ik} = 1 \quad \forall i \quad (5)$$

$$D_i = \sum_{k=1}^K d_{ik} * x_{ik} \quad \forall k \quad (6)$$

$$\sum_{i=1}^N x_{ik} \leq N * y_k \quad \forall k \quad (7)$$

where $i = 1 \dots N$ are the internal TAZs, $j = 1 \dots J$ are the MCL options, d_{ij} is the distance from TAZ i to MCL j , OT_i is the total of the originating and terminating truck trips for TAZ i , D_i the distance to the MCL assigned to TAZ i and p is the number of MCLs allowed. In equation 2, M is the sum of the OT_i values:

$$M = \sum_{i=1}^N OT_i \quad (8)$$

Equation (2) computes the OT-weighted average distance from the TAZs to the MCLs. By using the OT values, more importance is placed on the TAZs with large OT values. Equation (3) computes the maximum distance from any TAZ to its assigned MCL. (It is common in solving location problems to base the choice on both the average and the maximum distance and consider non-dominated tradeoffs between the two.) Equation (4) ensures that only p MCLs are selected, where p is a user input. Equation (5) ensures that every TAZ is assigned to an MCL. Equation (6) computes the distance from each TAZ to its assigned MCL. (Only one term in the sum will be non-zero, the one for which the assignment variable x_{ik} is non-zero.) Equation (7) ensures that TAZs are assigned only to MCLs that have been selected. LINGO (22), a commercial math optimization software product was used to obtain the solution.

One more equation was included, for ex-post-facto analysis, which calculated the actual average distance from the TAZs to the assigned MCLs:

$$d_{avg} = \sum_{i=1}^N D_i \quad (9)$$

Figure 1.6 shows the location of the MCL location chosen if only one was allowed. Not surprisingly it is in the middle of the region.

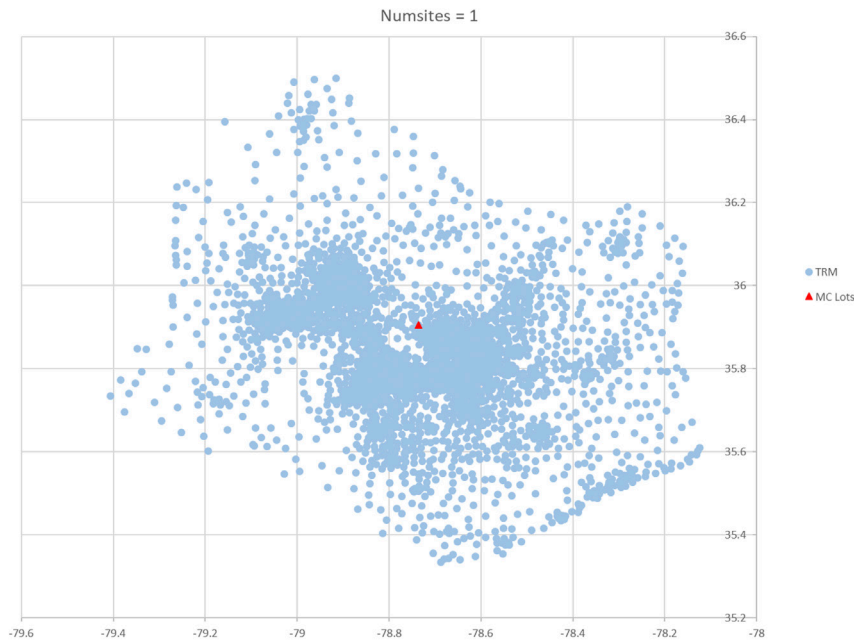


Fig. 1.6 Mode Change Lot location if only one is allowed

Figure 1.7 shows the downward trend in the weighted and unweighted average distances to the TAZs as the number of allowable MCL locations increases. There is no minimum. The trend will continue until zero is reached if the number of MCL locations is allowed to equal the number of TAZs. However, it is clear that the most significant drop occurs until the number of MCLs is about 8-14.

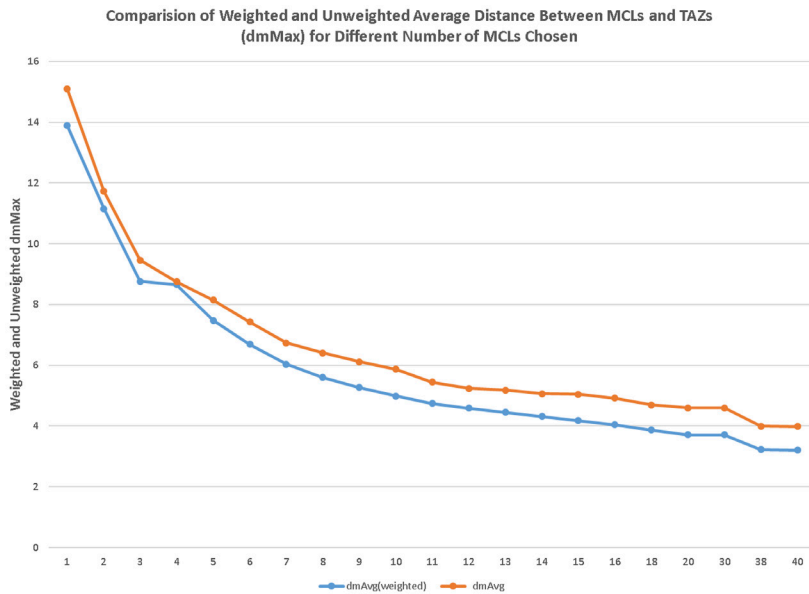


Fig. 1.7 Downward trend in the weighted and unweighted distances to the internal TAZs as the number of MCLs increases

Figure 1.8 shows a similar downward trend in the maximum distance to any of the internal TAZs. It does differ from the trend in the average in that a long plateau in the value occurs from four sites until 40. So when trying to minimize both average and maximum distances between MCLs and TAZs, there is not much to be gained from the perspective of maximum distance after four sites. But since the average distance still reduces significantly even after four sites, it was deemed practical to choose more than four MCL locations and in the range of 8-14 in order to gain some leverage in average distances. Since adding more MCL locations would increase costs, eight MCLs were deemed as the most cost-effective number for this study.

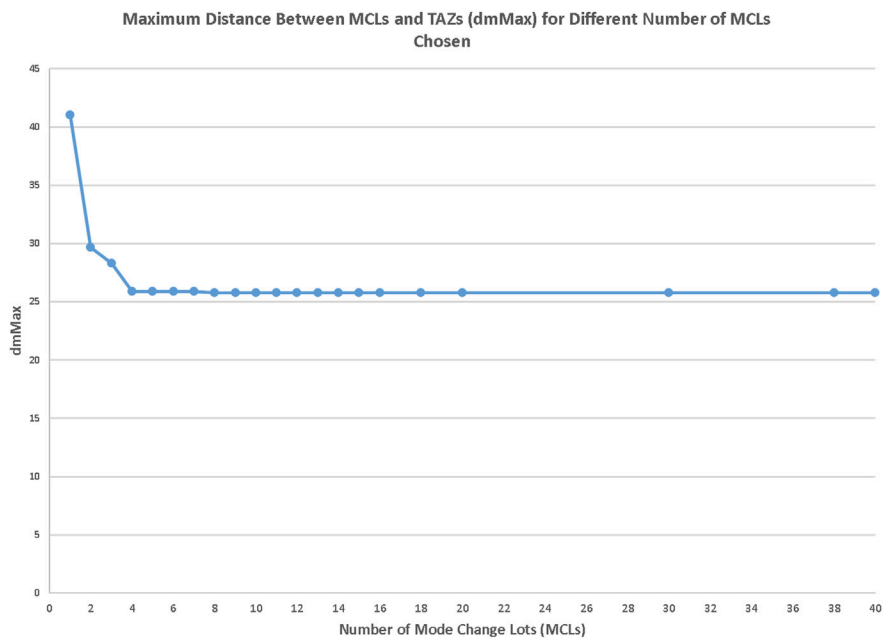


Fig. 1.8 Downward trend in the maximum distance to any internal TAZ as the number of MCLs increases

It is very important to realize that the actual locations chosen changes, dramatically at first, as the allowable number of sites increases. Figure 1.9 illustrates this fact. The chosen sites are highlighted in light purple. Notice, for example that the site chosen when $p = 1$, the very first site, does not reappear in the chosen set until the number of allowable sites is 12. In contrast, site "9" is selected when $p = 2$ (two sites allowed) and in every solution thereafter. The frequency with which the sites are selected is important information in determining which site should be selected. A trend we notice is that at 8 sites there is permanence in the selections. That is, the sites chosen when $p = 8$ remain chosen as part of the "best" set thereafter. Hence, from an investment standpoint, not only is the $p = 8$ solution a "good" one, based on Figures 1.7 and 1.8, but investments in those 8 sites would remain valuable if, "in the future", investments were made in more.

		Mode Change Lots Selected																																														
		1	2	3	4	5	6	7	8	9	10	11	12	13	14	15	16	17	18	19	20	21	22	23	24	25	26	27	28	29	30	31	32	33	34	35	36	37	38	39	40							
Number of Mode Change Lots	1																																															
	2																																															
	3																																															
	4																																															
	5																																															
	6																																															
	7																																															
	8																																															
	9																																															
	10																																															
	11																																															
	12																																															
	13																																															
	14																																															
	15																																															
	16																																															

Fig. 1.9 Trends in the sites chosen as the number of allowable MCL sites increases.

The locations of the sites in the $p = 8$ solution are shown in Figure 1.10. They tend to cover the Raleigh, Durham, and Chapel Hill urban areas with two additional sites along I-95.

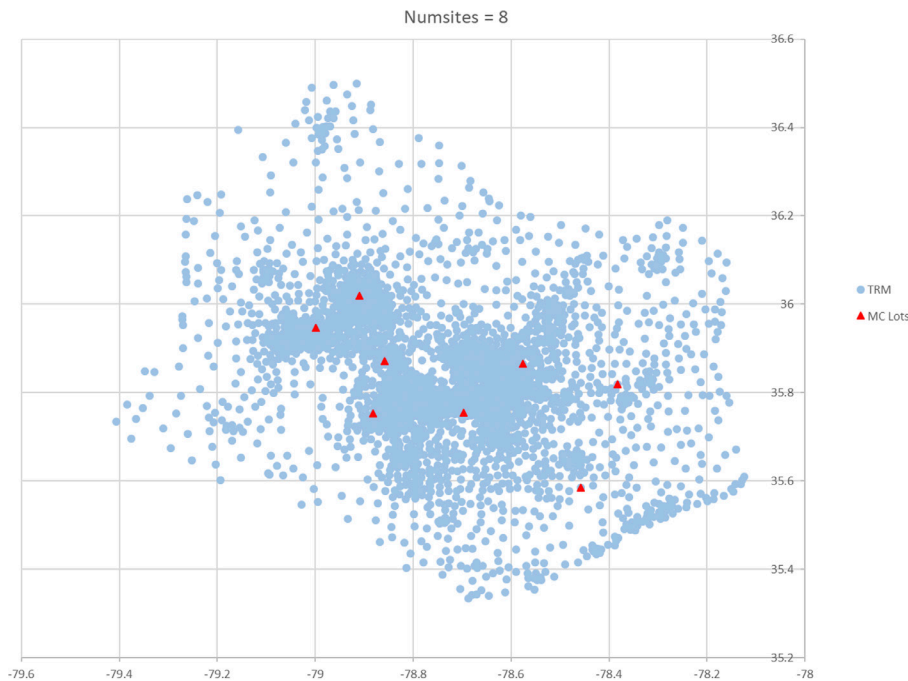


Fig. 1.10 Location of the MCLs chosen in the "8 site" solution

Figure 1.11 shows the location of these MCLs from the 8-site solution as they relate to the highway network. It is easy to see that most of them are adjacent to interchanges on the freeway network. The one exception is the site south of Clayton which likely appears to be off the freeway network because no TAZ was immediately adjacent to US-70 in that location. (If we had been able to add nodes to the TRM network for the MCL site options, this anomaly would have disappeared.)

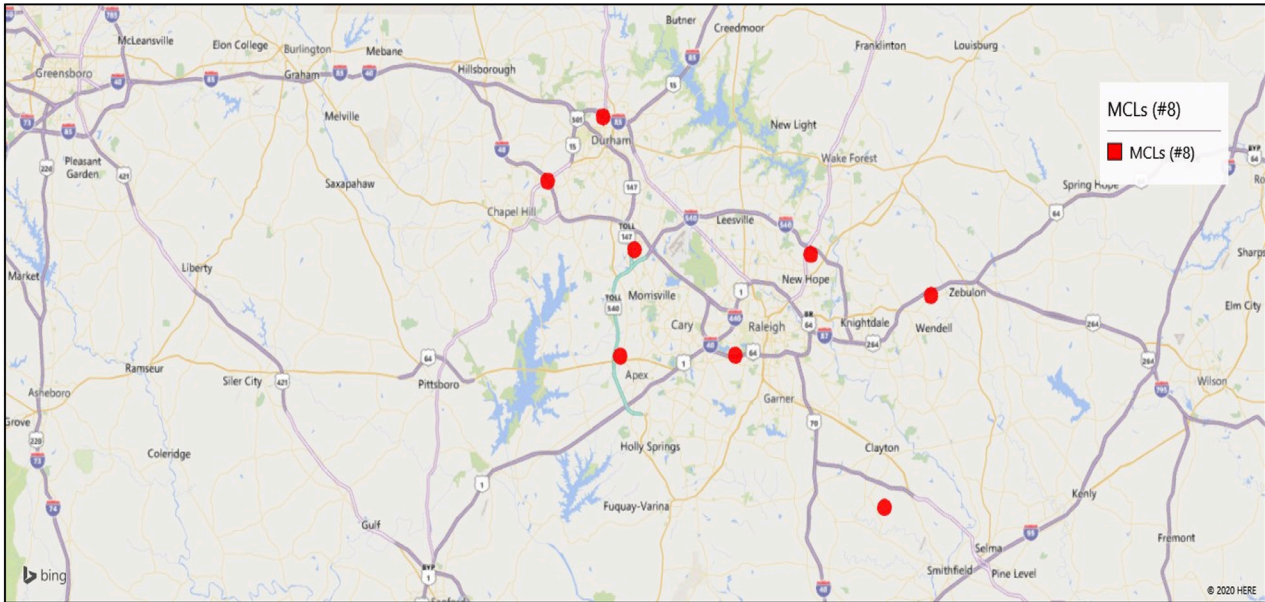


Fig. 1.11 MCL Locations on the Highway Network for the 8-site solution

Mode Split / Diversion

For mode split, which is the same as TAV diversion, we used five rules when considering each OD pair. The first was that the number of trips had to exceed a minimum threshold. The second was that only a certain percentage of the trips could be diverted. We explored two values, 30% and 100%. The third was that, for simplicity, straight-line distances could be used to estimate the trip lengths (rather than distances across the actual network links). The fourth was that the length of the TAV trip could not be any more than P percent longer than the original TV trip. We used $P = 20\%$. The fifth was that the length of the AV portion of the trip had to exceed a minimum length. We used 20 miles.

We examined every OD pair based on these five rules and identified those OD pairs for which diversion to TAV would be possible. Then for those, we adjusted the 2045 SUT and MUT goods movement trip tables so that they reflected the results of these diversions. The appropriate percentage (30% or 100%) of the trips for the “eligible” OD pairs were removed, and appropriate new TV and AV trip segments were added back in. This meant two TV and one AV segment for every II, IU, UI, and UU trip (appropriate combinations of IM, MI, UM, and MU segments in the first case, and MM segments in the second); one TV and one AV segment for every IC, UC, CI and CU trip (IM, UM, MI, MU, CM, and MC segments as appropriate). In the latter case, it was assumed that the MC and

CM segments could be removed from the PM time period and moved to another uncongested time period.

We did not attempt to compute a “defensible” mode split between traditional trucks (TVs) and TAVs. Instead, we were interested in seeing the impacts of diverting traditional trucks to AVs. Hence, two specific “diversion” percentages were assumed: 30%, which we thought was a “reasonable” value, and 100%, which would produce the greatest impacts. From a planning perspective, these choices are like “mode split” decisions, but we did not derive either value based on a procedure akin to Huang and Kockelman, for example (17).



The OD pairs whose trips could be diverted to TAV trips was assessed using exhaustive enumeration. The five rules presented previously were employed. To repeat: 1) the flow f_{ij} was at least F_{min} , 2) a specific percentage of the trips would be diverted (either 30% or 100%), 3) straight line distances could be used to approximate the node-to-node distances, 4) the extra distance added by the diversion would increase the total trip length

by no more than E percent greater than d_{ij} and 5) the total distance traversed between the MCLs needed to be at least d_{MMmin} . The pseudo code describing the process is as follows:

For all TAZ pairs ij such that $f_{ij} \geq F_{min}$, search all mode change lot combinations M_1M_2

- 1) Set the distance for the TAV trip $d_{TAV} = \infty$ and M_{1Best} and M_{2Best} to null
- 2) Select M_1M_2 without duplication, checking that $d_{M_1M_2} \geq MM_{min}$
- 3) Compute $d_{test} = d_{iM_1} + d_{M_1M_2} + d_{M_2j}$
- 4) If $d_{test} \leq (1+E) * d_{ij}$ and $d_{test} \leq d_{TAV}$, then set $d_{TAV} = d_{test}$ and set $M_{1Best} = M_1$ and $M_{2Best} = M_2$
- 5) Repeat steps 2, 3, and 4 until all M_1M_2 combinations are exhausted
- 6) If M_{1Best} and M_{2Best} are both not null, then TAZ pair ij has $P\%$ of its trips diverted to the path using path $i - M_{1Best} - M_{2Best} - j$, otherwise, no trips are converted to TAV trips.

Once this analysis was complete, the list of ij pairs for which diversions could occur was known.

To describe the adjustment process, some matrix notations are useful. Let T be the set of all trips for a given truck and trip type in time period n . (The “subscripts” for truck type, trip type, and time period are omitted for now to simplify the notation. The time period subscript will be reintroduced later.) T_{ij} is an element of matrix T and represents the number of trips for OD pair ij implicitly in time period n . We want to partition T based on whether the origin and the destination are of type I, M, U , or C . Doing this

creates 16 mutually exclusive submatrices: ***TII, TIM, TIU, TIC, TMI, TMM, TMU, TMC, TUI, TUM, TVU, TVC, TCI, TCM, TCU, and TCC***. Allowing that the nodes in *U* and *C* were originally in set *E*, nine of these submatrices are original: *II, IU, IC, UI, UU, UC, CI, CU, and CC*. These sub-matrices were used to capture the trips that were not converted to TAVs. The five new ones – *IM, MI, MU, MC, UM, UC, and CM* – were employed to capture the segments of the new TAV trips.

The action taken depended on the *ij* pair. For *II, IU, UI, and UU* trips, there was no change in when the trips occurred, including the AV (*MM*) segment. For the *IC, UC, CU, CI, and CC* trips, the AV segment was moved out of the original time period to some other time period when congestion is not an issue.

For the *II, IU, UI, and UU* trips, the “value” in utilizing the AV segments lies in lowering costs, simplifying driver logistics, and increasing labor productivity. For example, for a converted *II* trip, the driver that used to take the truck from *I* to *I* could now take it from *I* to *MCL_i*, drop if off, put it in AV mode, pick up another AV truck and bring it back to *i*. The same could happen on the *j* end of the trip. This means the “carrier” can reduce its labor cost because the driver does not have to accompany the truck for the entire trip. To illustrate numerically, assume the trip origin and destination are 30 miles apart. Also assume there are ten (10) truck trips each way between them every day (20 trips total). Of the 30 miles, 10 are on “local highways” and 20 are on freeways. The speed on the “highway” portions averages 15 mph while the speed on the freeway averages 50 mph. (This means for each trip 40 minutes is spent on the “local highways” and 24 minutes

on the freeways. Moreover, assume the cost per mile is \$2 and the cost per hour is \$60. If these trips are “driver-driven”, each day the total miles driven is 600 miles, the total hours is 21.33, and the total cost is \$2480. If these trips become TAV trips, the “driver-driven mileage” falls to 200 miles and the driver hours drops to 13.33 hours. If we assume there is no savings in mileage cost, then the TAV-based cost is \$2000, or 19.3% less than the TV cost. If *P*% of these trips are diverted to TAVs, then the driver-driven trips will be reduced by *P*%. If the trip is of type *II*, then *P*% of T_{ij} is added to cells in the submatrices ***TIM, TMM, and TMI*** for the original time period. Borrowing from the notation used earlier, *P*% of T_{ij} is added to $T_{iM1Best'}$, $T_{M1BestM2Best'}$ and $T_{M2Bestj}$. The same is true for trips of type *IU, UI, and UU*. For trips of types *IC* and *UC*, additions are made to the T_{*M} and T_{MC} matrices and for those of type *CI* and *CU*, additions are made to matrices T_{CM} and T_{M*} . However, in these cases, the AV portions of the trips are added to the overnight time period. For trip type *CC*, additions are made to the T_{CC} matrix overnight. Put in pseudo-code, the process is:



For all ij pairs in time period n such that diversions to TAVs occur, the following pseudo code describes the logic that was followed:

- 1) Decrement T_{ij} by $P\%$
- 2) For II , IU , UI , and UU trips, add $P\% * T_{ij}$ to $T_{iM1Best}$, $T_{M1BestM2Best}$ and $T_{M2Bestj}$ in time period n
- 3) For IC and UC trips, add $P\% * T_{ij}$ to $T_{iM1Best}$ in time period n and $T_{M1Bestj}$ in an uncongested time period.
- 4) For CI and CU trips, add $P\% * T_{ij}$ to $T_{iM1Best}$ in an uncongested time period and add T_{M1Best} to time period n .
- 5) For CC trips, add $P\% * T_{ij}$ to T_{ij} in an uncongested time period.

Figure 1.12 shows a simple TAV adjustment example. Starting from ten II trips that were found to qualify for diversion to TAV, 30%, or three trips, based on the diversion rate, are converted to TAV trips. Since these trips are of type II , two MCLs will be involved. Hence the three diverted TAV trips have three segments each. For each trip, one from the origin to the first MCL, one from the first MCL to the second, and a third from the second MCL to the destination. Even though the number of trip segments has increased, the new trips have a "long-enough" AV portion of the trip to be able to produce cost savings. The original 3 trips are subtracted from the II pair, and the new segments are added to the IM (IC), MM (CC), and MI (CI) pairs, since MCLs are a part of controlled facilities the trips show up in IC , CC and CI part of the matrix.

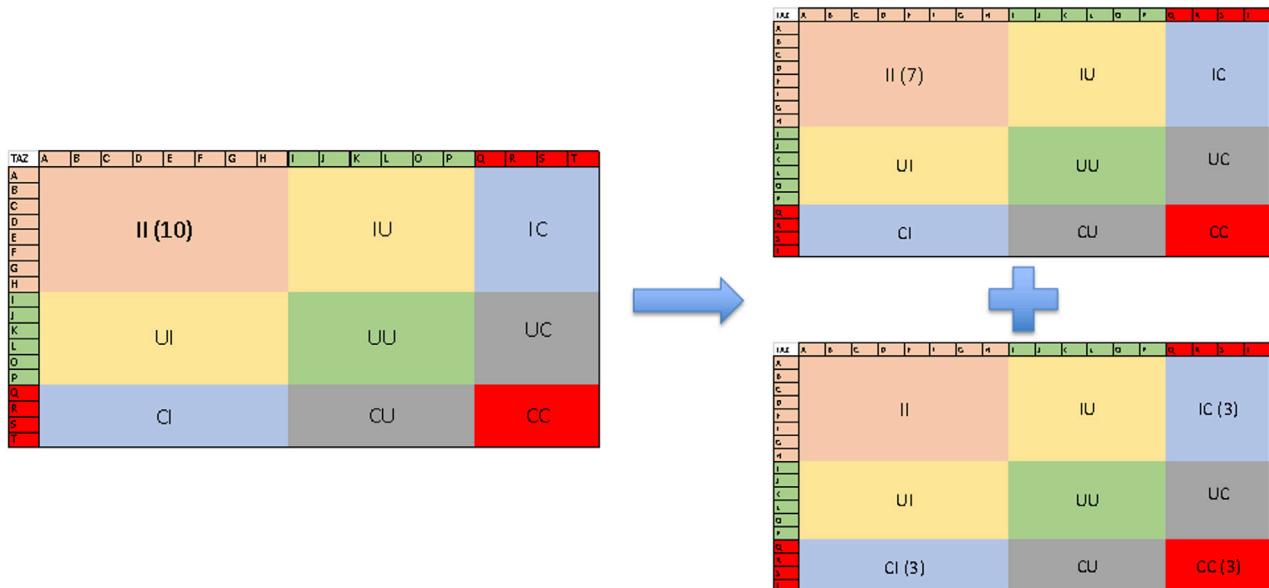


Fig. 1.12 MCL Illustration of the quantitative analysis

Traffic Assignment

For traffic assignment, a modified version of the normal TRMv6 process was employed. The TRMv6 would normally use a time equivalent for the path teq_p based on the congested travel time $time_p$ plus the sum of the tolls $toll_p$ divided by a value of time vot (SUT or MUT):

$$teq_p = time_p + toll_p / vot \quad (10)$$

Technically, the times are arc dependent, tolls exist only on some arcs, and the tolls are distance dependent with rate r . This means equation (10) can be rewritten based on the arcs $a \in A_p$ that are in path p :

$$teq_p = \sum_{a \in A_p} [time_a + r * dist_a / vot] \quad (11)$$

The modification to (11) that was used for the SUTs and MUTs started by computing a generalized cost:

$$C_p = \alpha * time_p + \beta * toll_p + \gamma * dist_p + \delta * pen_p \quad (12)$$

Respectively, the terms in this formula capture time-dependent costs for the trucks, the tolls, distance-dependent costs, and a penalty for choosing lower class facilities (implicitly, a toll).

Since the third term uses a distance-based rate and the penalties are distance-and-facility-type dependent, the generalized cost could be rewritten as:

$$C_p = \sum_{a \in A_p} \alpha * time_a + \sum_{a \in A_p} \beta * toll_a + \sum_{a \in A_p} \gamma * dist_a + \sum_{a \in A_p} \delta * pen_a \quad (13)$$

The distance dependency for the second, third, and fourth terms meant we could combine them into an equivalent toll for each arc $eToll_a = \beta * r * dist_a + \gamma * dist_a + \delta * pen_a * dist_a$. Then we could sum these $eToll_a$ values across the arcs to create $eToll_p$:

$$C_p = \alpha * time_p + \beta * eToll_p = \sum_{a \in A_p} \alpha * time_a + \sum_{a \in A_p} \beta * eToll_a \quad (14)$$

Finally, since the value of time vot is the same as the coefficient α which appears in the first term, equation (14) can be divided by α on both sides to yield:

$$teq_p = time_p + (\beta * eToll_p) / vot = \sum_{a \in A_p} time_a + \left(\sum_{a \in A_p} \beta * eToll_a \right) / vot \quad (15)$$

We used $\alpha = \$1$ per minute, $\beta = \$0.15$ per mile, $\gamma = \$1.73$ per mile. The pena values were facility type dependent as shown in Table 1.1:

	Functional Class												
	11	12	13	14	15	16	21	22	23	24	25	26	99
New Penalty (pena) (\$/mile)	0	0	0.3	1	2	3	0	0	0.3	1	2	3	0

Table 1.1 Penalties for facility use (\$/mile) by facility type

The values of time (VOTs) by vehicle class were adjusted to match the trends in TRM median income in terms of 2016 dollars:

Vehicle Class	VOT US median income 2016\$	VOT NC median income 2016\$	VOT TRM median income 2016\$
Median Income 2016	\$57,617	\$50,584	\$61,004
SOV	\$14	\$12	\$15
HOV2 (1.75 x SOV)	\$24	\$21	\$26
SUT	\$35	\$30	\$37
MUT	\$70	\$60	\$75

Table 1.2 Values of Time by Vehicle Type

SUTs and MUTs were also prohibited from using High Occupancy Toll (HOT) links by employing a flag for that facility class.

As with the TRMv6, the MUTs were assigned first, choosing paths on an all-or-nothing basis using $teqp$ from equation (15). These pre-loads resulted in a downward adjustment to the capacity remaining on the links used (by direction) and an upward adjustment to the starting values of the travel times.

The SUTs were subsequently assigned as part of the standard multi-modal equilibrium assignment process where equation (15) was used for the SUTs and equation (10) was used for the SOVs and HOVs.

Findings

Identifying a way to see the impacts and assess the change proved challenging. We tried looking at color-coded pictures of highway network, tables of values, total VMT (vehicle miles traveled), total VHT (vehicle hours of travel), differences in VMT and VHT by link, and several other ideas. Our finding was that, because the changes only pertain to SUTs and MUTs, and those flows are such a small portion of the overall trip table, and the VMT and VHT, that it was not possible to see significant changes in aggregate measures. This is a significant finding. Put another way, it should not be expected that a shift from TVs to a mixture of TVs and TAVs will not have a profound impact on the way in which the urban network functions during the peak hours. (This cannot be said for shifts from SOVs and HOVs to auto-related AVs.)

Reflecting on the changes introduced (shifting TV trips to TAV trips; rerouting the TAV trips, with greater circuitry, so that they made use of the freeways, and shifting the AV trips out of the peak) a mixed bag of impacts should be expected. The shift toward longer trips for the TAVs should increase VMT and maybe increase VHT. Removing the AV portions of some trips from the peak should lower VMT and VHT. The overall impact is unclear. Moreover, for some facilities the VMT and VHT might increase. For others, both might decrease.

The clearest picture we found of the impacts was provided by showing by the change in total VMT and VHT, splayed out for all the links in the network, sorted by functional class and then by link number. A more sophisticated way to present the results was elusive. So, in Figure 1.13, the freeway or interstate with the lowest link number is at the left-hand end of the x-axis. The rural collector with the highest link number is at the right-hand end of the x-axis. (Actually, the centroid connectors are last.)

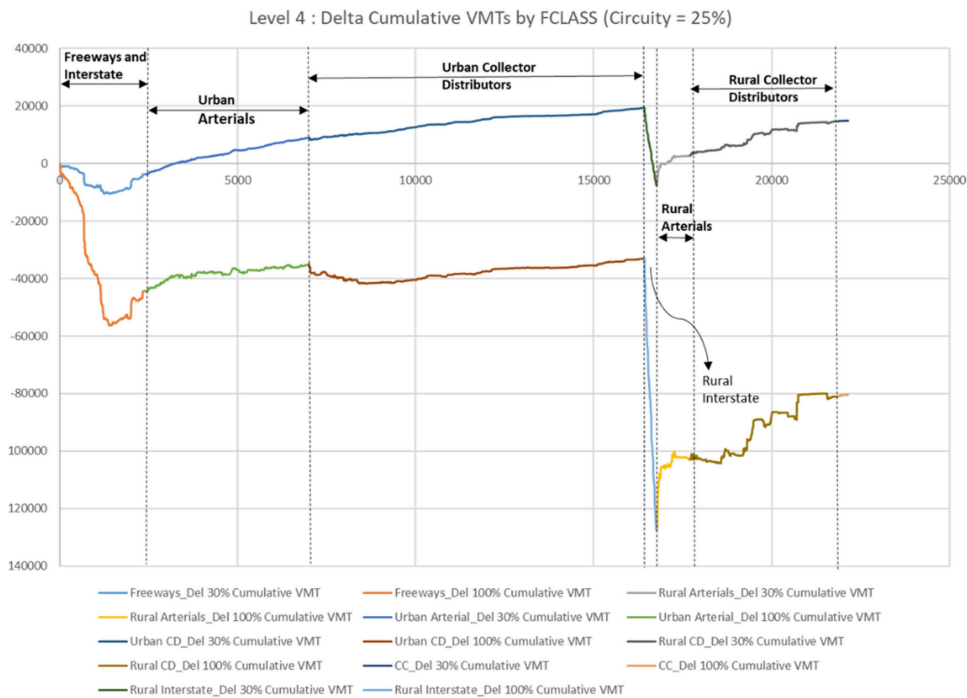


Fig. 1.13 The cumulative change in VMT for the 30% (top graph) and the 100% (bottom graph) diversion scenarios for a circuitry limit of 25%

Hence, in the figure, the way to interpret the results is as follows, from left to right. The “lower numbered” freeway links all show a decline in VMT. (These tend to be the links in the urban areas.) In net, for all the freeways and interstates, the VMT is lower than in the base case (a net of 0) for both the 30% and 100% diversion scenarios. However, for the urban arterials, the trend is upward, in both cases. For the urban collector-distributors, the trend is slightly different for the two scenarios. For the 30% diversion case, the net VMT continues to increase; for the 100% case, there is an initial dip followed by a climb. In both scenarios, for the rural freeways, there is a drop in VMT that is then offset by increases for the rural arterials and the rural collector-distributors. All-in-all, for the 30% diversion scenario, the net effect is positive, the total VMT does not decrease, it increases. For the 100% diversion scenario, the net effect is negative i.e. total VMT decreases.

Figure 1.14 shows the trends for VHT. In both scenarios the overall effect is positive. VHT increases. The increase is more dramatic for the 30% scenario than for the 100%. The same initial decreases can be seen for the urban freeways, although the decline is not as dramatic for the 30% scenario. The rural freeways also exhibit decreases. Our conclusion is that the 25% circuitry allowance is encouraging longer TAV trips with the result that the overall net changes are positive, except for VMT in the 100% diversion case.

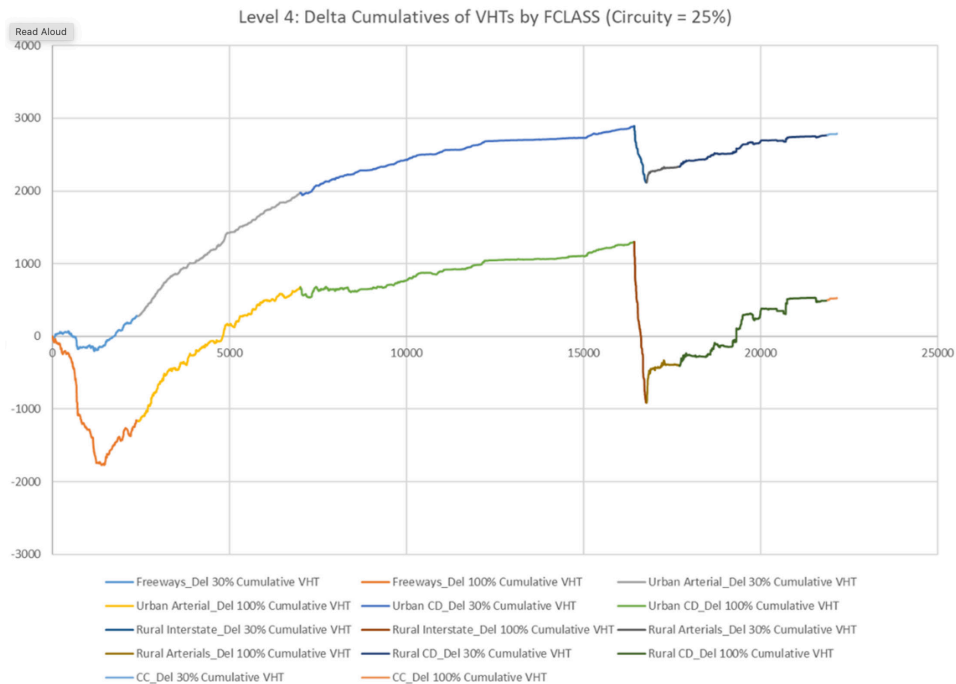


Fig. 1.14 The cumulative change in VHT for the 30% (top graph) and the 100% (bottom graph) diversion scenarios for a circuitry limit of 25%

Figures 1.15 and 1.16 show the trends for the scenarios where the upper bound on circuitry is 15%. The net changes are smaller, but the trends are the same. Except for VMT for 100% diversion, the VMT and VHT increase.

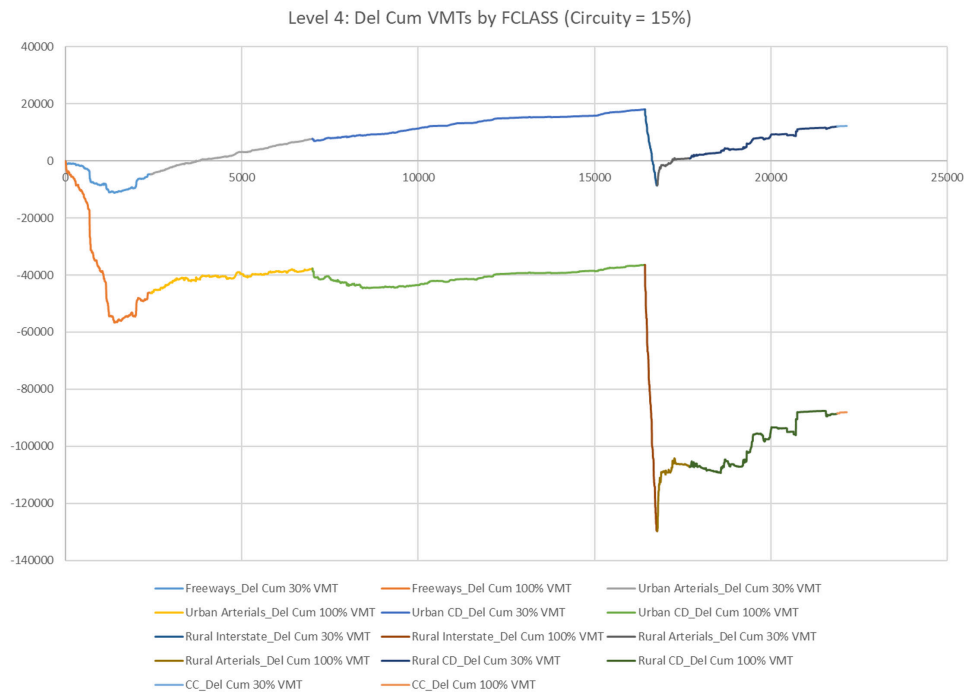


Fig. 1.15 The cumulative change in VMT for the 30% (top graph) and the 100% (bottom graph) diversion scenarios for a circuitry limit of 15%

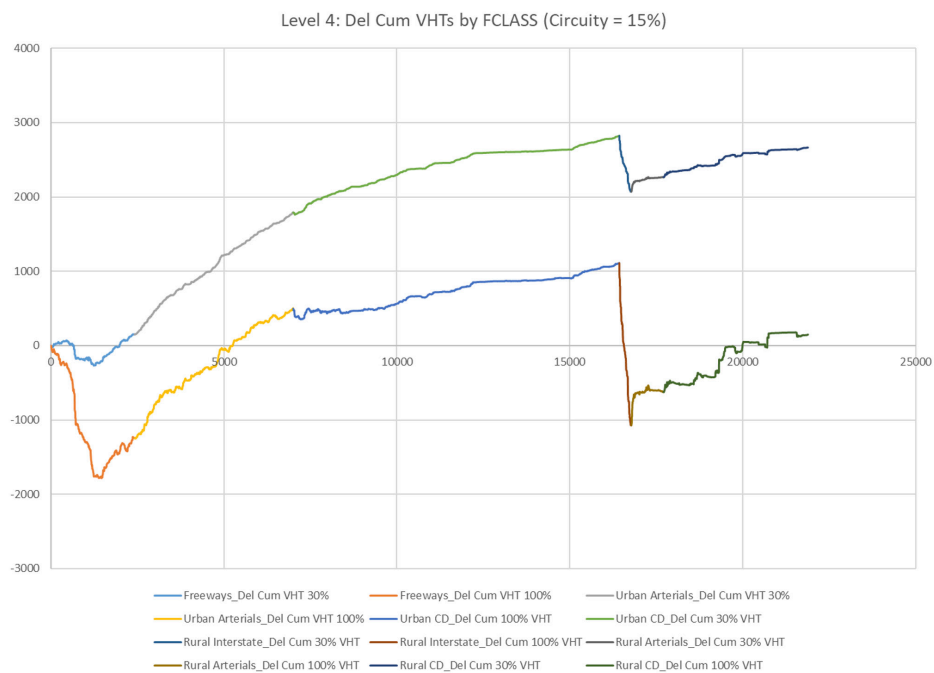
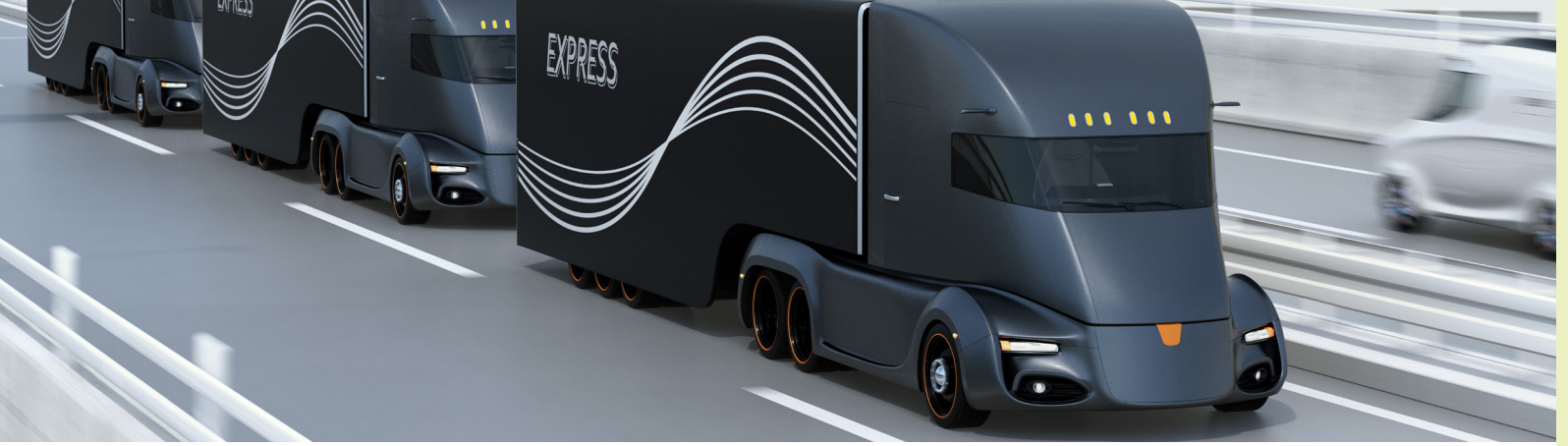


Fig. 1.16 The cumulative change in VMT for the 30% (top graph) and the 100% (bottom graph) diversion scenarios for a circuitry limit of 15%

Our conclusion is that, while shifts toward autonomous trucks may be beneficial for many reasons, expecting these shifts to produce savings in VMT or VHT during the peak hours may not be defensible.





1.4 Level 5 Analysis

For the level 5 analysis, we focused on both “goods” trips and the “service” trips. We also focused on the LCV trips in addition to those for the SUTs and MUTs.

Problem Set-Up

Setting up the Level 5 analysis was much simpler than Level 4. Mainly, this was because it was assumed that the AV trucks could operate anywhere on the network. That being said, we did structure the generalized cost for the traffic assignment so that higher-type facilities were favored. The main hypotheses were these:

- The logic pertaining to the SUTs and MUTs would be the same.
- A percentage $p_g\%$ of the SUT, MUT and LCV trips would be diverted to AVs. For SUTs and MUTs, a 100% for $p_g\%$ was examined. For the LCVs, two values of $p_g\%$ i.e. 30% and 100% were explored.
- The AV trips between EE and EI TAZs would be moved out of the peak congested period. (While one could argue that some of these trips would “need to” remain in the

congested period, we were interested in exploring the maximum impact that this shift to AVs might have.

- The LCV trips that were converted to AVtrips would be removed from the LCV trip matrix and, through a PCE equivalency, added to the SUT trips.

For trip generation there was no change. The same SUT, MUT, and LCV initial trip matrices were employed.

For “mode split” (trip diversion) there would only be AV trips. TV trips would be diverted to AV trips. There no longer were any TAV trips.



Traffic Assignment

For traffic assignment, we used the same process employed in level 4. The teqp values for the SUTs and MUTs were based on the generalized cost described in Equation (15). The MUTs were pre-loaded, and the SUTs were assigned as part of the normal multi-modal equilibrium assignment process. Moreover, since the LCV trips that were converted to AV trips were folded into the SUT trip matrix, the LCV-related AV trips were also subjected to the teqp calculation based on generalized cost.

Findings

The same changes in cumulative VMT and VHT proved to provide the clearest indication of the impacts. The changes in VMT and VHT were again summed in a sorted order by functional class and link number and then plotted.

Figure 1.17 shows the change in total VMT for a 30% diversion of LCVs and a 100% diversion of SUT and MUT trips. The change is substantial across all functional classes.

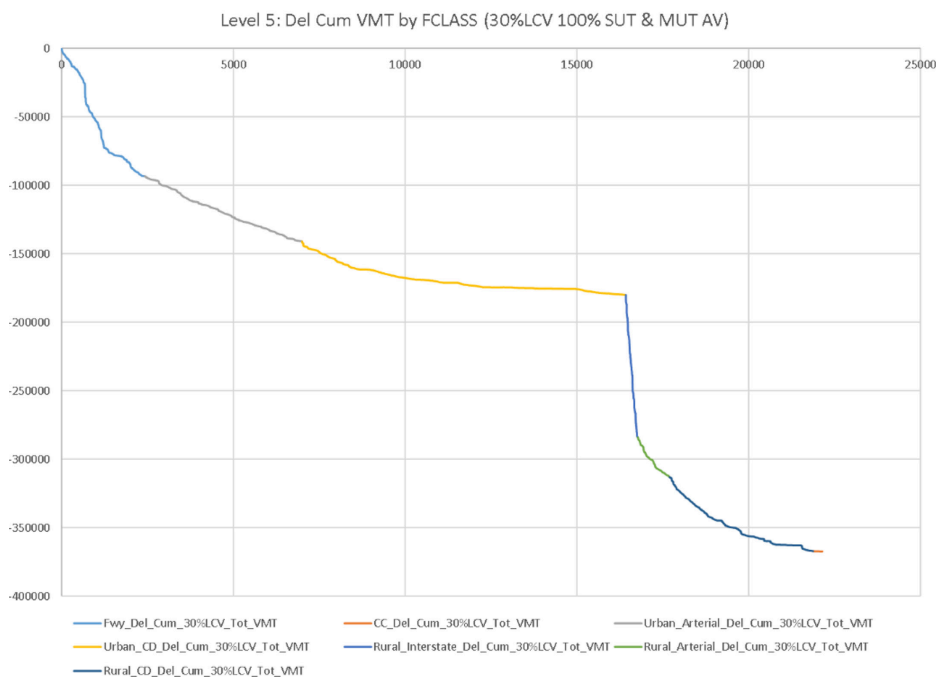


Fig. 1.17 The cumulative change in VMT for a 30% diversion of LCV trips and 100% diversion of SUT and MUT trips to AV trips in level 5

Figure 1.18 shows the corresponding change in VHT for a 30% diversion of LCVs and a 100% diversion of SUT and MUT trips. The VHT decreases as well although not as substantially as the VMT, but the rural interstate links show a very sharp decline for VHT values.

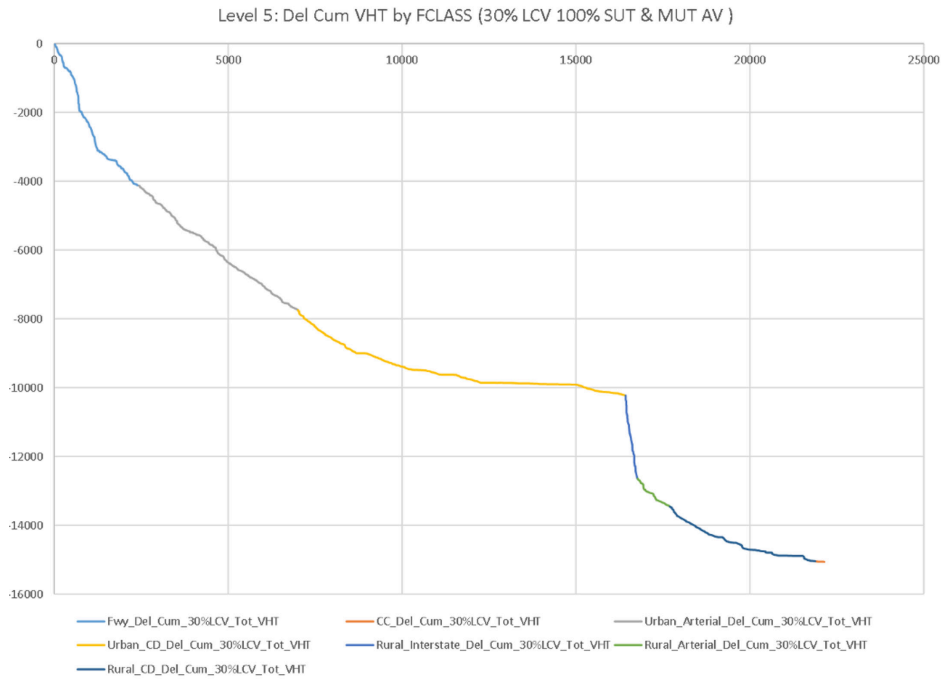


Fig. 1.18 The cumulative change in VHT for a 30% diversion of LCV trips and 100% diversion of SUT and MUT trips to AV trips in level 5

Figure 1.19 shows the cumulative change in VMT for the scenario where 100% of the SUT, MUT, and LCV trips are shifted to AVs. As was the case for the 30% diversion, the total VMT decreases.

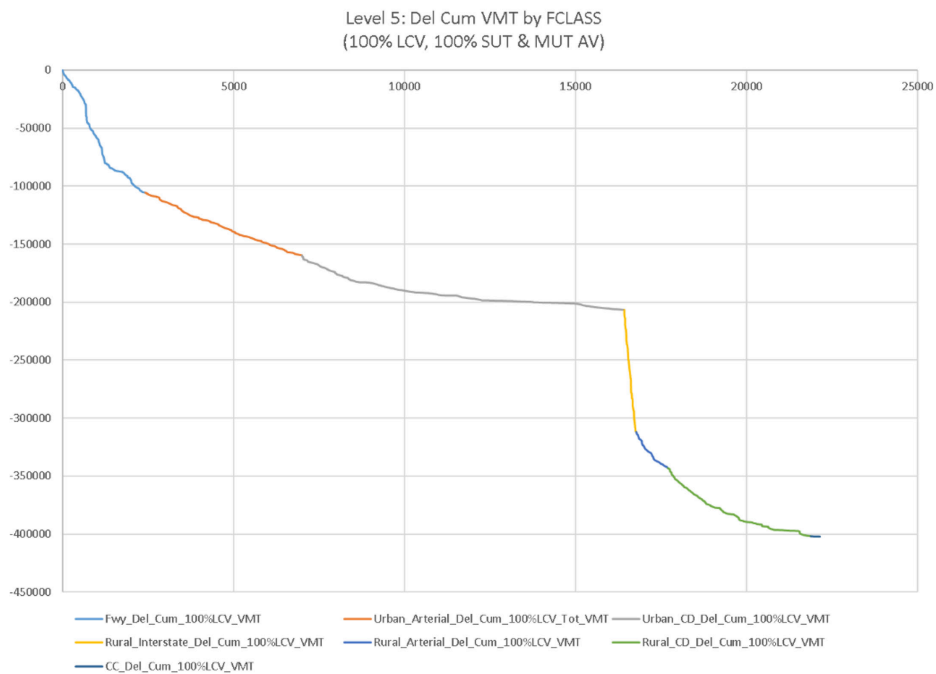


Fig. 1.19 The cumulative change in VMT for a 100% diversion of LCV, SUT and MUT trips to AV trips in level 5

Figure 20 shows the change in cumulative VHT for the case where 100% of the LCV, SUT, and MUT trips are diverted to AVs.

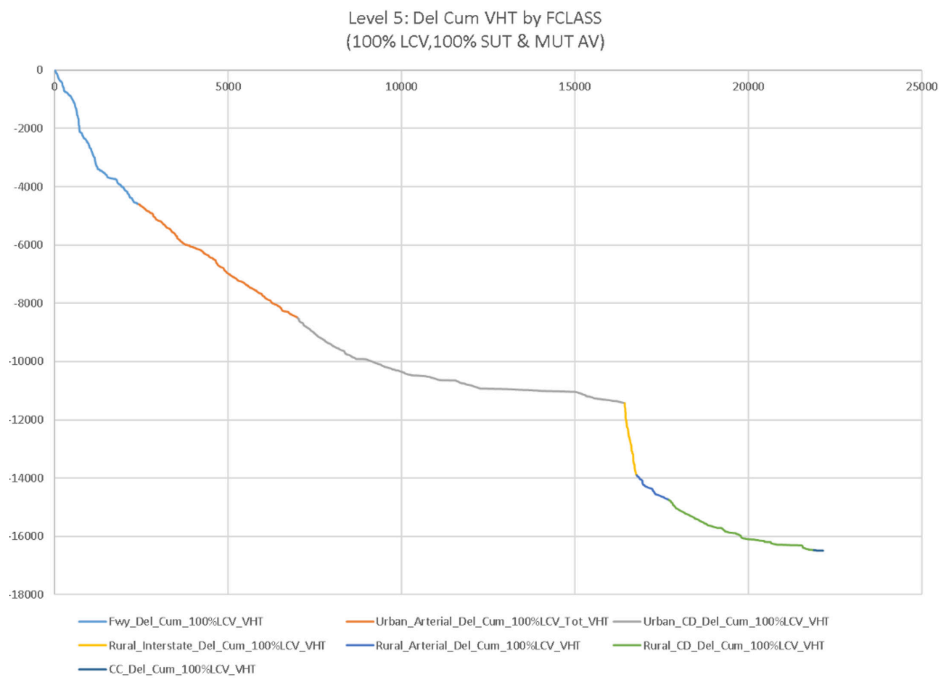


Fig. 1.20 The cumulative change in VHT for a 100% diversion of LCV, SUT and MUT trips to AV trips in level 5



1.5 Summary and Conclusions

This study presents the findings of a travel demand modeling study focused on autonomous freight trips in an urban area, in this case the Triangle region of North Carolina. The Triangle Regional Model (TRM), which is a planning model employed by the Capital Area Metropolitan Planning Organization (CAMPO), was used as the analysis tool. The analysis year was chosen to be 2045 simply because the TRM is presently validated for that horizon year.

We study autonomy levels 4 and 5 as specified by the Society of Automotive Engineers (SAE)(2). For level 4, we assume the AVs can operate autonomously on controlled access facilities like freeways; they will be more amenable to AV operation than “lower class” facilities. For level 5, we assume they can use any link although we encourage them, through preferential weights, to use “higher-type” facilities where possible. We do not distinguish between AVs with and without communication/connection capabilities. We assume all of the AVs are connected as well as autonomous. The study focuses on peak period operation where capacity is scarce and congestion, common.

The three main questions we address are:

1. To what extent can AVs reduce the peak period levels of congestion?
2. what operational changes will be needed?
3. what if any special facilities might be needed to accommodate these flows?

There are different treatments done for AV trips depending on the level of automation. The following sections explain the level 4 and level 5 treatments and results in detail.

In the case of level 4, we assume a probability that traditional truck (TV) trips will be converted to blended conventional-automated trips (TAVs); and for level 5 we assume a likelihood that all TV trips will become AV trips. Level 4 also imposes a “circuitry restriction” on trips: that is, an eligible TV-to-AV conversion will only become a TAV trip if the extra distance traveled by the TAV trip is at or below a maximum “extra distance” threshold. Two sub-scenarios were considered: one where 30% of both the SUT and MUT trips and another 100% of both the SUT and MUT

trips would be diverted to AVs. The latter was examined to observe results from the maximum impacts. None of the LCV trips were converted to AV, since this was thought to be a much more advanced scenario for level 4 in 2045. This is because LCVs are primarily “service” trips where the service person often provides a customized/expertise based service which might not be as easy to automate in the near future (examples are cleaning/ plumbing based services).



Analysis of level 4 trips is more involved because we assumed only a portion of the network allows AV trips like freeways. So, AV portions of the diverted trips would take place on the freeways, and other segments of the trip would be human driven (TV). In order to have safe “mode transitions” between AV and TV modes, TAZs were flagged as “mode change lots” (MCLs). A TV can enter an MCL to shift from TV to AV mode, let the driver disembark (the driver also might stay with the vehicle). At the end of the AV segment of the trip, the truck would enter a second MCL and undergo a similar mode change, in reverse. The AV would enter the MCL, stop, a driver would board (or resume control), and then continue. A limited

number of MCLs were created, keeping cost effectiveness in mind. We examined numbers of MCLs ranging from one (1) to forty two (42) using a bi-objective p-Median / p-Center problem and determined that eight (8) MCLs were enough to serve the regions demands.

Next in order to model the mode split from TV to TAV trips, the following five rules were applied when considering each OD pair: (a) the number of trips had to exceed a minimum threshold (b) only a certain percentage of the trips could be diverted (30% and 100% diversion rates were tested) (c) straight-line distances could be used to estimate the trip lengths (rather than distances across the actual network links) (d) The length of the TAV trip could not be any more than P percent longer than the original TV trip (P = 20% was used) and (e) the length of the AV portion of the trip had to exceed a minimum length (we used 20). Once this analysis was complete, the list of OD pairs for which diversions could occur was known. The TV trips were then adjusted based their OD pair, some trips were also moved out of the peak period to examine how that effects network performance. For II, IU, UI, and UU trips, there was no change in when the trips occurred, including the AV (MM i.e. trip occurring between MCLs) segment. For the IC, UC, CU, CI, and CC trips, the AV segment was moved out of the original time period to some other time period when congestion is not an issue. For the II, IU, UI, and UU trips, the “value” in utilizing the AV segments lies in lowering costs, simplifying driver logistics, and increasing labor productivity.

For traffic assignment, a modified version of the normal TRM process was

employed. To begin with a generalized cost was estimated for the SUTs and MUTs. The generalized cost equation used had four components: a time-dependent cost for the trucks, the tolls, distance-dependent costs, and a penalty for choosing lower class facilities (implicitly, a toll). Value of time (VOT) was then used to factor this cost into the time equivalent for a particular path. The VOT values were also adjusted to match the trends in TRM median income in terms of 2016 dollars, which was the most recent data available on VOTs. Exclusion sets were employed to prohibit SUTs and MUTs from using High Occupancy Toll (HOT) links. After these changes were made, the usual TRM highway assignment process was applied: MUTs were assigned first, choosing paths on an all-or-nothing basis using the new time equivalents. These pre-loads resulted in a downward adjustment to the capacity remaining on the links used (by direction) and an upward adjustment to the starting values of the travel times. The SUTs were subsequently assigned as part of the standard multi-modal equilibrium assignment using time equivalents pertaining to SUTs.

The level 4 study findings are as follows:

1. Because the changes only pertain to SUTs and MUTs, and those flows are such a small portion of the overall trip table, and the VMT and VHT, that it was not possible to see significant changes in aggregate measures. This is a significant finding. Thus, it should not be expected that a shift from TVs to a mixture of TVs and TAVs will not have a profound impact on the way in which the urban network functions during the peak hours.
2. The various treatments applied like shifting TV trips to TAV trips; rerouting the TAV trips, with greater circuitry, so that they made use of the freeways, and shifting the AV trips out of the peak, created a mixed impacts. The shift toward longer trips for the TAVs increased VMTs and VHTs in some facilities while reduced the VMTs and VHTs in others.
3. The clearest picture was obtained by examining change in total VMT and VHT, splayed out for all the links in the network. This representation of results showed that there was decrease in VMTs and VHTs on urban freeways, urban and rural interstate, but an increase in other facilities like urban & rural collector-distributors and urban & rural arterials. This trend was observed for both 30% and 100% AV diversion rates and also for their respective sub-scenarios where circuitry was 15% and 25%.



For the level 5 analysis, we focused on LCV trips in addition to the SUT and MUT trips. Here the logic pertaining to the SUTs and MUTs would be the same. A percentage of the SUT, MUT and LCV trips would be diverted to AVs: for SUTs and MUTs, a 100% was examined; for

the LCVs, 30% and 100% were explored. The AV trips between EE and EI facilities would be moved out of the peak congested period. The motivation for doing this was to be able to explore the maximum impact that the shift to AVs might have. Lastly, the LCV trips that were converted to AV trips would be removed from the LCV trip matrix and, through a PCE equivalency, added to the SUT trips.

There was no change in trip generation. For “mode split” (trip diversion) since there were only AV trips in level 5 (i.e. no TAV trips), TV trips would be diverted to AV trips. For traffic assignment, the same process as level 4 was employed. The time equivalents for the SUTs and MUTs were based on the generalized cost as described earlier. The MUTs were pre-loaded, and the SUTs were assigned as part of the normal multi-modal equilibrium assignment process. Since the LCV trips were converted to AV by folding them into the SUT trip matrix, the LCV-related AV trips were also subjected to the time equivalents calculated based on generalized cost.

The same trends in cumulative VMT and VHT as level 4 were observed. The decrease in VMTs and VHTs was more substantial as compared to level 4 which is understandable given the assumptions for the two studies.

REFERENCES

1. Waymo. On the Road – Waymo. <https://waymo.com/ontheroad/>. Accessed Mar. 8, 2019.
2. SAE International Releases Updated Visual Chart for Its “Levels of Driving Automation” Standard for Self-Driving Vehicles. <https://www.sae.org/news/press-room/2018/12/sae-international-releases-updated-visual-chart-for-its-“levels-of-driving-automation”-standard-for-self-driving-vehicles>. Accessed Jul. 10, 2021.
3. Waymo. On the Road – Waymo. <https://waymo.com/ontheroad/>.
4. Zattero, D. A., and S. E. Weseman. Commercial Vehicle Trip Generation in Chicago Region. *Transportation Research Record*, 1981, pp. 12–15.
5. Southworth, F., Y. J. Lee, and D. Zattero. A Motor Freight Planning Model for Chicago. No. 9, 1982.
6. Freight Matters: Trucking Industry Guide to Freight and Intermodal Planning Under ISTEA. 1993.
7. Cohen, H. S., R. M. Alfelor, K. L. Rhoades, A. J. Horowitz, S. Chatterjee, M. McAdams, D. W. Matherly, and A. Sosslau. *Quick Response Freight Manual*. 1996.
8. Ruiters, E. R. Development of an Urban Truck Travel Model for the Phoenix Metropolitan Area. Arizona. Dept. of Transportation, 1992.
9. Fischer, M. J., and E. K. Constantine. Innovative Approaches to Regional Freight Transportation Planning: Case Study of Monterey Bay Region. *Transportation Research Record: Journal of the Transportation Research Board*, Vol. 1522, No. 1, 1996, pp. 27–37. <https://doi.org/10.1177/0361198196152200104>.
10. List, G. F., L. A. Konieczny, C. L. Durnford, and V. Papayanoulis. Best-Practice Truck-Flow Estimation Model for the New York City Region. *Transportation Research Record*, Vol. 1790, No. 1790, 2002, pp. 97–103. <https://doi.org/10.3141/1790-12>.
11. Holguín-veras, J., G. F. List, A. H. Meyburg, K. Ozbay, R. E. Passwell, H. Teng, and S. Yahalom. An Assessment of Methodological Alternatives for a Regional Freight in the NYMTC Region. *New York Metropolitan Transportation Council*, 2001, p. 181.
12. Prem, C. E., and P. Yu. Applying Urban Transportation Modeling Techniques to Model Regional Freight and Vehicle Movement. *Transportation Research Record: Journal of the Transportation Research Board*, Vol. 1518, No. 1, 1996, pp. 22–24. <https://doi.org/10.1177/0361198196151800105>.

13. Marker, J. T., and K. G. Goulias. Truck Traffic Prediction Using Quick Response Freight Model Under Different Degrees of Geographic Resolution: Geographic Information System Application in Pennsylvania. *Transportation Research Record: Journal of the Transportation Research Board*, Vol. 1625, No. 1, 1998, pp. 118–123. <https://doi.org/10.3141/1625-15>.
14. Slavin, H. Enhanced Framework for Modeling Urban Truck Trips. 1998.
15. Faris, J. M., and D. Ismart. Freight Modeling Techniques for Small and Medium-Sized Areas. 1999.
16. Hasnat, M. M., E. Bardaka, M. S. Samandar, N. M. Roupail, G. F. List, and B. Williams. Impacts of Private Autonomous and Connected Vehicles on Transportation Network Demand in the Triangle Region, NC. *Publishing in ASCE Journals*, 2020, pp. 13–21. <https://doi.org/10.1061/9780784479018.ch03>.
17. Huang, Y., and K. M. Kockelman. What Will Autonomous Trucking Do to U.S. Trade Flows? Application of the Random-Utility-Based Multi-Regional Input–Output Model. *Transportation*, 2019, pp. 1–28. <https://doi.org/10.1007/s11116-019-10027-5>.
18. Cantarella, G. E., and A. Di Febbraro. Transportation Systems with Autonomous Vehicles: Modeling Issues and Research Perspectives. 5th IEEE International Conference on Models and Technologies for Intelligent Transportation Systems, MT-ITS 2017 - Proceedings, 2017, pp. 1–6. <https://doi.org/10.1109/MTITS.2017.8005580>.
19. Southworth, F., C. Ross, A. Amekudzi-Kennedy, M. Meyer, R. Pendyala, K. Haynes, M. Caldwell, S. Caldwell, R. Haynes, S. Haynes, L. Haynes, and E. Gordon. Modeling And Understanding The Implications Of Future Truck Technology Scenarios For Performance-Based Freight Corridor Planning. No. December, 2016.
20. Nasri, M. I., T. Bektaş, and G. Laporte. Route and Speed Optimization for Autonomous Trucks. *Computers and Operations Research*, Vol. 100, 2018, pp. 89–101. <https://doi.org/10.1016/j.cor.2018.07.015>.
21. Triangle Regional Model Information - NC Capital Area Metropolitan Planning Organization. <https://www.campo-nc.us/mapsdata/triangle-regional-model/trm-information>. Accessed Jul. 10, 2021.
22. Cunningham, K., and L. Schrage. *The LINGO Algebraic Modeling Language*. Springer, Boston, MA, 2004.

Chapter 2

Impacts of Connected and Autonomous Trucks on Freeway Operations

George List, Professor
North Carolina State University

Soumya Sharma, Graduate Research Assistant
North Carolina State University

Shoaib Samandar, Research Associate
North Carolina State University





2.1 Introduction

While connected and autonomous automobiles seem to be the major media focus presently, it may be autonomous trucks that emerge first in significant numbers. There are economic drivers, like reduced labor costs, that will drive carriers, shippers, and receivers toward the use of this technology.

The question is: how will this technology be accommodated? How will it fit into the existing highway environment? Will it be disruptive? Will truck AVs be compatible with the existing mix of highway traffic? Will this depend on the percentage of the traffic stream that is truck AVs? It is not clear. Pictures of truck AV prototypes suggest they will look very different from existing trucks. For example, they do not have cabs. They look more like the push-back tractors that move planes at airports - low and boxy - or overgrown sports cars than present tractor-trailers or single unit trucks.

While questions about the visual acceptance of this technology are beyond the scope of an analytical study; we can examine the extent to which they will be compatible with existing highway flows in the sense of

highway operations. We can model the highway-environment and explore their impact.

This study examined the way in which autonomous trucks might inter-relate with the existing traffic stream using microsimulation. We created a model of a hypothetical section of freeway that included both a basic freeway section with no ramps and one that included an on and off ramp in sequence. We conducted simulation studies of this facility for reasonable, but not at-capacity flow rates, and examined the travel rate distributions and lane changing activity with and without truck AVs. We also explored what seemed to be reasonable ideas about how truck AVs might be accommodated, like setting a policy that they should make use of the middle lane and not operate anywhere on the facility.

Technically, we modeled CAV trucks, not AVs. That is, we assumed the autonomous trucks could talk to one another. While there is evidence of AV autos, that lack communication capabilities, and in some ways, they are already here, it seems far less likely that AV trucks will emerge that cannot communicate. Most trucks, particularly the ones that are large, over-the-



road tractor-trailers, are already equipped with communication technology and sensors. What is missing is robotic control. That is the feature we assume will be added. So anywhere in this report where we are talking about AV trucks, whether we say so or not, and whether the acronym employed is AV or CAV trucks, the implicit assumption is that the autonomous trucks are CAVs, they not only can operate autonomously but they can communicate with each other. Moreover, to keep the wording short, we will use the acronym T-CAV to refer to autonomous truck AVs, rather than writing out the words each time.

Our representation of the T-CAVs is based on a premise that they would behave differently based on where they were in the traffic stream relative to other vehicles. If they were following another T-CAV, they would behave one way; and when following a traditional vehicle, differently. Hence, the T-CAV headways were modeled as dynamic and made dependent on whether a T-CAV was following another T-CAV or not. We adjusted model parameters used to represent vehicular “car following” and lane changing; and models of both that were more consistent with anticipated T-CAV behavior. We assumed the T-CAVs would use shorter time and/or space headways and that they can operate in a platoon mode when in a string of T-CAV trucks, while maintaining longer headways when following other vehicles. This was done by having the T-CAVs use a car following that depended on the vehicle in front of it.

The other vehicles in the traffic stream were assumed to be traditional vehicles, including autos and non-CAV trucks. These vehicles were presumed to be human driven. Since trucks are generally more limited in their maneuverability, our analysis included a major

focus on lane changing. We monitored the extent to which lane changing was affected by the presence of the T-CAV trucks. This included an investigation of the extent to which lane use restrictions, imposed on the T-CAVs, might affect the operation of the freeway.

This remainder of the report is organized as follows. First, a review of the technical literature focused on modeling autonomous and connected trucks in a mixed traffic environment is presented. Second, the methodology is explained; where the algorithms used to model the behavior of each vehicle type are provided. Third, the analysis and results are described, and finally the summary and conclusions from the study are presented.



2.2 Literature Review

Hurtado-Beltran and Rilet studied the impact of CAV Truck Platooning on the Highway Capacity Manual's Capacity and Passenger Car Equivalent Values. They used the equal capacity passenger car equivalent (EC-PCE) methodology from the manual to estimate capacity and EC-PCEs for CAV truck platoons on freeway segments. The EC-PCE values for CAV trucks were on an average, 34.3% lower compared to the values for non-CAV trucks. The study shows that CAV platoons can have a positive effect on highway capacity. The decrease in the EC-PCE value depends on the CAV operational assumptions made by the study. (1) Yang et. al. assessed the safety performance of the Wyoming Connected Vehicle pilot deployment program under adverse weather conditions. A 23-mile section representative of the I-80 corridor was chosen for the microsimulation model. Field data under winter snowy weather condition were collected to calibrate the base model. Various connected vehicle (CV) demand levels and CV penetration rates were studied and the reductions in conflicts displayed a decreasing trend with the increase of CV penetration rates. When all trucks were CVs,

a maximum reduction in in conflicts of 85% was observed (2). Song et. al. developed a cellular automata (CA) model to simulate the influence of autonomous truck platoons (ATPs) on traffic flow. The model used a fine cell size as 0.5 m (length) plus 3.5 m (width). To examine the necessity of dedicated lane for ATPs, three scenarios were developed based on a three-lane expressway. In scenario 1, light vehicles were allowed on all three lanes and trucks on the two right most lanes. In the scenario 2, both the single truck and ATPs were allowed on the two right most lanes. In the scenario 3, the ATPs were limited to only the rightmost lane. They observed queuing in all three scenarios but scenario 3 was observed to have longer queues as compared to the other scenarios. With the increase of vehicles density, scenario 3 may encounter serious congestion eventually. An examination of the lane changing behavior showed that there was no significant difference in lane changing frequency among the three scenarios. The light vehicles were found switching lanes frequently when their front vehicle was a truck or ATPs, this was especially true for scenario 3. This caused longer ATPs to form

naturally such that the rightmost lane nearly became a truck only lane. For scenario 3, the two rightmost lanes had worse congestion than the other scenarios.(3) Calvert et. al. studied the effects of truck platooning on traffic flow. They proposed extensions to simulation to better model truck platoon interactions. They observed that traffic flow was negatively affected by truck platooning, especially in saturated states. Effects on merging were also explored. Merging was found to be effected but the impact was not too detrimental for short platoon sizes. (4) Lee et. al. proposed a framework for exploring traffic mobility and safety performance for different market penetration rate (MPR) of truck platoons. Their study was based on microscopic traffic simulation in VISSIM using a platoon formation algorithm developed by the team. The results indicated that the difference in network mobility performance was not significant up to MPR of 80%. For the truck-designated lane, the average speed was found to be lower than in other lanes. Moreover, the on-ramp section in the truck-designated lane had an average speed that was 33% lower. Increasing truck platoon MPRs were found to have a positive effect on longitudinal safety but a negative effect on lateral safety. (5) Duret et. al. devised an efficient method for splitting a platoon of vehicles near network merges. A model-based bi-level control strategy was proposed. The main motivation was to provide a solution to the problem of active platoon maneuver near merges for both CAV and mixed traffic conditions. The hierarchical framework proposed uses an analytical car-following model to decide optimal tactical decisions. It then uses a more detailed model to predict and control operational acceleration dynamics of trucks. The tactical part of the

provides optimal vehicle indexes in the platoon to yield gaps for merging vehicles and time instants they should start the yielding process. This was decided taking into account a speed drop that they can accept compared to the equilibrium speed. The operational part utilizes a third-order longitudinal dynamics model to estimate optimal truck accelerations so that new equilibrium gaps can be formed when the merging vehicles begin lane changing.(6) Mesa-Arango and Fabergas assessed the impacts of ATPs on travel time and travel time reliability at freeway diverge areas. They proposed a framework to integrate ATPs into a microscopic traffic simulator. The impact of four experimental variables on travel time and reliability was examined: (i) traffic volume projections, (ii) ATP penetration rates, (iii) ATP sizes, and (iv) ATP gaps. Two performance metrics were employed, and statistical analysis was done to measure impacts on through and divergent traffic. The results indicated the significance and impact of experimental variables on travel time and reliability.(7)

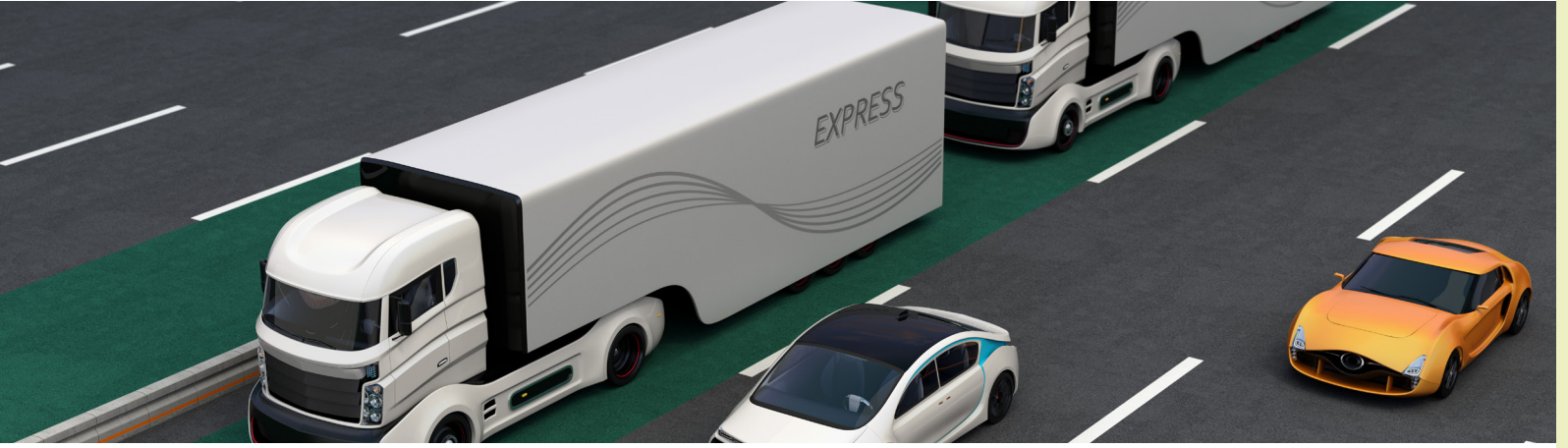
Research on autonomous trucks is dominated by autonomous trucking related work, however, another largely explored area



worth mentioning is the challenges that come with human interactions with autonomous and connected vehicle technologies. A slew of studies focus on the behavioral impacts on trucks drives in the context of autonomous driving. Zhang et. al. studied how safe and comfortable transitions of control from the automated system back to the human drivers can be made. They examined truck drivers' take-over response times after a system-initiated request to take back control in non-critical truck platooning scenarios. Truck driving simulator experiment was conducted on 22 professional truck drivers and subjects were instructed to drive under three conditions during highly automated driving:

- Driver monitoring condition i.e., drivers were instructed to monitor the surroundings,
- Driver not-monitoring condition where drivers were provided with a hand-held tablet and were asked to use it, and
- Eyes-closed condition where the drivers were not allowed to open their eyes. The take-over response time was assumed to comprise the perception response time and the movement response time.

Results indicated longer total take-over times with high variability for the Driver not-monitoring and Eyes-closed conditions. Hand movement response time was observed to be the major component of the total take-over time. It was influenced by the movements done to resume physical readiness before taking over control, like putting away the tablet, or adjusting the seat. (8) Many other researchers have looked into the taking-over process for truck drivers operating AV, CAV, and CV trucks. (9-14)



2.3 Methodology

Our main objective was to explore the extent to which highway operations, especially on freeways, might be affected by the presence of the T-CAVs. We perceived that the best way to do this was to create a microscopic simulation model of this mixed vehicular environment and apply that model to typical freeway situations; namely, a basic freeway section and a typical urban setting that involved an on ramp followed by an off-ramp. We also wanted to explore the impacts of specifying which lanes could be used by the T-CAVs, either all lanes or just the middle lane.

Many microscopic simulation software options exist – VISSIM, PARAMICS, TransModeler, and CORSIM. Of these, TransModeler is the platform that NCDOT typically employs. However, for this study, we did not want to be dependent upon pre-programmed logic for how the T-CAVs would operate. We wanted the ability to directly control the T-CAV lane changing and car-following. Hence, we sought a microsimulation software platform that would be open source, and found SUMO (15). SUMO was chosen because it allows the user to select from models available in

the literature rather than relying solely on models provided in the application framework. It also offers easy to use output file formats that provide a detailed picture of lane changing maneuvers/ events during simulation.

Since lane changing behavior was of significant interest, we will describe how SUMO handles that activity first. The default lane changing model in SUMO i.e. LC2013 (16) uses a four-layered hierarchy of motivations to determine what a vehicle will do in terms of its lateral behavior. Four incentives are employed to determine if a lane change will take place:

- 1) strategic change,
- 2) cooperative change,
- 3) tactical change, and
- 4) regulatory change.

A strategic lane change is one when a vehicle must change its lane in order to be able to reach the next edge on its route. A cooperative represents the real-world situations when vehicles/ drivers change lanes solely to help another vehicle with lane changing towards their lane. Tactical lane changing refers to maneuvers where a vehicle attempts to avoid following a slow leader. Regulatory lane changes are motivated by



mandatory traffic laws. For example in countries with right-handed driving, drivers are under the obligation to clear the passing lane whenever they do not use it for an overtaking maneuver.

The lane-changing model has several parameters, but only four values were changed from their defaults to emulate the T-CAVs. As research on this area grows, we will have more information about parameter values specific to a vehicle type, but at present, no reference sources exist. We elected to modify the following parameters: 1) *lcStrategic*, the look-ahead distance for strategic decision making, which we set to 1000 meters for the T-CAVs and human driven trucks; 2) *lcLookaheadLeft*, the distance that vehicles look ahead for lane changing opportunities, which we set at 1000 meters for all vehicles, and 3) *lcAssertive*, the willingness to accept lower front and rear gaps on the target lane (The required gap is divided by this value), which we set at 2 for all vehicles.

Insofar as car-following is concerned, we employed a model built on the work of Xiao et al.(17), Nowakowski et al.(18), Milanes and Shladover(19) and Xiao et al. (20). It is assumed that the T-CAVs obtain information about their surroundings using onboard communication and sensing equipment. Driving decisions are made using line-of-sight and signals received or intercepted from other connected vehicles and/or the infrastructure. The communication capability

enables the T-CAVs to ascertain the real-time motion of other vehicles, respond to driving changes of vehicles in their vicinity and the traffic stream almost instantaneously (mechanical delay and communication latency make up the essential parts of the delay for the T-CAVs. We assumed that the T-CAVs can communicate with all other T-CAVs in their vicinity and that the T-CAVs can form platoons that involve shorter following time gaps. The T-CAV can operate in three modes:

- Cruising: the T-CAV maintains either a user-defined desired speed or posted speed limit in absence of a preceding vehicle;
- Car-following: the T-CAV maintains a fixed time gap to its preceding vehicle; and
- Gap closing: the T-CAV transitions from the cruising mode to car-following mode when it approaches a preceding vehicle that was a long distance away.

The cruising mode for the T-CAVs is treated like AVs. It is activated when there are no preceding vehicles in the range covered by the sensors or when the time-gap with the leading vehicle is larger than two (2) seconds. However, the car-following mode for CAVs is quite different from that for AVs and is triggered when the gap and speed deviations are simultaneously smaller than 0.2 m and 0.1 m/s, respectively.

Vehicle speed under this mode is calculated from the vehicle speed in the previous time step, as well as the gap error in the previous time step and its derivative. The details of this calculation for the T-CAV car-following mode are provided below.

$$v_{n,j} = v_{n,j-1} + k_p * e_{n,j-1} + k_d \frac{(e_{n,j-1} - e_{n,j-2})}{\Delta t} \quad (1)$$

The gap error ($e_{n,j-1}$) in equation 1 is determined as:

$$e_{n,j} = x_{n-1,j-1} - x_{n,j-1} - L - d_0 - \tau * v_{n,j-1} \quad (2)$$

where:

- $e_{n,j}$ = time gap error in the current time step (j),
- $e_{n,j-1}$ = time gap error in the previous time step,
- k_b, k_d = feedback gain with 0.45 s^{-1} and 0.0125 from (46) and (50) , respectively,
- $x_{n-1,j-1}$ = position of the preceding vehicle in the previous time step,
- $x_{n,j-1}$ = position of subject vehicle in the previous time step,
- d_0 = spacing margin,
- τ = desired time-gap in seconds, a value of 0.6 sec adopted from (51) ,
- $v_{n,j}$ = speed of subject vehicle,
- $v_{n,j-1}$ = speed of subject vehicle in the previous time step,
- L = vehicle length (5 meters),

The dynamic spacing margins for the T-CAVs, d_0 , is a function of the vehicle speed as follows:

$$d_0 = \begin{cases} 0 & v \geq 10 \text{ m/s} \\ -0.125v & v < 10 \text{ m/s} \end{cases} \quad (3)$$

The third, gap-closing mode, regulates the transition from the cruising mode to the car following mode when a CAV approaches its leader from a long distance. This mode is triggered when the time-gap is less than 1.5 seconds. Under this mode, the mathematical formulation of speed is identical to that of the car-following mode. However, the values for k_p and k_d parameters are 0.005 s^{-1} and 0.05 , respectively.

For traditional vehicles, the widely used psycho-physical model by Wiedemann (21, 22) was utilized. The model asserts that the driver of a faster moving vehicle approaching a slower vehicle will initiate deceleration upon reaching their personal perception threshold. At any given moment, a driver is assumed to be in one of the four modes: free driving, approaching, following, or braking. Acceleration by mode is determined by the current speed, speed difference, space headway and the individual characteristics of driver and vehicle. The parameter values for autos and non-CAV trucks in this study are given in Table 1 below (the values changed are shown in bold, rest of the values are defaults for the parameter):

Parameter	Autos	Non-CAV trucks
CC0 (Stand still distance)	1.5 m	1.5 m
CC1 (Headway time)	1 s	1.8 s
CC2 (Following variation)	2 m	2.4 m
CC3 (Threshold for entering following)	-8	-8
CC4 (Negative following threshold)	-0.35	-0.35
CC5 (Positive following threshold)	0.35	0.35
CC6 (Speed dependency of Oscillation)	11.4	11.4
CC7 (Oscillation Acceleration)	0.25 m/s ²	0.25 m/s²
CC8 (Standstill Acceleration)	3.50 m/s ²	1.97 m/s²
CC9 (Acceleration with 80 km/h)	1.5 m/s ²	0.82 m/s²

Table 2.1: Parameter values in car following for Autos and Non-CAV Trucks

The simulation runs can be thought of as being of two types: 1) a basic freeway segment or 2) a “weaving” segment, technically an on-ramp followed by an off-ramp.

For the basic segment case, a hypothetical freeway was created comprised of three freeway sections, each 3 miles in length as shown in Figure 2.1. We treated the first segment as the “loading” segment, the second as the “observation” or “test” segment, and the third as the “exit” or “post-experiment” segment.

Vehicles entered the system at the left-hand edge of the first segment, transited through the system and exited at the right-hand edge of the third segment. The first segment was

included to buffer out any transients created by vehicle entry. The third segment was included to ensure that the operating conditions at the right-hand edge of the “test”, second segment would implicitly match those at the left-hand edge. That is, no traffic-condition-induced constraints on operation would not be removed because the second segment simply ended abruptly.

Within the “test” segment, we collected detailed information about vehicle trajectories. We installed loop detectors 100 ft inside the left- and right-hand edges of the “test” segment. With these detectors, we collected the vehicle ID, lane location, and a timestamp for every vehicle. We also used a pre-defined report provided by SUMO

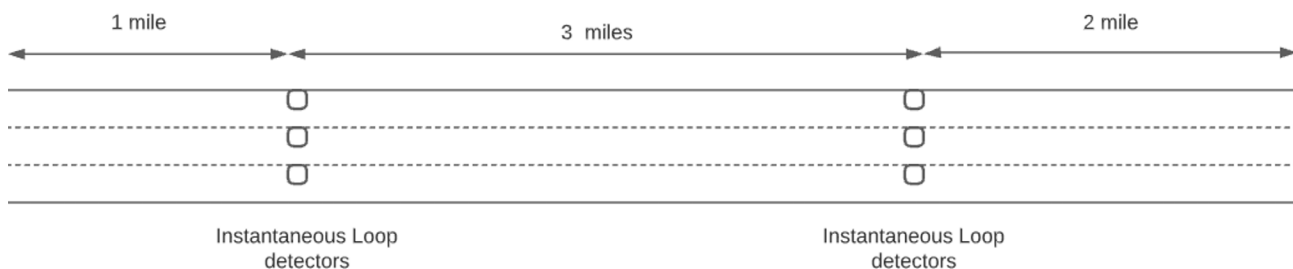


Figure 2.1: The Basic Segment

that reports all the lane changes that occurred between specific lanes within a given segment.

Different percentages of total trucks were examined, from 10% to 40%. For each of these, the percentage of T-CAVs was explored from 0% (all traditional trucks) to 100% (all T-CAVs). To label the scenarios for analysis purposes, we used a three-number scheme – the T-CAV percent, the conventional truck percent, and the auto percent. So, 10-10-80 would imply 10% T-CAVs, 10% conventional trucks and 80% autos.

We explored two variants of the operation policy for the T-CAVs. One in which they could use any lane and another in which they were required (strongly encouraged) to use the middle lane. In the latter case, since all vehicles were allowed to enter any lane at the left-hand edge of the first segment, the T-CAVs had to transition

from their entry lane to the middle lane by the time they reached the second segment. To make this happen, we provided a look-ahead ability for the T-CAVs so that they could see in advance when they needed to be in the middle lane. To see that this worked, we viewed the vehicle movements during simulation, and saw that the T-CAVs were able to comply with this requirement and did transition to the middle lane prior to entering the second segment.

The weaving section model involved a network of 5 segments, each 1 mile long except for the weaving portion which was determined to be 3450 ft. based on HCM recommendation of maximum weaving length.(23). The physical arrangement of the weaving model is shown in Figure 2.2 below.

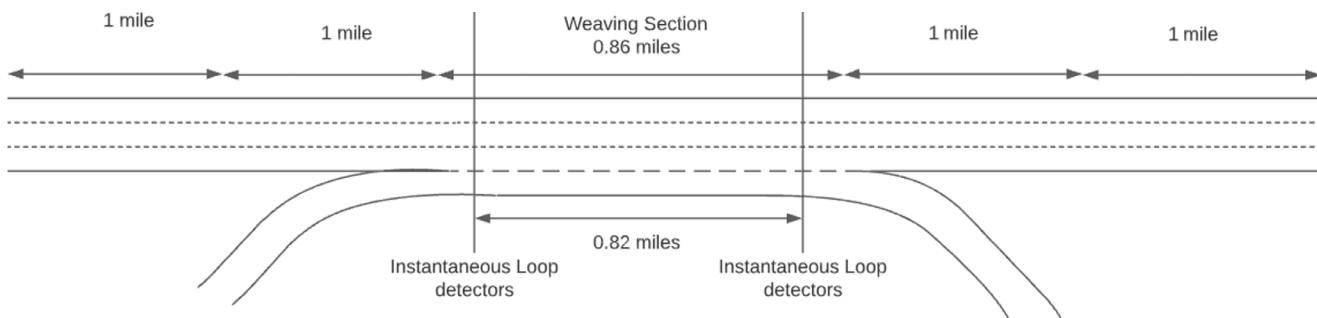


Figure 2.2: The Weaving Section Model

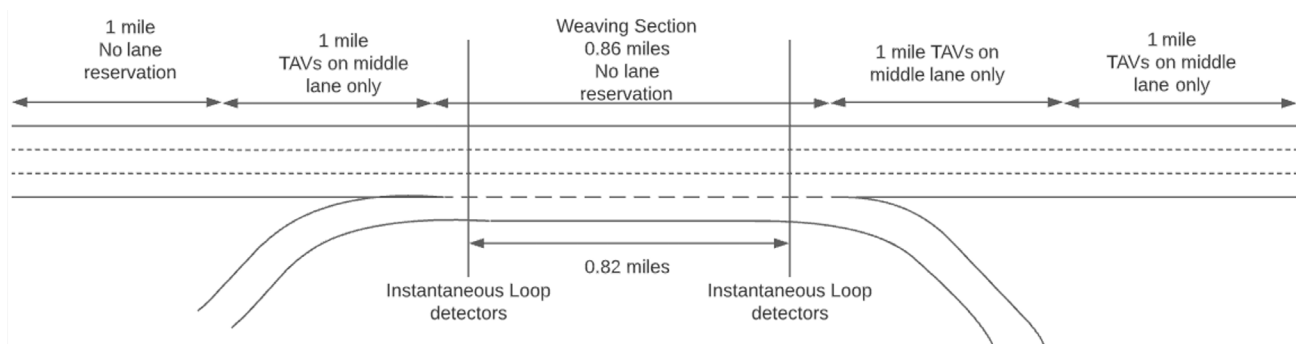


Figure 2.3: Weaving Segment with Lane Reservation

As with the basic freeway section model, we introduced loop detectors that would provide detailed information about the vehicular movements within the weaving section. The detectors were placed 100' inside the boundaries of the weaving section, 4330' apart. are allowed on all lanes. Loop detectors were placed 100 ft inside the weaving segment.

Also, as with the basic freeway section model, we examined two variants insofar as the operating conditions are concerned. One where the T-CAVs could use any lane (implicitly shown in Figure 2) and one where they were "required" to use the middle lane. The imposition of these lane use restrictions is shown in Figure 2.3. It is mandatory that they be varied so that the T-CAVs can both exit and enter the freeway.

Two main outputs from the SUMO simulations were utilized. The first was the lane change file. It provides information about all lane change events that took place within a given segment. For each it shows a time stamp (defined as the moment where the center line of the vehicle enters the new lane) and a reason for the lane change maneuver. The reasons for the lane change reasons can be:

- a. speedGain (i.e. to increase speed)
- b. strategic (i.e. focused on the future route)
- c. cooperative (i.e. to yield to another vehicle)
- d. keepRight (i.e. if the vehicle parameters have been set such that it always tries to keep to the rightmost lane)
- e. sublane (i.e. due to a sublane model employed)
- f. traci (i.e. if a user manually forced a lane change using SUMO's interface traci)

The second type of output came from loop detector output files. These files indicate a vehicle ID, a time, and an event type for each vehicle detected. The event type is one of three options:

- a. "enter": indicates that a vehicle has entered the detector in the simulation step
- b. "stay": indicates a vehicle which entered the detector in a prior step is still on the detector
- c. "leave": indicates that a vehicle has left the detector in the simulation step



2.4 Results and Discussion

The results from the analysis are both informative and reassuring. As previously indicated, we explored truck percentages ranging from 10% to 40%, and percentages of T-CAVs ranging from 0% to 100%. As stated earlier, a three-number scheme was used to identify the vehicle mix. For example, 20-0-80 indicates 20% T-CAVs, no conventional trucks, and 80% autos.

Many traffic mixes and operating conditions were explored. A select set for the basic freeway section analysis are shown in Table 2. The first four rows show results for situations where all vehicles could use any lanes. The last shows the results when the T-CAVs are required to use the middle lane. The specific vehicle mixes are shown in the second, third, and fourth columns, using, implicitly, the three-number identification scheme described in the previous paragraph. The next three columns show the 5th, 50th, and 95th percentiles of the travel rate distributions. (The travel rates are in minutes per mile, where one minute per mile is 60 mph). The last three columns show the percentages of lane changes that occurred.

As can be seen, the effects of the T-CAVs are minor. Even when the percentage of T-CAVs is 40%, there is not a dramatic impact on the travel rates. There appears to be a minor change in the percentage of lane changes that occur, especially from the right-hand lane (lane 0) to the middle lane (lane 1). But the increase from 29% to 32% may not be significant statistically.

Moreover, when use of the middle lane is mandated for the T-CAVs, there does not appear to be a major impact on either the travel rates or the lane changing behavior. This is good news in that, if a policy decision is made to require T-CAVs to use the middle lane, that decision will not have an adverse effect on freeway operations, at least for T-CAV percentages up to 40%.

Table 2.3 presents selected run results for the weaving section analysis. As with Table 2.2, the first column indicates whether the T-CAVs could use any lane or only the middle lane. The next three columns show the vehicle mix. The middle three show the 5th, 50th, and 95th percentile travel rates, and the last six (6) show the percentages of lane change maneuvers.

Lane Use	Vehicle Mix (%)			Travel Rates (min/mi)			Lane Changes (%)			
	T-CAV	TT	CA	5%	50%	95%	01	10	12	21
All	0	10	90	0.847	0.901	0.963	28%	26%	24%	22%
All	0	20	80	0.860	0.912	0.975	29%	27%	23%	22%
All	20	0	80	0.854	0.898	0.966	29%	28%	22%	21%
All	40	0	60	0.856	0.891	0.960	32%	29%	21%	18%
Middle	20	0	80	0.854	0.898	0.966	29%	28%	22%	21%
Key:										
T-CAV: Connected and autonomous truck										
TT: Traditional (non-autonomous) truck										
CA: Conventional auto										

Table 2.2: Basic Freeway Segment Performance for Various Vehicle Mixes and Operating Conditions

Lane Use	Vehicle Mix (%)			Travel Rates (min/mi)			Lane Changes (%)					
	T-CAV	TT	CA	5%	50%	95%	01	10	12	21	23	32
All	0	20	80	0.867	0.924	1.028	19%	22%	14%	25%	9%	12%
All	20	0	80	0.867	0.925	1.021	18%	21%	16%	26%	8%	11%
Middle	0	20	80	0.867	0.925	1.030	19%	22%	14%	24%	9%	13%
Middle	20	0	80	0.871	0.928	1.041	21%	24%	13%	21%	9%	12%
Key:												
T-CAV: Connected and autonomous truck												
TT: Traditional (non-autonomous) truck												
CA: Conventional auto												

Table 2.3: Weaving Segment Performance for Various Vehicle Mixes and Operating Conditions

The key take-aways from Table 2.3 appear to be the following. First, the travel rates are somewhat higher than for the basic freeway section, which should be expected since weaving movements are taking place. Second, the percentage of T-CAVs in the traffic stream, at least up to 20% does not appear to have a significant impact on either the travel rates or the percentages of lane changes. Third, restricting the T-CAVs to use of the middle lane does not appear to have a significant impact either. So, as was observed for the basic freeway section analysis, if there is desire to implement a policy where T-CAVs are “required” to use the center lane, this will not have an adverse impact on the performance of the weaving section.



2.5 Conclusion

Our conclusions from this analysis are as follows. First, it is possible to create a simulation model that makes it possible to study the effects of T-CAVs on the performance of basic freeway segments and weaving sections. Second, it is possible to separately control the behavior of the T-CAVs and differentiate that behavior, in a meaningful way, from that of the conventional trucks and other vehicles. Third, it does not appear that, for reasonable ranges of both truck percentage (up to 40%) and for the percentage of T-CAVs, from 0% up to 100% of the truck flows, that the introduction of the T-CAVs has an adverse effect on the performance of the freeway facility. Moreover, if a policy decision to have the T-CAVs use a specific lane (e.g., the center lane) is of interest, such a policy decision will not have an adverse effect on freeway operation, at least for the operating conditions that were examined.

REFERENCES

1. Hurtado-Beltran, A., and L. R. Rilett. Impact of CAV Truck Platooning on HCM-6 Capacity and Passenger Car Equivalent Values. *Journal of Transportation Engineering, Part A: Systems*, Vol. 147, No. 2, 2021, p. 04020159. <https://doi.org/10.1061/jtepbs.0000492>.
2. Yang, G., M. Ahmed, and E. Adomah. An Integrated Microsimulation Approach for Safety Performance Assessment of the Wyoming Connected Vehicle Pilot Deployment Program. *Accident Analysis and Prevention*, Vol. 146, 2020, p. 105714. <https://doi.org/10.1016/j.aap.2020.105714>.
3. Song, M., F. Chen, and X. Ma. A Simulation of the Traffic Behavior with Autonomous Truck Platoons Based on Cellular Automaton. *ICTIS 2019 - 5th International Conference on Transportation Information and Safety*, 2019, pp. 416–423. <https://doi.org/10.1109/ICTIS.2019.8883834>.
4. Calvert, S. C., W. J. Schakel, and B. van Arem. Evaluation and Modelling of the Traffic Flow Effects of Truck Platooning. *Transportation Research Part C: Emerging Technologies*, Vol. 105, 2019, pp. 1–22. <https://doi.org/10.1016/J.TRC.2019.05.019>.
5. Qiao, Y., and Y. Hu. The Impact of Connected and Autonomous Trucks on Freeway Traffic Flow. 2021, pp. 97–103. https://doi.org/10.1007/978-3-030-68017-6_15.
6. Duret, A., M. Wang, and A. Ladino. A Hierarchical Approach for Splitting Truck Platoons near Network Discontinuities. *Transportation Research Part B: Methodological*, Vol. 132, 2020, pp. 285–302. <https://doi.org/10.1016/J.TRB.2019.04.006>.
7. Mesa-Arango, R., and A. Fabregas. *Assessing Sustainability of Road Tolling Technologies*. 2017.
8. Zhang, B., E. S. Wilschut, D. M. C. Willemsen, and M. H. Martens. Transitions to Manual Control from Highly Automated Driving in Non-Critical Truck Platooning Scenarios. *Transportation Research Part F: Traffic Psychology and Behaviour*, Vol. 64, 2019, pp. 84–97. <https://doi.org/10.1016/j.trf.2019.04.006>.
9. Brandenburg, S., and L. Chuang. Take-over Requests during Highly Automated Driving: How Should They Be Presented and under What Conditions? *Transportation Research Part F: Traffic Psychology and Behaviour*, Vol. 66, 2019, pp. 214–225. <https://doi.org/10.1016/J.TRF.2019.08.023>.
10. Ito, T., A. Takata, and K. Oosawa. Time Required for Take-over from Automated to Manual Driving. *SAE Technical Papers*, Vol. 2016-April, No. April, 2016. <https://doi.org/10.4271/2016-01-0158>.

11. Jamson, A. H., N. Merat, O. M. J. Carsten, and F. C. H. Lai. Behavioural Changes in Drivers Experiencing Highly-Automated Vehicle Control in Varying Traffic Conditions. *Transportation Research Part C: Emerging Technologies*, Vol. 30, 2013, pp. 116–125. <https://doi.org/10.1016/J.TRC.2013.02.008>.
12. Körber, M., C. Gold, D. Lechner, and K. Bengler. The Influence of Age on the Take-over of Vehicle Control in Highly Automated Driving. *Transportation Research Part F: Traffic Psychology and Behaviour*, Vol. 39, 2016, pp. 19–32. <https://doi.org/10.1016/J.TRF.2016.03.002>.
13. Zeeb, K., A. Buchner, and M. Schrauf. Is Take-over Time All That Matters? The Impact of Visual Cognitive Load on Driver Take-over Quality after Conditionally Automated Driving. *Accident Analysis & Prevention*, Vol. 92, 2016, pp. 230–239. <https://doi.org/10.1016/J.AAP.2016.04.002>.
14. van den Beukel, A. P., M. C. van der Voort, and A. O. Eger. Supporting the Changing Driver's Task: Exploration of Interface Designs for Supervision and Intervention in Automated Driving. *Transportation Research Part F: Traffic Psychology and Behaviour*, Vol. 43, 2016, pp. 279–301. <https://doi.org/10.1016/J.TRF.2016.09.009>.
15. Lopez, P. A., M. Behrisch, L. Bieker-Walz, J. Erdmann, Y. P. Flotterod, R. Hilbrich, L. Lucken, J. Rummel, P. Wagner, and E. Wiebner. Microscopic Traffic Simulation Using SUMO. No. 2018-Novem, 2018, pp. 2575–2582.
16. Data, J. E.-M. M. with O., and undefined 2015. SUMO's Lane-Changing Model. Springer.
17. Xiao, L., M. Wang, and B. Van Arem. Realistic Car-Following Models for Microscopic Simulation of Adaptive and Cooperative Adaptive Cruise Control Vehicles. *Transportation Research Record*, Vol. 2623, 2017, pp. 1–9. <https://doi.org/10.3141/2623-01>.
18. Nowakowski, C., J. O'Connell, S. E. Shladover, and D. Cody. Cooperative Adaptive Cruise Control: Driver Acceptance of Following Gap Settings Less than One Second. *Proceedings of the Human Factors and Ergonomics Society Annual Meeting*, Vol. 54, No. 24, 2010, pp. 2033–2037. <https://doi.org/10.1177/154193121005402403>.
19. Milanés, V., and S. E. Shladover. Modeling Cooperative and Autonomous Adaptive Cruise Control Dynamic Responses Using Experimental Data. *Transportation Research Part C: Emerging Technologies*, Vol. 48, 2014, pp. 285–300. <https://doi.org/10.1016/J.TRC.2014.09.001>.

20. Xiao, L., M. Wang, W. Schakel, and B. van Arem. Unravelling Effects of Cooperative Adaptive Cruise Control Deactivation on Traffic Flow Characteristics at Merging Bottlenecks. *Transportation Research Part C: Emerging Technologies*, Vol. 96, 2018, pp. 380–397. <https://doi.org/10.1016/J.TRC.2018.10.008>.
21. Wiedemann, R. *Simulation Des Straßenverkehrsflusses*. Institut Für Verkehrswesen Der Universität Karlsruhe. 1974.
22. Wiedemann, R. Modelling of RTI-Elements on Multi-Lane Roads. Drive Conference, 1991.
23. Kashani, A., and B. Shirgir. Development of Maximum Weaving Length Model Based on HCM 2016: <https://doi.org/10.1177/0361198120973667>, Vol. 2675, No. 4, 2020, pp. 135–145. <https://doi.org/10.1177/0361198120973667>.

Chapter 3

Fuel Use and Emission Rates Reduction Potential for Light-Duty Gasoline Vehicle Eco-Driving

Chris Frey, Professor
North Carolina State University

Weichang Yuan, Graduate Research Assistant
North Carolina State University





3.1 Introduction

Light-duty gasoline vehicles (LDGVs) account for over 95% of the U.S. light-duty vehicle fleet (U.S. EPA, 2019b) and contributed 58% of U.S. transportation energy use and CO₂ emissions in 2018 (Davis & Boundy, 2020). LDGVs directly emit CO, hydrocarbons (HC), NO_x, and particulate matter (PM), which are linked to adverse health effects (Health Effects Institute, 2010; K.-H. Kim, Jahan, Kabir, & Brown, 2013; U.S. EPA, 2010, 2016, 2019a). Locations with above-threshold tailpipe emission rates are emission hotspots (Fernandes, Salamati, Roupail, & Coelho, 2015; Khan, Frey, Rastogi, & Wei, 2020; Unal, Frey, & Roupail, 2004). Hotspots worsen localized air quality and increase human exposure to traffic-related air pollution (Alexeeff et al., 2018; Apte et al., 2017; Robinson et al., 2019). Therefore, strategies are needed to reduce fuel use and emission rates (FUERs).

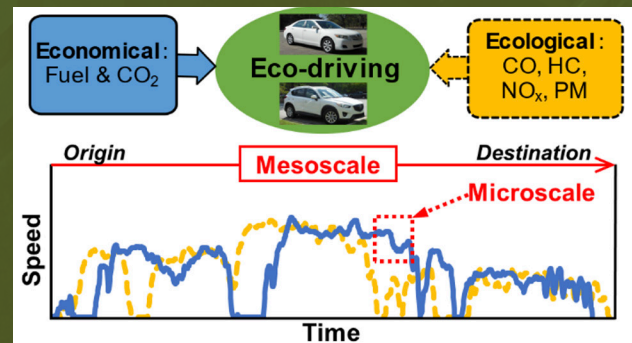
One potential strategy is eco-driving, referring to economical or ecological driving depending on interest in reducing fuel use or air pollutant emissions, respectively (Felicitas Mensing, Bideaux, Trigui, Ribet, & Jeanneret, 2014). Eco-driving requires modification of

vehicle speed trajectories (hereafter referred to as trajectories) (He, Liu, & Liu, 2015; F. Mensing, Trigui, & Bideaux, 2011; Felicitas Mensing, Bideaux, Trigui, & Tattetrain, 2013; Xu, Li, Liu, Rodgers, & Guensler, 2017; Yuan & Frey, 2020). A trajectory is a continuous series of speed versus time data points, typically at 1 Hz (U.S. EPA, 2017). The U.S. Department of Energy promotes eco-driving practices, such as reducing idling, peak speed, acceleration, and braking, and using cruise control on freeways (U.S. Department of Energy, n.d.-b). Future autonomous vehicles (AVs) could enable fleet-wide eco-driving adoption (Wadud, MacKenzie, & Leiby, 2016). AVs can include LDGVs (Mersky & Samaras, 2016).

There is not a standard approach to quantify fuel-saving potential for eco-driving (Huang et al., 2018; Wadud et al., 2016). Comparisons have been made among different simulated trajectories in optimization-based studies (He et al., 2015; F. Mensing et al., 2011; Felicitas Mensing et al., 2014, 2013; Rakha & Kamalanathsharma, 2011; Yang, Almutairi, & Rakha, 2020). Optimal trajectories are characterized by ideal driving, such as constant

cruise speeds (He et al., 2015; F. Mensing et al., 2011; Yang et al., 2020). However, in real-world driving, variations in posted speed limit (PSL), road grade (RG), and traffic lead to speed fluctuations (Liu & Frey, 2015a). Optimal trajectories can overestimate fuel-saving potential compared to real-world trajectories (Felicitas Mensing et al., 2013). Future AVs can be assumed to be operated similarly to those of the most energy-efficient human driving with traditional vehicles, and fuel savings can be estimated by comparing to average real-world driving (Brown, Gonder, & Repac, 2014).

Eco-driving studies typically focus on economical driving for reducing fuel use and CO₂ emissions (Huang et al., 2018; Saboohi & Farzaneh, 2009; Sciarretta & Vahidi, 2020; Xing, Lv, Cao, & Lu, 2020; Zhou, Jin, & Wang, 2016). More than 99.8% of the carbon in gasoline is emitted as CO₂ (H. C. Frey, Unal, Roupail, & Colyar, 2003). Thus, LDGV fuel-optimal trajectories are typically CO₂-optimal. However, eco-driving can lead to co-benefits and tradeoffs for other air pollutants. For example, based on engine dynamometer measurements of a gasoline engine for which engine load was controlled to simulate a moving vehicle, an economical trajectory reduced fuel use and emission rates of CO₂ and NO by 16% to 32% but increased CO and HC emission rates by 181% and 76%, respectively, compared to a baseline (Felicitas Mensing et al., 2014). In contrast, in the same study, an ecological trajectory, for which CO, HC, and NO emissions rates decreased by 46% to 62%, had a 5% increase in fuel use and CO₂ emission rates, compared to the same baseline (Felicitas Mensing et al., 2014). Compared to the ecological trajectory, the economical trajectory penalized CO and HC and NO emissions by 165%, 84%, and 90%, respectively, due to high



episodic accelerations (Felicitas Mensing et al., 2014). However, co-benefits or inter-species tradeoffs have not been quantified based on real-world trajectories.

Previous research has separately evaluated economical driving at mesoscale (Felicitas Mensing et al., 2014, 2013) or microscale (He et al., 2015; Rakha & Kamalanathsharma, 2011; Yang et al., 2020). On a spatial basis, mesoscale refers to routes between an origin and a destination, on the order of miles, whereas microscale refers to short road segments, such as ¼ mile (Khan et al., 2020; U.S. EPA, 2001). Mesoscale fuel-optimal trajectories typically include a period of acceleration to achieve the lowest possible cruise speed that meets a travel time constraint (Felicitas Mensing et al., 2014, 2013). However, episodes of acceleration can produce microscale emission hotspots (Khan et al., 2020). Thus, eco-driving needs to be jointly evaluated at mesoscale and microscale.

The objective is to quantify the mesoscale and microscale FUERs reduction potential associated with LDGV eco-driving. Research questions include: (1) are there co-benefits or tradeoffs in emissions for economical driving; and (2) does eco-driving oriented to reduce mesoscale FUERs reduce microscale FUERs?



3.2 Materials and Methods

From 2008 to 2019, NC State University (NCSU) has conducted real-world trajectory measurements for over 200 LDGVs measured on eight local one-way routes (H. C. Frey, Zhang, & Rouphail, 2008; Khan & Frey, 2018; Khan et al., 2020; Liu & Frey, 2015b; Wei & Frey, 2020; Yuan et al., 2019). The routes were divided into segments for joint evaluation of mesoscale and microscale eco-driving.

Mesoscale routes

Figure 3.1a shows a map of eight one-way routes, including four outbound routes from NCSU to Research Triangle Park via North Raleigh and inbound routes in the reverse direction. The eight routes have lengths varying from 10 mi to 18 mi, with a total of 110 miles. The routes include three types of traffic control and five road types. PSLs range from 25 mph to 70 mph. RG varies within $\pm 10\%$ (Khan et al., 2020).

Microscale segments

To enable evaluation of microscale eco-driving, the one-way routes were divided into segments based on separating traffic controls

and road types. Traffic control and road type affect microscale variability in trajectories and variability in microscale FUERs (Khan et al., 2020), and can also affect FUERs reduction potential via eco-driving (Asadi & Vahidi, 2011; Barth & Boriboonsomsin, 2009).

As illustrations of factors considered in defining segments, example signalized intersection segments (Figure 3.1b) and example ramp segments (Figure 3.1c) are shown. For intersection segments 149 and 180, which represent opposite directions between common endpoints, the endpoints were selected to enclose an influence area of 1,000 ft before and after the signalized intersection. Based on empirical trajectories at signalized intersections with a red phase, over $\frac{3}{4}$ of the vehicles started deceleration at 1,000 ft or closer to signalized intersections. After the red phase, over $\frac{3}{4}$ of the vehicles reached arterial Free Flow Speed (FFS) within 1,000 ft beyond the signalized intersections. For ramp segments 101 and 119, endpoints were selected to be 2,000 ft before the beginning of deceleration lanes or after the end of acceleration lanes. Over $\frac{3}{4}$ of the

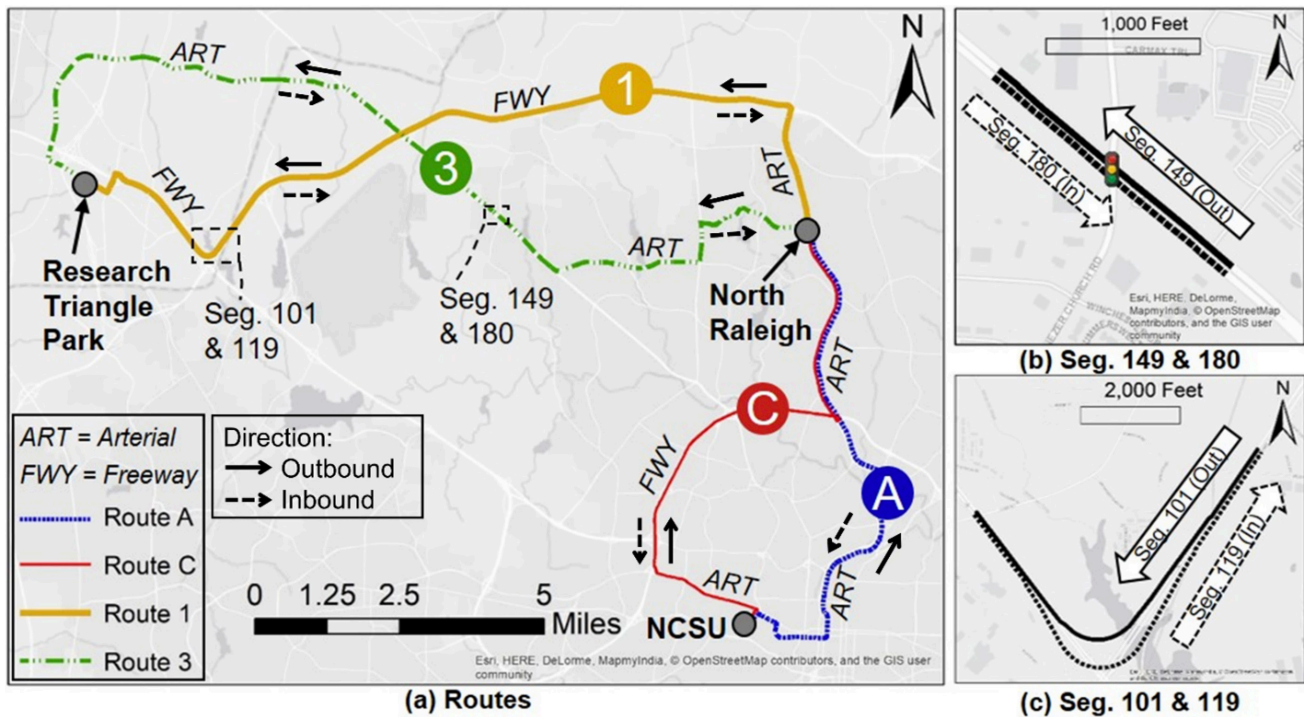


Figure 3.1 Maps of (a) study area routes, indicating inbound and outbound directions, (b) an example of segments at a signalized intersection (segment 149 & 180), and (c) an example of segments at a ramp (segment 101 & 119). The paths of the outbound routes overlap with the corresponding inbound routes except for ramps. Traffic control includes signalized intersection, roundabout, and stop-yield. Road types include collector, minor arterial, major arterial, freeway, and ramp.

vehicles started deceleration from freeway FFS at 2,000 ft or closer to the beginning of deceleration lanes. Likewise, over $\frac{3}{4}$ of the vehicles reached freeway FFS within 2,000 ft beyond the end of acceleration lanes.

Trajectory measurements

Real-world 1 Hz trajectories were measured using an on-board diagnostic (OBD) scan tool. Trajectories of 214 LDGVs from prior studies (H. C. Frey et al., 2008; Khan & Frey, 2018; Khan et al., 2020; Liu & Frey, 2015b; Wei & Frey, 2020; Yuan et al., 2019) were augmented with trajectories of 18 LDGVs measured in 2019. The 232 LDGVs were recruited from NCSU students, NCSU motor pool, North Carolina Department

of Transportation, or rental agencies. There were no supercars or high-performance modified vehicles. On each route, five LDGVs were each measured four times (Yuan et al., 2019), and the other 227 LDGVs were measured once. Each LDGV was driven by one driver, including 153 NCSU students and seven researchers. One hundred and fifty-two drivers drove only one LDGV, and the remaining eight drivers drove between 2 and 32 LDGVs. About 60% of the measurements were made on weekdays. The start time of the measurements varied from 6 am to 7 pm. A measurement typically took 5-6 hours to complete.

No eco-driving training was given to drivers prior to the measurements. Drivers were

encouraged to drive naturally, except for a few cases. For example, the driver of a 2017 Honda Accord Hybrid (hereafter referred to as Accord) intended to maximize fuel economy. Cruise control was used on freeways of Routes C and 1 for a study in which five vehicles were each measured four times (Yuan et al., 2019).

Trajectory-average FUERs for each trajectory were estimated for a typical LDGV, including a Tier 3 passenger car (PC) and a Tier 3 passenger truck (PT). Tier 3 is the current emission standard for light-duty vehicles in the U.S. except for California (U.S. Environmental Protection Agency, 2016). Tier 3 is assumed to continue for the foreseeable future (H. C. Frey, 2018) and, therefore, to be applicable to future AVs. PCs and PTs are able to operate according to any of the observed empirical trajectories of each route. No significant differences were observed between 63 passenger cars and 32 passenger trucks regarding the range of accelerations in real-world speeds from 0 mph to > 75 mph (Liu & Frey, 2015a). Also, the choice of vehicle is not a significant factor affecting naturalistic driving (Tanvir, Frey, & Rouphail, 2018).

Route- and segment-trajectories are based on driving on a route and a segment, respectively. Route- and segment-trajectories that had > 5% missing data with respect to travel time or travel distance were excluded.

Vehicle Specific Power (VSP) modal model

VSP is an indicator of engine power demand and is a function of speed, acceleration, and RG (H. Frey, Unal, Chen, Li, & Xuan, 2002; Jiménez-Palacios, 1998). VSP accounts for changes in kinetic and potential energy, rolling resistance,

and aerodynamic drag. VSP for a typical LDGV was calculated at 1 Hz (Equation S1).

To calibrate VSP modal models, previously reported 1 Hz real-world FUERs (g/s) for 14 PCs and 11 PTs (Wei & Frey, 2020; Yuan et al., 2019) were supplemented with new measurements of one PC and one PT. The measurements and data quality assurance procedures of these 27 vehicles were the same (Sandhu & Frey, 2013). The measurements were conducted on the routes shown in Figure 3.1a. FUERs of CO₂, CO, HC, NO_x, and PM were measured using a GlobalMRV Axion Portable Emission Measurement System (PEMS). This PEMS has been independently evaluated (Myers, Kelly, Dindal, Willenberg, & Riggs, 2003; Vu, Szente, Loos, & Maricq, 2020). The 27 vehicles cover nine makes, 23 models, rated horsepower from 98 to 375, and curb weight from 2,278 lb to 5,534 lb. Over 95% of the raw data were valid. A combined 160,000 and 130,000 seconds of valid data were measured for the 15 PCs and the 12 PTs, respectively.

In model calibration, 1 Hz FUERs for each vehicle were binned into 14 VSP modes (H. Frey et al., 2002). This modeling approach



is accurate within $\pm 10\%$ in predicting emission rates associated with route-trajectories (Wei & Frey, 2020). To represent modal-average FUERs for a typical PC and a typical PT, the modal-average FUERs for the 15 PCs and the 12 PTs, respectively, were averaged. For each route- or segment-trajectory, trajectory-average FUERs (g/mi) were estimated based on the sum-product of VSP modal-average FUERs (g/s), for a typical PC and a typical PT, and time in each VSP mode, divided by route or segment length, respectively.

Sources of inter-trajectory variability in FUERs

To identify dynamic factors for eco-driving, sources of inter-trajectory variability in trajectory-average FUERs were quantified. Trajectory-average FUERs are sensitive to variability in average speed, peak speed, and travel time (Khan et al., 2020; Liu & Frey, 2015b). Engine idling and frequent stops adversely affect FUERs (Sanguinetti, Kurani, & Davies, 2017). Aggressive driving contributes to excess FUERs (Faria, Duarte, Varella, Farias, & Baptista, 2019). Driving aggressiveness has been quantified based on peak speed, relative positive acceleration (RPA), and the 95th percentile of the product of speed and acceleration (va+[95]) (Hooftman, Messagie, Van Mierlo, & Coosemans, 2018). Effective acceleration accounts for the effect of RG on acceleration (Bachman, 1998). RPA estimated based on effective acceleration is defined as relative positive effective acceleration (RPEA). Seven dynamic factors were quantified and evaluated simultaneously to explain inter-trajectory variability in FUERs for each route, including: (1) average speed; (2) peak speed; (3)

travel time; (4) idle time; (5) number of stops; (6) RPEA; and (7) va+[95].

Collinearity refers to two or more factors that are closely linearly related to each other (James, Witten, Hastie, & Tibshirani, 2013). It is difficult to separate the individual effects



of collinear factors on the response variable (James et al., 2013). To avoid collinearity, factors with Variance Inflation Factors (VIFs) > 5 were excluded (James et al., 2013). For a given route, significant sources of variability in trajectory-average FUERs were evaluated using multi-factor analysis of variance (ANOVA). ANOVA enables quantification of the proportion of variance explained by each factor (Tabachnick, Fidell, & Ullman, 2007). In particular, η^2 was used to quantify the relative importance of each factor to the response variable.

Mesoscale route-eco-driving

To represent mesoscale average real-world driving, the route-average rate ($RAR_{s,r,vt}$ g/mi) for each species (s), route (r), and vehicle type (vt) was quantified based on the mean of trajectory-average rates of all empirical route-trajectories. To represent the most efficient mesoscale real-world driving, the route-minimum rate ($RMR_{s,r,vt}$ g/mi) for each species,

route, and vehicle type was quantified based on the minimum of the trajectory-average rates of all empirical route-trajectories. The trajectories associated with $RMR_{s,r,vt}$ are defined as empirical route-eco-driving trajectories. Mesoscale FUERs reduction potential was quantified as the difference between $RMR_{s,r,vt}$ and $RAR_{s,r,vt}$.

Route-trajectory simulation

To infer possible route-eco-driving trajectories that concurrently reduce microscale FUERs for any segment, a simulator was developed based on bootstrapping and concatenating empirical segment-trajectories into route-trajectories. The concatenations require meeting speed and acceleration continuity constraints. The speed continuity constraints are based on limiting the rate-of-change between the final speed of the trajectory in a preceding segment and the initial speed of the trajectory in an adjacent successive segment. Similarly, the acceleration continuity constraints are based on limiting the rate-of-change between the final acceleration of the trajectory in a preceding segment and the initial acceleration of the trajectory in an adjacent successive segment. The rate-of-change of speed is acceleration, and the rate-of-change of acceleration is jerk (Fernandes, Tomás, Ferreira, Bahmankhah, & Coelho, 2020). The continuity constraints were quantified based on a Speed and Acceleration Activity Envelope (Figure S7) and an Acceleration and Jerk Activity Envelope (Figure S9). To simulate a route-trajectory, segment-trajectories were randomly selected, tested for continuity, resampled and retested as needed, and concatenated.

The simulator was evaluated regarding whether simulated route-trajectories that met

continuity constraints had estimated trajectory-average FUERs comparable to those of empirical route-trajectories. The simulator was calibrated to all segment-trajectories. To obtain a wide range of variations in trajectory-average FUERs, bootstrapping was performed iteratively until 20,000 simulated route-trajectories that met the continuity constraints were accepted. Route-average and route-minimum FUERs were quantified based on 20,000 simulated route-trajectories that met continuity constraints. For each of the six species and two vehicle types, linear least squares regressions without intercept were used to quantify the goodness-of-fit of route-average and route-minimum rates for the simulated versus empirical route-trajectories on eight routes.

Microscale segment-eco-driving

To represent microscale average real-world driving, the segment-average rate ($SAR_{s,seg,vt}$ g/mi) for each species (s), segment (seg), and vehicle type (vt) was quantified based on the mean of trajectory-average rates of all empirical segment-trajectories. $SAR_{s,seg,vt}$ was used as the baseline for evaluating segment-eco-driving.

To evaluate whether empirical route-eco-driving trajectories reduce $SAR_{s,seg,vt}$ the empirical route-eco-driving trajectories were disaggregated into segments, referred to as dependent segment-eco-driving trajectories. For dependent segment-eco-driving trajectories, the initial speed and acceleration of a segment are dependent on the final speed and acceleration, respectively, of the preceding segment. The rates estimated for dependent segment-eco-driving trajectories were defined as segment dependent rates ($SDR_{s,seg,vt}$ g/mi).

To represent the most efficient microscale real-world driving, the segment-minimum rate ($SMR_{s,seg,vt}$ g/mi) for each species, segment, and vehicle type was quantified separately for each segment based on the minimum of trajectory-average rates of all empirical segment-trajectories. The trajectories associated with $SMR_{s,seg,vt}$ were defined as independent segment-eco-driving trajectories, based on assuming independence of the final speed and acceleration of a preceding segment and the initial speed and acceleration, respectively, of an adjacent successive segment. Thus, these trajectories typically do not satisfy continuity constraints with adjacent segments but are used to identify a localized upper bound on reduction potential.

To identify segment-eco-driving with rates lower than $SAR_{s,seg,vt}$ while satisfying continuity constraints, the simulator was re-run based on constraining the rates of segment-trajectories to be lower than the corresponding $SAR_{s,seg,vt}$. For each route, bootstrapping was conducted iteratively until 20,000 simulated route-trajectories met the continuity and $< SAR_{s,seg,vt}$ constraints. The simulated route-trajectory with the minimum rate for a given species, route, and vehicle type was referred to as a simulated route-eco-driving trajectory. The segment rates for a simulated route-eco-driving trajectory are defined as segment constrained rates ($SCR_{s,seg,vt}$ g/mi). The segment-trajectories associated with $SCR_{s,seg,vt}$ are identified as constrained segment-eco-driving trajectories.

Segments were categorized into hotspots or non-hotspots. Various criteria have been used to define thresholds for hotspots (Fernandes et al., 2015; Khan et al., 2020; Mudgal, Hallmark, Carriquiry, & Gkritza, 2014;

Unal et al., 2004). Based on a hotspot definition proposed by Khan et al. (Khan et al., 2020), hotspots were defined as the segments with $\geq 90^{\text{th}}$ percentile of segment-average rates of a species among all segments.



3.3 Results and Discussion

The eight routes were divided into 199 segments. Segment lengths range from 0.08 to 2.40 (mean = 0.56) miles. A route-trajectory includes 18 to 32 segment-trajectories, depending on the route. Typically, $\leq 15\%$ of the route- and segment-trajectories were excluded, except for segments at the beginning and end of each route. There are 209 to 220 (mean = 214) route-trajectories, depending on the route, and 143 to 241 (mean = 229) segment-trajectories, depending on the segment. Missing data were due to temporary OBD scan tool failure. About 20% to 40% segment-trajectories at the beginning and end of each route were excluded because of variations in travel distances associated with differing parking locations with designated parking areas.

VSP modal model

VSP modal average FUERs for an average PC and average PT are shown in Figure 3.2. For both PC and PT, modal average FUERs increase monotonically with positive VSP; however, inter-modal ratios of rates differ among species. For example, for PC, the inter-modal ratio for

mode 14 versus mode 3 is the smallest for fuel use and CO_2 , at 10, and the highest for CO, at 388. The large increment in CO modal average rates from mode 13 to 14 is related to fuel enrichment, which reduces the fraction of CO oxidized to CO_2 to prevent the catalyst from overheating (Eriksson & Nielsen, 2014). CO emission rates are more sensitive to high engine power demand compared to rates of the other five species.



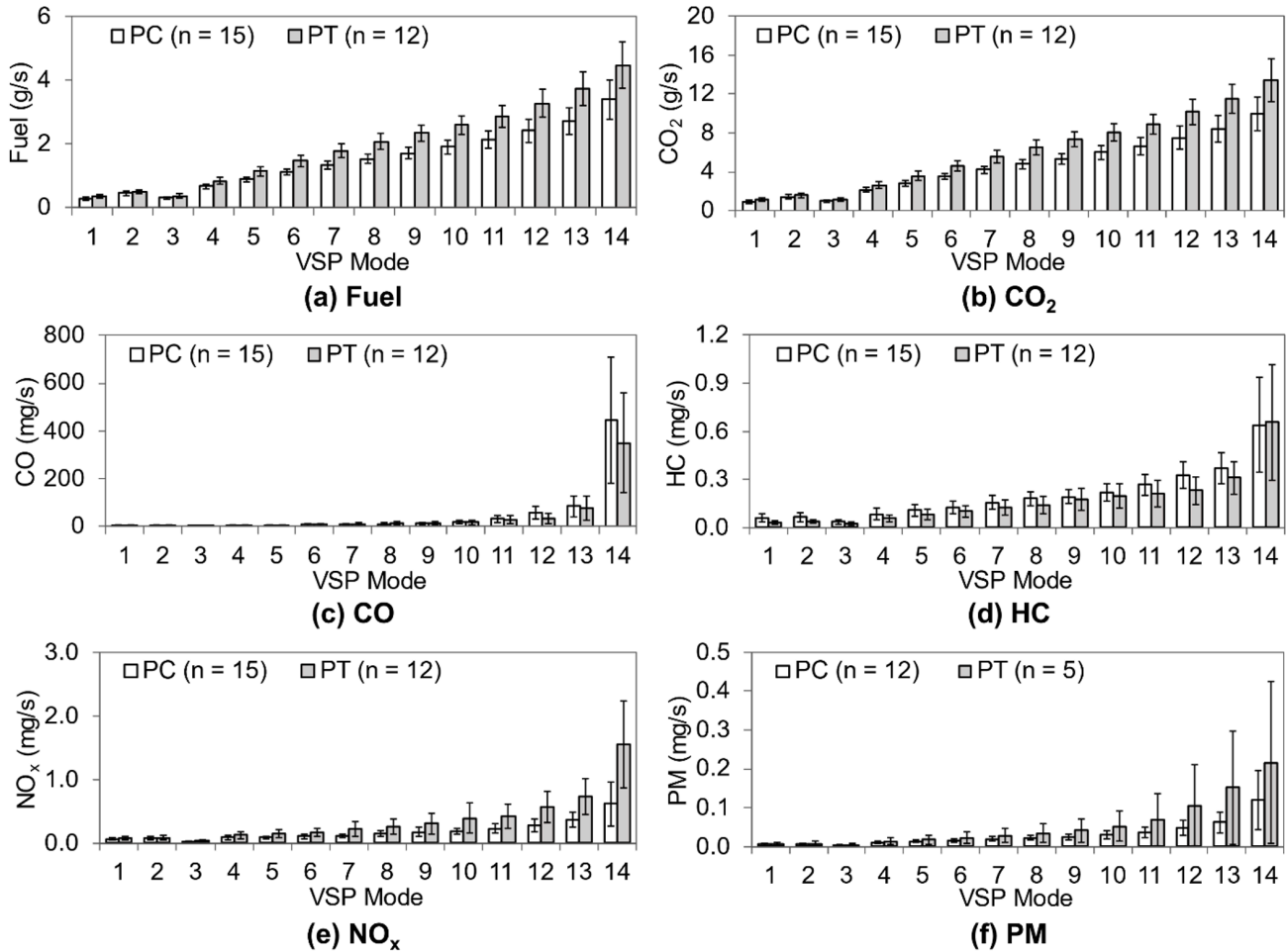


Fig. 3.2 Vehicle Specific Power (VSP) modal average fuel use and emission rates (FUERs) for an average Tier 3 passenger car (PC) and an average Tier 3 passenger truck (PT): (a) fuel use; (b) CO₂, (c) CO, (d) hydrocarbons (HC), (e) NO_x, and (f) particulate matter (PM). All 15 PCs and 12 PTs were measured for fuel, CO₂, CO, HC, and NO_x. PM was measured for 12 PCs and 5 PTs. Error bars are 95% confidence intervals based on the average rates in each VSP mode for each vehicle. The upper bounds of VSP (kW/ton) modes are: Mode 1, -2; Mode 2, 0; Mode 3, 1; Mode 4, 4; Mode 5, 7; Mode 6, 10; Mode 7, 13; Mode 8, 16; Mode 9, 19; Mode 10, 23; Mode 11, 28; Mode 12, 33; Mode 13, 39 (H. Frey et al., 2002). Modes 1 and 2 indicate vehicle deceleration or coasting downhill. Mode 3 includes idling. Modes 4 to 14 indicate cruising, acceleration, or uphill driving.

Mesoscale inter-trajectory variability in FUERs

Wide ranges of inter-trajectory variability in route trajectory-average FUERs were estimated, as illustrated in Figure 3.3 for fuel use and CO emission rates. For a given route and species, the ratios of the maximum to the minimum trajectory-average rates range from 1.2 to 5.2, indicating wide ranges of driving activities. For a given route and vehicle type, the distributions of trajectory-average CO emission rates are more skewed than those of fuel use rates, attributable to the more highly non-linear increments for high VSP modal average rates, such as from modes 13 to 14.

Only a small fraction of empirical trajectories was associated with intentional eco-driving. However, intentional eco-driving can reduce FUERs. For example, the minimum Route 3-In CO and PM emission rates are associated with trajectories measured with the Accord. The other trajectories measured with the Accord have FUERs in the lowest decile among all trajectories. Route-minimum rates can be achieved with or without using cruise control on freeways. For example, based on PC, several route-minimum rates, including those for all six species for Route C-Out, HC for Routes C-In, NO_x for Route 1-Out, and CO for Route 1-In, were achieved by trajectories with cruise control, whereas the remaining route-minimum rates were achieved solely by human driving. Route-minimum rates are similar to the corresponding second-lowest rates within < 1% to 5% (mean = 2%), depending on species, route, and vehicle type.

Based on multi-factor ANOVA, five dynamic factors explain 65% to 95% of the inter-trajectory variability in trajectory-average FUERs, as illustrated in Figure 3.4 for fuel and CO based on PC. Average speed and travel time were

excluded because of VIFs > 5. The most important factor, indicated by the largest Eta², explains 30% to 80% of the variability, depending on species, route, and vehicle type. For all species, the most important factor is approximately 2 to 10 times more important than the other factors. The most important factor differs by species and route but not vehicle type. For example, for fuel, CO₂, HC, NO_x, and PM, idle time is the most important factor for six to eight routes, accounting for approximately 40% to 80% of FUERs variability. In contrast, peak speed is the most important factor for inter-trajectory variability in CO emission rates for all eight routes, accounting for 30% to 57% of the variability. Reducing idle time is recommended for reducing fuel use and emission rates of CO₂, HC, NO_x, and PM, while reducing peak speed is recommended for reducing CO emission rates.

FUERs reduction potential is more sensitive to species and route than vehicle type, as shown in Figure 3.3. Inter-route differences in idle time and peak speed contribute to inter-route variability in FUERs reduction potential. For example, Routes 1-Out and 1-In have the lowest average idle time at about 100 seconds per trajectory and the highest average peak speed at 77 mph among all eight routes, which are on average 40% lower and 20% higher than the other six routes, respectively. Routes 1-Out and 1-In have about 80% freeway in terms of length, with a maximum PSL of 70 mph. Therefore, Routes 1-Out and 1-In typically have less fuel-saving potential but more CO reduction potential than other routes.

Mesoscale co-benefits and tradeoffs

Figure 3.5 shows the empirical route-eco-driving trajectories for fuel and CO of Route 3-In based on PC. The fuel eco-driving trajectory has CO

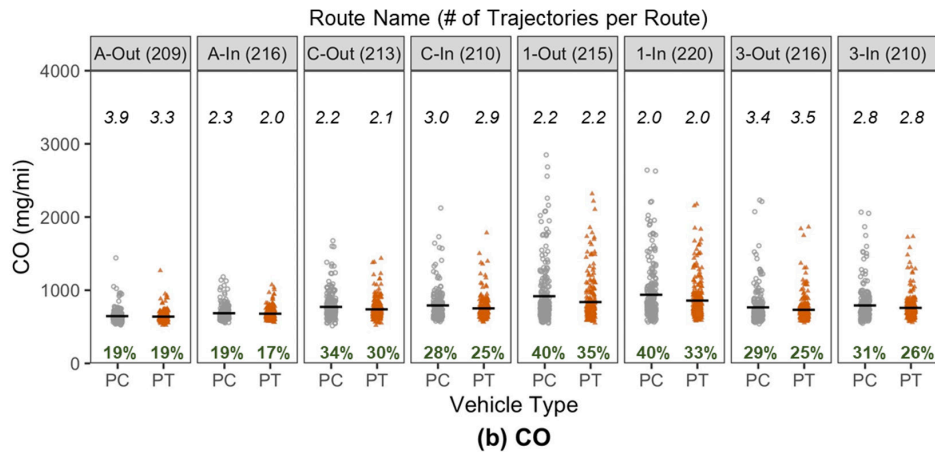
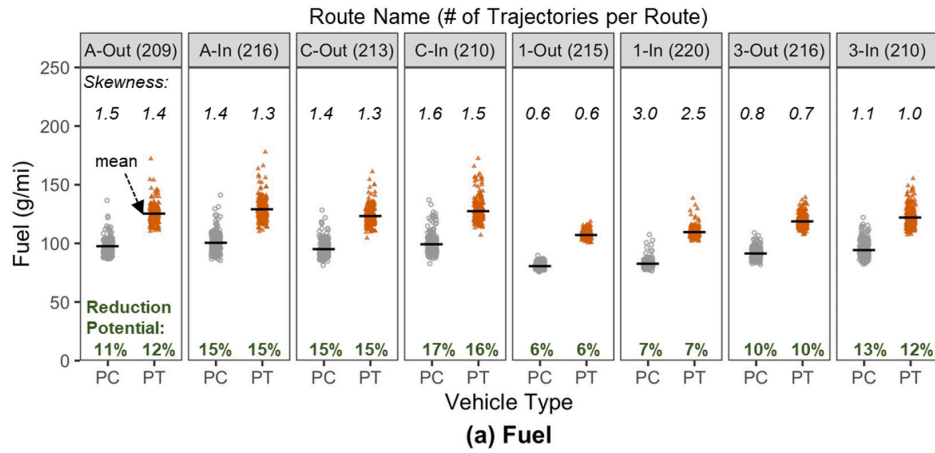


Fig. 3.3 Distributions of route trajectory-average rates of: (a) fuel use and (b) CO emission for empirical route-trajectories based on the Vehicle Specific Power (VSP) modal model (see Figure 2). For each route, the trajectory-average fuel use and CO emission rates were estimated based on an average passenger car (PC) and an average passenger truck (PT). The skewness of each distribution, quantified based on the third standardized moment, is indicated above each distribution in italics. Reduction potential, estimated based on the differences of the mean and minimum rates, is labeled at the bottom.

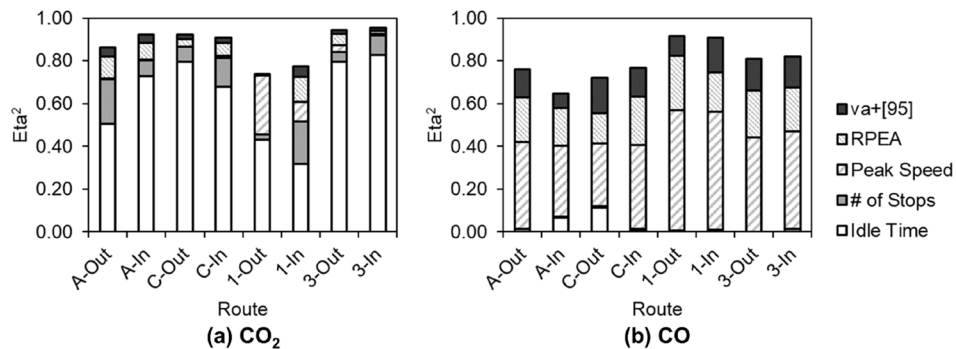


Fig. 3.4 Sources of inter-trajectory variability in trajectory-average (a) fuel use rates and (b) CO emission rates based on an average passenger car (PC). η^2 was quantified based on multi-factor analysis of variance (ANOVA). Five factors with low collinearity were included: idle time, number of stops, peak speed, relative positive effective acceleration (RPEA), and the 95th percentile of the product of speed and acceleration ($va^+[95]$).

emission rate 17% lower than the route-average CO emission rate. Similarly, the CO eco-driving trajectory has fuel use and emission rates of CO₂, HC, NO_x, and PM 7% to 12% lower than the corresponding route-average rates, depending on the species. Thus, there are potential co-benefits of eco-driving in reducing air pollutant emissions even if the goal is to save fuel and vice versa.

Choosing the Route 3-In fuel eco-driving trajectory over the CO eco-driving trajectory would lead to 20% increase in CO emission rate compared to route-minimum CO emission rate. Similarly, choosing the CO eco-driving trajectory over the fuel eco-driving trajectory would lead to increase in fuel use and emission rates of CO₂, HC, NO_x, and PM by 2% to 11%, depending on the species, compared to their route-minimums.

Thus, there are inter-species tradeoffs in FUERs associated with empirical route-eco-driving trajectories.

Based on PC or PT, inter-species eco-driving tradeoffs were estimated for seven routes except for Route C-Out. For Route C-Out, the lowest rates of all species are associated with the same trajectory. For the seven routes, the tradeoffs among empirical route-eco-driving trajectories for fuel, CO₂, HC, NO_x, and PM are typically within 5%. Empirical route-eco-driving trajectories for CO are associated with 1% to 10% (mean = 5%) tradeoffs in fuel use and emission rates of CO₂, HC, NO_x, and PM. Similarly, empirical route-eco-driving trajectories for HC, NO_x, and PM are typically associated with < 10% tradeoffs in CO emission rates. However, empirical route-eco-

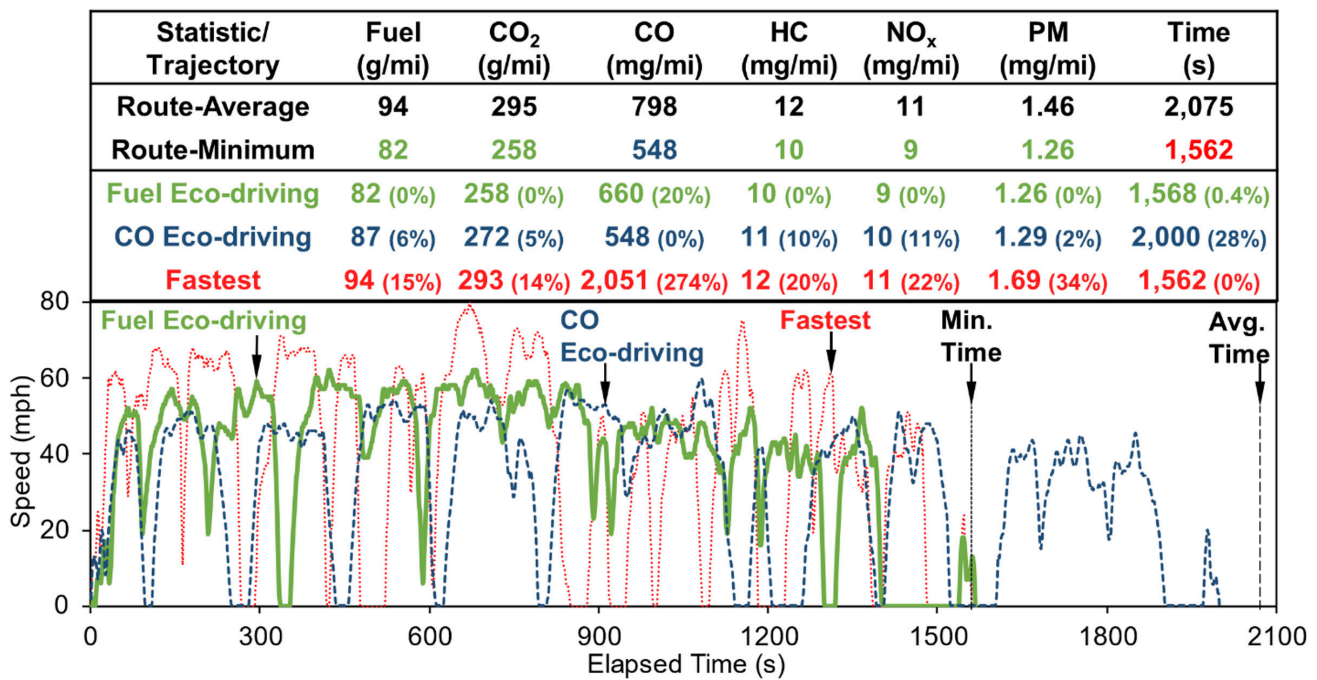


Fig. 3.5 Examples of fuel use and emission rates (FUERs) and travel time based on three empirical route-trajectories of Route 3-In, including the eco-driving trajectory for fuel, the eco-driving trajectory for CO, and the fastest trajectory. The FUERs were estimated based on an average passenger car (PC). Route-average and route-minimum were estimated based on the 210 empirical route-trajectories. Tradeoffs, based on increases from route-minimum FUERs or travel time, are indicated in parentheses. The empirical route-eco-driving trajectories for CO₂, HC, NO_x, and PM are the same as the fuel eco-driving trajectory.

driving trajectories for fuel are associated with 20% to 79% (mean = 33%) CO emission rate tradeoffs for Routes C-In, 1-Out, 3-Out, and 3-In, depending on the route and vehicle type. Thus, fuel eco-driving can cause larger tradeoffs in CO emission rates than the corresponding tradeoffs in fuel use rates associated with CO eco-driving, attributable to greater sensitivity to high engine power demand for CO emission rates versus fuel use rates. The disparity in fuel and CO tradeoffs is consistent with those based on dynamometer measurements (Felicitas Mensing et al., 2014).

As shown in Figure 3.5, the fuel eco-driving trajectory has travel time approximately the same as the fastest trajectory, indicating the potential, at least for some situations, to achieve eco-driving without sacrificing travel time. Although the fastest trajectory has 54% more idle time than the fuel eco-driving trajectory, it has 29% higher peak speed, which compensates for the time loss due to idling. However, compared to the fuel eco-driving trajectory, the fastest trajectory leads to 15% to 34% higher fuel use and emission rates of CO₂, HC, NO_x, and PM, and 211% higher CO emission rate. The fuel eco-driving trajectory and the fastest trajectory have 0.3% and 5%, respectively, time in VSP modes 13 and 14. Thus, although high peak speed can compensate for idling, it leads to FUERs tradeoffs, especially for CO, due to more high engine power demand episodes.

As shown in Figure 3.5, the CO eco-driving trajectory has 4% less travel time than the route-average travel time, indicating that eco-driving can have a co-benefit of reducing travel time. However, the CO eco-driving trajectory penalizes travel time by 28% compared to the fastest trajectory and has 25% lower peak speed. Thus, real-world eco-driving can lead to travel

time tradeoffs compared to the fastest trajectory. However, choosing the fastest trajectory over the CO eco-driving trajectory would lead to 8% to 31% higher fuel use and emission rates of CO₂, HC, NO_x, and PM, and 274% higher CO emission rate. Compared to the fastest trajectory, the CO eco-driving trajectory reduces high engine power demand episodes and eliminates time spent in VSP modes 12 to 14.

Among the eight routes, empirical route-eco-driving trajectories typically have less travel time than the route-average but more travel time than the fastest trajectories. Compared to the fastest trajectories, travel time tradeoffs associated with empirical route-eco-driving trajectories are substantially larger for CO versus other species, with an average difference of 14 percentage points. CO eco-driving typically requires peak speed reduction. Thus, eco-driving aimed at reducing CO typically induces travel time tradeoffs compared to the fastest trajectories. Such tradeoffs could be a challenge in promoting eco-driving because drivers tend to prioritize time savings over fuel savings (Dogan, Steg, & Delhomme, 2011; Harvey, Thorpe, & Fairchild, 2013). With future AVs, potential travel time increases associated with eco-driving could become less important since drivers can engage in activities other than driving (Manawadu, Ishikawa, Kamezaki, & Sugano, 2015). With connected vehicle technologies, travel time tradeoffs could be reduced by improved traffic management (Oh & Peng, 2018).

Among the eight routes, the rates associated with the fastest trajectories are 1% to 52% (mean = 18%) higher than the route-minimum rates for fuel, CO₂, HC, NO_x, or PM, and 15% to 284% (mean = 151%) higher than the route-minimum rates for CO. The fastest

trajectories have more episodes of high engine power demand. Hence, the fastest trajectories are typically associated with more tradeoffs in CO emission rates than other species.

Route-trajectory simulation

Simulated route-trajectories that met continuity constraints had estimated trajectory-average FUERs comparable to those of empirical route-trajectories. For example, for all six species, eight routes, and two vehicle types, the simulated route-trajectories are accurate within $\pm 5\%$ and precise with $R^2 \geq 0.98$ in estimating route-average and route-minimum rates.

Microscale co-benefits and tradeoffs

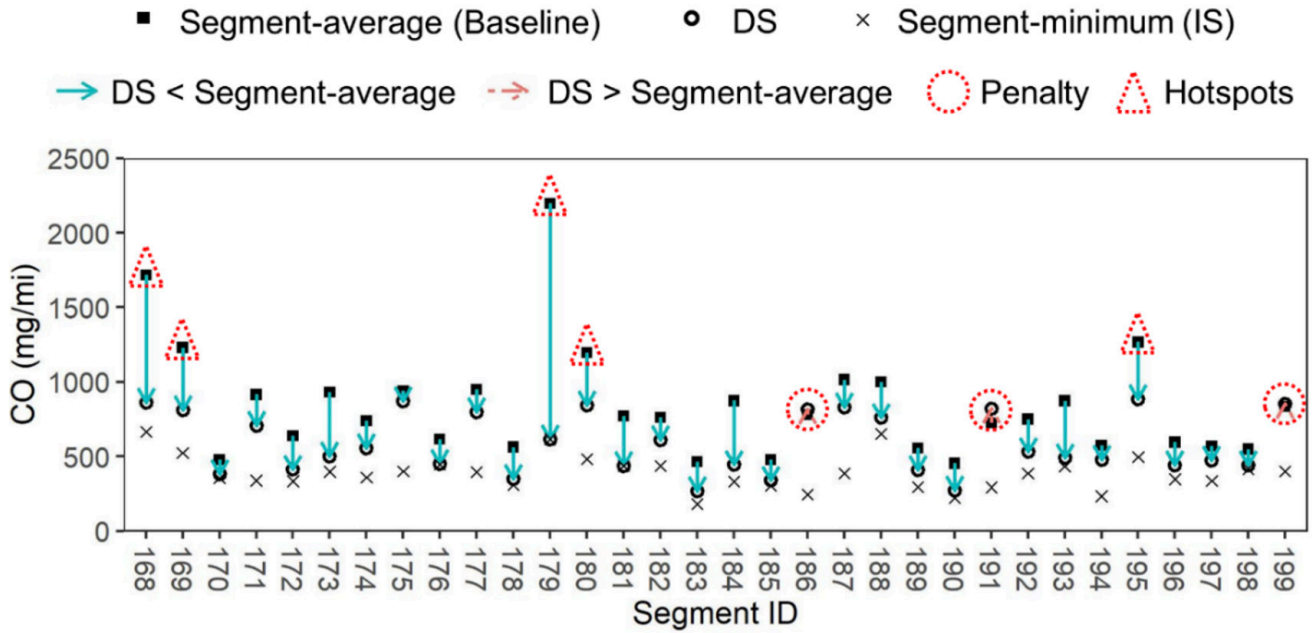
For a given segment, dependent segment-eco-driving typically has lower microscale emission rates compared to segment-average rates among all trajectories, including those of hotspots. For example, dependent segment-eco-driving based on PC is compared to segment-average rates in Figure 3.6 for Route 3-In CO and NO_x emission rates. For all five CO hotspots of Route 3-In, dependent segment-eco-driving has 29% to 72% lower CO emission rates compared to the corresponding segment-average CO emission rate. For three of the four NO_x hotspots of Route 3-In, dependent segment-eco-driving has 12% to 40% lower NO_x emission rates compared to the corresponding segment-average NO_x emission rate. However, for segment 199, which is a NO_x hotspot, dependent segment-eco-driving has 23% higher NO_x emission rate than the average NO_x emission rate for segment 199.

Among all species, routes, and vehicle types, over 99% of hotspots are associated with traffic control, ramps, or both. Dependent segment-eco-driving was estimated to have rates

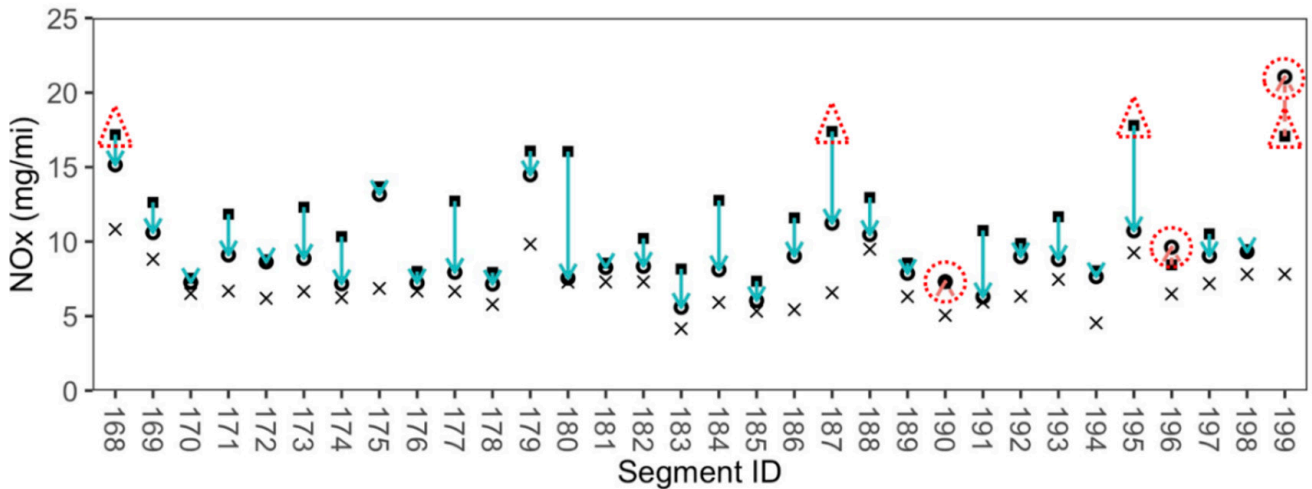
0.2% to 72% (mean = 24%) lower than segment-average rates among 85% to 95% of the hotspots, depending on the species, segment, vehicle type. However, dependent segment-eco-driving was also estimated to have rates 0.4% to 61% (mean = 15%) higher than segment-average rates among 5% to 15% of the hotspots, depending on the species, segment, vehicle type. Thus, eco-driving for a route typically has co-benefits in reducing microscale emissions, such as those of most hotspots, but can exacerbate hotspots at some locations.

Nevertheless, dependent segment-eco-driving rates are typically higher than the corresponding segment-minimum rates. For example, as shown in Figure 3.6, among the all 32 segments of Route 3-In, 29 segments have dependent segment-eco-driving CO emission rates higher than the corresponding segment-minimum rates, by 5% to 230%, while the remaining three segments have dependent segment-eco-driving CO emission rates the same as the corresponding segment-minimum rates. All 32 segments of Route 3-In have dependent segment-eco-driving NO_x emission rates higher than segment-minimum rates, by 4% to 170%. Independent segment-eco-driving trajectories are characterized by high entry (e.g., PSL ± 5 mph) but low exit (e.g., < 10 mph) speeds, indicating dominance of deceleration. Deceleration (i.e., VSP modes 1 and 2) has lower FUERs compared to cruising, acceleration, or uphill driving (VSP modes 4 to 14).

The FUERs reduction potential estimated based on dependent segment-eco-driving is more realistic than that based on independent segment-eco-driving. For example, as illustrated in Figure 3.7, the weighted mean, by segment length, of NO_x reduction potential for independent



(a) Route 3-In Microscale CO Emission Rates



(b) Route 3-In Microscale NO_x Emission Rates

Fig. 3.6 Selected examples of the effects of dependent segment-eco-driving (DS) and independent segment-eco-driving (IS) on microscale emission rates for Route 3-In: (a) CO, and (b) NO_x. Based on the 90th percentiles of segment-average rates among all 199 segments, CO and NO_x hotspots are segments with segment-average rates > 1,132 mg/mi and > 17 mg/mi, respectively. The rates were estimated based on an average passenger car (PC).

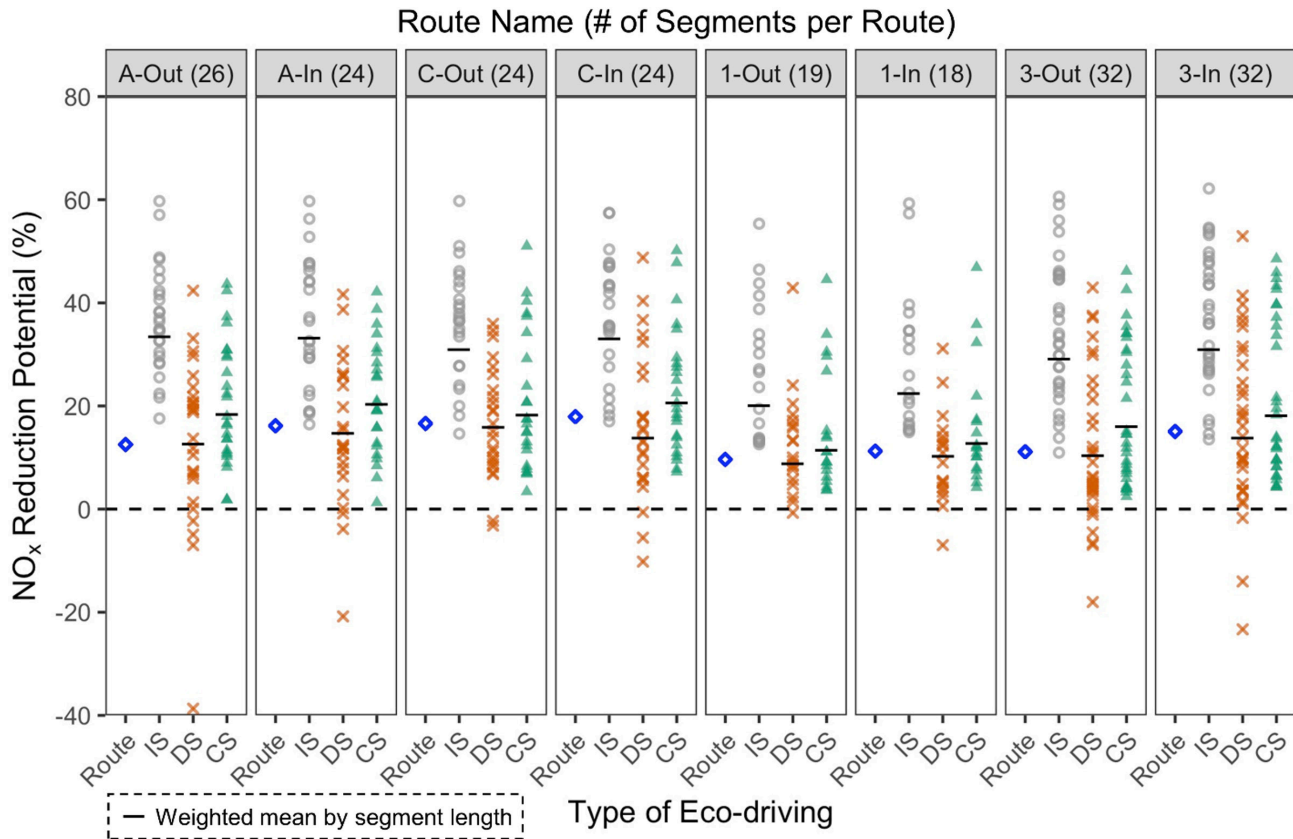


Fig. 3.7 Comparisons of NO_x reduction potential, based on an average passenger car (PC), for four types of eco-driving, including mesoscale route-eco-driving, independent segment-eco-driving (IS), dependent segment-eco-driving (DS), and constrained segment-eco-driving (CS). For a given route, the number of segments is the same among IS, DS, and CS.

segment-eco-driving is consistently higher than the route reduction potential, by 6 to 20 percentage points. In contrast, the weighted mean of NO_x reduction potential for dependent segment-eco-driving is similar to the route reduction potential within ± 3 percentage points. Thus, continuity constraints between adjacent segments are needed to reduce overestimation of segment FUEs reduction potential.

Constrained segment-eco-driving eliminates microscale FUEs tradeoffs. For example, Figure 3.7 illustrates that compared to dependent segment-eco-driving, for which 23 segments among eight routes have negative reduction potential, there are no segments with negative reduction potential for constrained segment-eco-driving. Moreover, constrained segment-eco-driving typically leads to more reduction potential on a route-average basis compared to dependent segment-eco-driving. For example, constrained segment-eco-driving has more NO_x reduction potential for 127 segments, by a partial mean of 12 percentage points, versus less NO_x reduction potential for only 72 segments, by a partial mean of only six percentage points.





3.4 Conclusions

At mesoscale, eco-driving is an effective strategy to reduce LDGV fuel use and tailpipe emission rates of CO_2 , CO, HC, NO_x , and PM. Depending on species, route, and vehicle type, mesoscale rate reduction potential ranges from 6% to 40%, compared to average rates estimated based on all trajectories. FUERs reduction potential varies by route and species and is typically similar within three percentage points between PC and PT.

For a given route and vehicle type, real-world route-eco-driving trajectories typically differ by species. Compared to route-average rates, there are co-benefits of economical driving in reducing air pollutant emission rates, and, similarly, there are co-benefits of ecological driving in saving fuel. However, compared to route-minimum rates, there are inter-species tradeoffs in rates associated with eco-driving due to different sensitivity to engine power demand among species. Mesoscale eco-driving typically leads to travel time tradeoffs, on average 20%, compared to the fastest

trajectories. However, compared to the route-minimum rates, choosing the fastest trajectories would cause on average 18% tradeoffs for rates of fuel, CO_2 , HC, NO_x , and PM and on average 151% tradeoffs for CO emission rates due to more high engine power demand episodes compared to eco-driving.

Real-world mesoscale eco-driving for a route typically has co-benefits in reducing microscale emissions, such as on average 24% FUERs reduction potential for 85% to 95% of the hotspots, but can exacerbate FUERs of the remaining hotspots by an average 15%. Constrained segment-eco-driving illustrates that eco-driving trajectories can be developed such that mesoscale and microscale FUERs are concurrently reduced.

This study is novel because it quantifies FUERs reduction potential associated with real-world LDGV eco-driving simultaneously based on six species (fuel, CO_2 , CO, HC, NO_x , and PM) and two spatial scales (mesoscale and microscale)

A close-up photograph of a person's hand resting on a steering wheel. The image is overlaid with a semi-transparent green grid pattern. The background is a solid, muted green color.

for the first time. This work contributes new generalizable insights into several environmental aspects of LDGV eco-driving: (1) real-world eco-driving focused on fuel savings typically reduced air pollutant emissions and vice versa; and (2) real-world mesoscale eco-driving for a route typically has co-benefits in reducing microscale emissions but can exacerbate hotspots at some locations. The estimated co-benefits and tradeoffs can be used to guide decisions related to adoption of eco-driving to reduce LDGV FUERs among the existing fleet and future AVs.



3.5 Recommendations for Future Work

These results focus on individual vehicles. However, eco-driving of one vehicle may affect eco-driving of other vehicles within a road network, such as due to conflicting movements of crossroads and main corridors (Huang et al., 2018; Xia, Boriboonsomsin, & Barth, 2013). Thus, evaluation of the effectiveness of eco-driving in mitigating road network FUERs is recommended.

The methods to collect and define mesoscale and microscale trajectories, the approaches to quantify sources of variability, the route-trajectory simulation method, and the approaches to quantify co-benefits and tradeoffs are applicable to other vehicle technologies, such as hybrid-electric vehicles (HEVs), plug-in hybrid electric vehicles (PHEVs), and battery-electric vehicles (BEVs). VSP modal models have been developed to estimate energy consumption and emissions of HEVs (Zhai, Frey, & Rouphail, 2011) and PHEVs (H. C. Frey, Zheng, & Hu, 2020). BEV energy consumption can also be estimated based on 1 Hz trajectories and RG (Fiori, Ahn, & Rakha, 2016).

When idling, HEVs and PHEVs are typically zero-emitting because of automatic engine shutoff (Graver, Frey, & Choi, 2011; Zhai et al., 2011). PHEVs running only on electricity during charge depleting mode, and BEVs, have no tailpipe emissions but have indirect emissions from power plants that are proportional to electricity usage (U.S. Department of Energy, n.d.-a). HEVs, PHEVs, and BEVs have regenerative braking for partial kinetic energy recovery (Fiori et al., 2016; H. C. Frey, 2018; Hodges & Potter, 2010). These features could lead to different FUERs reduction potential and eco-driving strategies compared to traditional LDGVs (Huang et al., 2018). For example, reducing idling may not be as effective for HEVs, PHEVs, and BEVs compared to traditional LDGVs. Nevertheless, reducing peak speed on freeways could be an important eco-driving practice for HEVs, PHEVs, and BEVs because of reduction in aerodynamic drag. For HEVs, PHEVs, and BEVs, additional eco-driving practices could focus on optimizing the use of regenerative braking for mitigating energy loss (Y. Kim et al., 2020; Sanguinetti et al., 2017).

REFERENCES

- Alexeeff, S. E., Roy, A., Shan, J., Liu, X., Messier, K., Apte, J. S., ... Van Den Eeden, S. K. (2018). High-resolution mapping of traffic related air pollution with Google street view cars and incidence of cardiovascular events within neighborhoods in Oakland, CA. *Environmental Health*, 17(1), 38. <https://doi.org/10.1186/s12940-018-0382-1>
- Apte, J. S., Messier, K. P., Gani, S., Brauer, M., Kirchstetter, T. W., Lunden, M. M., ... Hamburg, S. P. (2017). High-Resolution Air Pollution Mapping with Google Street View Cars: Exploiting Big Data. *Environmental Science & Technology*, 51(12), 6999–7008. <https://doi.org/10.1021/acs.est.7b00891>
- Asadi, B., & Vahidi, A. (2011). Predictive Cruise Control: Utilizing Upcoming Traffic Signal Information for Improving Fuel Economy and Reducing Trip Time. *IEEE Transactions on Control Systems Technology*, 19(3), 707–714. <https://doi.org/10.1109/TCST.2010.2047860>
- Bachman, W. H. (1998). A GIS-Based Modal Model of Automobile Exhaust Emissions: Final Report (No. EPA-600/R-98-097). Atlanta, Georgia.
- Barth, M., & Boriboonsomsin, K. (2009). Energy and Emissions Impacts of A Freeway-Based Dynamic Eco-driving System. *Transportation Research Part D: Transport and Environment*, 14(6), 400–410. <https://doi.org/10.1016/j.trd.2009.01.004>
- Brown, A., Gonder, J., & Repac, B. (2014). An Analysis of Possible Energy Impacts of Automated Vehicles. In G. Meyer & S. Beiker (Eds.), *Road Vehicle Automation* (pp. 137–153). Cham: Springer International Publishing. https://doi.org/10.1007/978-3-319-05990-7_13
- Davis, S. C., & Boundy, R. G. (2020). *Transportation Energy Data Book* (No. ORNL/TM-2019/1333). Oak Ridge, TN: Oak Ridge National Laboratory.
- Dogan, E., Steg, L., & Delhomme, P. (2011). The influence of multiple goals on driving behavior: The case of safety, time saving, and fuel saving. *Accident Analysis & Prevention*, 43(5), 1635–1643. <https://doi.org/10.1016/j.aap.2011.03.002>
- Eriksson, L., & Nielsen, L. (2014). *Modeling and control of engines and drivelines*. John Wiley & Sons.
- Faria, M. V., Duarte, G. O., Varella, R. A., Farias, T. L., & Baptista, P. C. (2019). How do road grade, road type and driving aggressiveness impact vehicle fuel consumption? Assessing potential fuel savings in Lisbon, Portugal. *Transportation Research Part D: Transport and Environment*, 72, 148–161. <https://doi.org/10.1016/j.trd.2019.04.016>

- Fernandes, P., Salamati, K., Roupail, N. M., & Coelho, M. C. (2015). Identification of emission hotspots in roundabouts corridors. *Transportation Research Part D: Transport and Environment*, 37, 48–64. <https://doi.org/10.1016/j.trd.2015.04.026>
- Fernandes, P., Tomás, R., Ferreira, E., Bahmankhah, B., & Coelho, M. C. (2020). Driving aggressiveness in hybrid electric vehicles: Assessing the impact of driving volatility on emission rates. *Applied Energy*, 116250. <https://doi.org/10.1016/j.apenergy.2020.116250>
- Fiori, C., Ahn, K., & Rakha, H. A. (2016). Power-based electric vehicle energy consumption model: Model development and validation. *Applied Energy*, 168, 257–268. <https://doi.org/10.1016/j.apenergy.2016.01.097>
- Frey, H. C. (2018). Trends in onroad transportation energy and emissions. *Journal of the Air & Waste Management Association*, 68(6), 514–563. <https://doi.org/10.1080/10962247.2018.1454357>
- Frey, H. C., Unal, A., Roupail, N. M., & Colyar, J. D. (2003). On-road measurement of vehicle tailpipe emissions using a portable instrument. *Journal of the Air & Waste Management Association*, 53(8), 992–1002. <https://doi.org/10.1080/10473289.2003.10466245>
- Frey, H. C., Zhang, K., & Roupail, N. M. (2008). Fuel use and emissions comparisons for alternative routes, time of day, road grade, and vehicles based on in-use measurements. *Environmental Science & Technology*, 42(7), 2483–2489. <https://doi.org/10.1021/es702493v>
- Frey, H. C., Zheng, X., & Hu, J. (2020). Variability in Measured Real-World Operational Energy Use and Emission Rates of a Plug-In Hybrid Electric Vehicle. *Energies*, 13(5), 1140. <https://doi.org/10.3390/en13051140>
- Frey, H., Unal, A., Chen, J., Li, S., & Xuan, C. (2002). Methodology for developing modal emission rates for EPA's multi-scale motor vehicle & equipment emission system (No. EPA420-R-02-027). Ann Arbor, Michigan. Retrieved from <http://www.epa.gov/otaq/models/ngm/r02027.pdf>
[http://scholar.google.com/scholar?hl=en](http://scholar.google.com/scholar?hl=en&btnG=Search&q=intitle:Methodology+for+Developing+Modal+Emission+Rates+for+EPA+?+s+Multi-Scale+Motor+Vehicle+and+Equipment#0%5Cnhttp://scholar.google.com/scholar?hl=en)
- Graver, B. M., Frey, H. C., & Choi, H.-W. (2011). In-Use Measurement of Activity, Energy Use, and Emissions of a Plug-in Hybrid Electric Vehicle. *Environmental Science & Technology*, 45(20), 9044–9051. <https://doi.org/10.1021/es201165d>
- Harvey, J., Thorpe, N., & Fairchild, R. (2013). Attitudes towards and perceptions of eco-driving and the role of feedback systems. *Ergonomics*, 56(3), 507–521. <https://doi.org/10.1080/00140139.2012.751460>

- He, X., Liu, H. X., & Liu, X. (2015). Optimal vehicle speed trajectory on a signalized arterial with consideration of queue. *Transportation Research Part C: Emerging Technologies*, 61, 106–120. <https://doi.org/10.1016/j.trc.2015.11.001>
- Health Effects Institute. (2010). *Traffic-Related Air Pollution: A Critical Review of the Literature on Emissions, Exposure, and Health Effects* (No. Special Report 17). Health Effects Institute.
- Hodges, T., & Potter, J. (2010). *Transportation's Role in Reducing US Greenhouse Gas Emissions: Volume 1: Synthesis Report and Volume 2: Technical Report*. Washington, DC: U.S. Department of Transportation.
- Hooftman, N., Messagie, M., Van Mierlo, J., & Coosemans, T. (2018). A review of the European passenger car regulations – Real driving emissions vs local air quality. *Renewable and Sustainable Energy Reviews*, 86, 1–21. <https://doi.org/10.1016/j.rser.2018.01.012>
- Huang, Y., Ng, E. C. Y., Zhou, J. L., Surawski, N. C., Chan, E. F. C., & Hong, G. (2018). Eco-driving technology for sustainable road transport: A review. *Renewable and Sustainable Energy Reviews*, 93, 596–609. <https://doi.org/10.1016/j.rser.2018.05.030>
- James, G., Witten, D., Hastie, T., & Tibshirani, R. (2013). *An Introduction to Statistical Learning* (Vol. 112). New York, USA: Springer.
- Jiménez-Palacios, J. L. (1998). *Understanding and Quantifying Motor Vehicle Emissions with Vehicle Specific Power and TILDAS Remote Sensing* (PhD Thesis). Massachusetts Institute of Technology, Boston, MA.
- Khan, T., & Frey, H. C. (2018). Comparison of real-world and certification emission rates for light duty gasoline vehicles. *Science of The Total Environment*, 622–623, 790–800. <https://doi.org/10.1016/j.scitotenv.2017.10.286>
- Khan, T., Frey, H. C., Rastogi, N., & Wei, T. (2020). Geospatial Variation of Real-World Tailpipe Emission Rates for Light Duty Gasoline Vehicles. *Environmental Science & Technology*, 54(14), 8968–8979. <https://doi.org/10.1021/acs.est.0c00489>
- Kim, K.-H., Jahan, S. A., Kabir, E., & Brown, R. J. C. (2013). A Review of Airborne Polycyclic Aromatic Hydrocarbons (PAHs) and Their Human Health Effects. *Environment International*, 60, 71–80. <https://doi.org/10.1016/j.envint.2013.07.019>

- Kim, Y., Figueroa-Santos, M., Prakash, N., Baek, S., Siegel, J. B., & Rizzo, D. M. (2020). Co-optimization of speed trajectory and power management for a fuel-cell/battery electric vehicle. *Applied Energy*, 260, 114254. <https://doi.org/10.1016/j.apenergy.2019.114254>
- Liu, B., & Frey, H. C. (2015a). Measurement and Evaluation of Real-World Speed and Acceleration Activity Envelopes for Light-Duty Vehicles. *Transportation Research Record*, 2503(2503), 128–136. <https://doi.org/10.3141/2503-14>
- Liu, B., & Frey, H. C. (2015b). Variability in Light-Duty Gasoline Vehicle Emission Factors from Trip-Based Real-World Measurements. *Environmental Science & Technology*, 49(20), 12525–12534. <https://doi.org/10.1021/acs.est.5b00553>
- Manawadu, U., Ishikawa, M., Kamezaki, M., & Sugano, S. (2015). Analysis of individual driving experience in autonomous and human-driven vehicles using a driving simulator. 2015 IEEE International Conference on Advanced Intelligent Mechatronics (AIM), 299–304. <https://doi.org/10.1109/AIM.2015.7222548>
- Mensing, F., Trigui, R., & Bideaux, E. (2011). Vehicle trajectory optimization for application in eco-driving. 2011 IEEE Vehicle Power and Propulsion Conference, 1–6. Chicago, IL: IEEE. <https://doi.org/10.1109/VPPC.2011.6042993>
- Mensing, Felicitas, Bideaux, E., Trigui, R., Ribet, J., & Jeanneret, B. (2014). Eco-driving: An economic or ecologic driving style? *Transportation Research Part C: Emerging Technologies*, 38, 110–121. <https://doi.org/10.1016/j.trc.2013.10.013>
- Mensing, Felicitas, Bideaux, E., Trigui, R., & Tattegrain, H. (2013). Trajectory optimization for eco-driving taking into account traffic constraints. *Transportation Research Part D: Transport and Environment*, 18, 55–61. <https://doi.org/10.1016/j.trd.2012.10.003>
- Mersky, A. C., & Samaras, C. (2016). Fuel economy testing of autonomous vehicles. *Transportation Research Part C: Emerging Technologies*, 65, 31–48. <https://doi.org/10.1016/j.trc.2016.01.001>
- Mudgal, A., Hallmark, S., Carriquiry, A., & Gkritza, K. (2014). Driving behavior at a roundabout: A hierarchical Bayesian regression analysis. *Transportation Research Part D: Transport and Environment*, 26, 20–26. <https://doi.org/10.1016/j.trd.2013.10.003>
- Myers, J., Kelly, T., Dindal, A., Willenberg, Z., & Riggs, K. (2003). Environmental Technology Verification Report: Clean Air Technologies International, Inc. Remote On-Board Emissions Monitor. Columbus, OH: Prepared by Battelle for the US Environmental Protection Agency. Retrieved from Prepared by Battelle for the US Environmental Protection Agency website: https://archive.epa.gov/research/nrmrl/archive-etv/web/pdf/01_vr_oem_report3.pdf

- Oh, G., & Peng, H. (2018). Eco-driving at Signalized Intersections: What is Possible in the Real-World? 2018 21st International Conference on Intelligent Transportation Systems (ITSC), 3674–3679. <https://doi.org/10.1109/ITSC.2018.8569588>
- Rakha, H., & Kamalanathsharma, R. K. (2011). Eco-driving at signalized intersections using V2I communication. 2011 14th International IEEE Conference on Intelligent Transportation Systems (ITSC), 341–346. <https://doi.org/10.1109/ITSC.2011.6083084>
- Robinson, E. S., Shah, R. U., Messier, K., Gu, P., Li, H. Z., Apte, J. S., ... Presto, A. A. (2019). Land-Use Regression Modeling of Source-Resolved Fine Particulate Matter Components from Mobile Sampling. *Environmental Science & Technology*, 53(15), 8925–8937. <https://doi.org/10.1021/acs.est.9b01897>
- Saboohi, Y., & Farzaneh, H. (2009). Model for developing an eco-driving strategy of a passenger vehicle based on the least fuel consumption. *Applied Energy*, 86(10), 1925–1932. <https://doi.org/10.1016/j.apenergy.2008.12.017>
- Sandhu, G. S., & Frey, H. C. (2013). Effects of Errors on Vehicle Emission Rates from Portable Emissions Measurement Systems. *Transportation Research Record*, 2340(1), 10–19. <https://doi.org/10.3141/2340-02>
- Sanguinetti, A., Kurani, K., & Davies, J. (2017). The many reasons your mileage may vary: Toward a unifying typology of eco-driving behaviors. *Transportation Research Part D: Transport and Environment*, 52, 73–84. <https://doi.org/10.1016/j.trd.2017.02.005>
- Sciarretta, A., & Vahidi, A. (2020). *Energy-Efficient Speed Profiles (Eco-Driving)*. Cham: Springer International Publishing. https://doi.org/10.1007/978-3-030-24127-8_6
- Tabachnick, B. G., Fidell, L. S., & Ullman, J. B. (2007). *Using Multivariate Statistics* (7th ed., Vol. 5). Boston, MA: Pearson.
- Tanvir, S., Frey, H. C., & Roupail, N. M. (2018). Effect of Light Duty Vehicle Performance on a Driving Style Metric. *Transportation Research Record*, 2672(25), 67–78. <https://doi.org/10.1177/0361198118796070>
- Unal, A., Frey, H. C., & Roupail, N. M. (2004). Quantification of Highway Vehicle Emissions Hot Spots Based upon On-Board Measurements. *Journal of the Air & Waste Management Association*, 54(2), 130–140. <https://doi.org/10.1080/10473289.2004.10470888>

- U.S. Department of Energy. (n.d.-a). Alternative Fuels Data Center: Emissions from Hybrid and Plug-In Electric Vehicles. Retrieved February 18, 2021, from https://afdc.energy.gov/vehicles/electric_emissions.html
- U.S. Department of Energy. (n.d.-b). Drive More Efficiently. Retrieved December 28, 2020, from <https://www.fueleconomy.gov/feg/driveHabits.jsp>
- U.S. Environmental Protection Agency. (2016). EPA Emission Standards for Light-Duty Vehicles and Trucks [Overviews and Factsheets]. Retrieved May 1, 2019, from Emission Standards Reference Guide website: <https://www.epa.gov/emission-standards-reference-guide/epa-emission-standards-light-duty-vehicles-and-trucks>
- U.S. EPA. (2001). EPA's New Generation Mobile Source Emissions Model: Initial Proposal and Issues (No. EPA420-R-01-007). Ann Arbor, MI: U.S. Environmental Protection Agency. Retrieved from U.S. Environmental Protection Agency website: <https://nepis.epa.gov/Exe/ZyPDF.cgi/P1002131.PDF?Dockey=P1002131.PDF>
- U.S. EPA. (2010). Integrated Science Assessment for Carbon Monoxide (No. EPA/600/R-09/019F). Research Triangle Park, NC: U.S. Environmental Protection Agency.
- U.S. EPA. (2016). Integrated Science Assessment for Oxides of Nitrogen-Health Criteria (No. EPA/600/R-15/068). Research Triangle Park, NC: U.S. Environmental Protection Agency.
- U.S. EPA. (2017, January 31). Dynamometer Drive Schedules [Data and Tools]. Retrieved September 13, 2019, from <https://www.epa.gov/vehicle-and-fuel-emissions-testing/dynamometer-drive-schedules>
- U.S. EPA. (2019a). Integrated Science Assessment (ISA) for Particulate Matter (No. EPA/600/R-19/188). Research Triangle Park, NC: U.S. Environmental Protection Agency.
- U.S. EPA. (2019b). The 2018 EPA Automotive Trends Report: Greenhouse Gas Emissions, Fuel Economy, and Technology since 1975 (No. EPA-420-R-19-002; p. 153). Ann Arbor, MI: U.S. Environmental Protection Agency.
- Vu, D., Szente, J., Loos, M., & Maricq, M. (2020). How Well Can mPEMS Measure Gas Phase Motor Vehicle Exhaust Emissions? SAE Technical Paper 2020-01-0369. <https://doi.org/10.4271/2020-01-0369>

- Wadud, Z., MacKenzie, D., & Leiby, P. (2016). Help or hindrance? The travel, energy and carbon impacts of highly automated vehicles. *Transportation Research Part A: Policy and Practice*, 86, 1–18. <https://doi.org/10.1016/j.tra.2015.12.001>
- Wei, T., & Frey, H. C. (2020). Evaluation of the Precision and Accuracy of Cycle-Average Light Duty Gasoline Vehicles Tailpipe Emission Rates Predicted by Modal Models: *Transportation Research Record*, 2674(7), 566–584. (Sage CA: Los Angeles, CA). <https://doi.org/10.1177/0361198120924006>
- Xia, H., Boriboonsomsin, K., & Barth, M. (2013). Dynamic Eco-Driving for Signalized Arterial Corridors and Its Indirect Network-Wide Energy/Emissions Benefits. *Journal of Intelligent Transportation Systems*, 17(1), 31–41. <https://doi.org/10.1080/15472450.2012.712494>
- Xing, Y., Lv, C., Cao, D., & Lu, C. (2020). Energy oriented driving behavior analysis and personalized prediction of vehicle states with joint time series modeling. *Applied Energy*, 261, 114471. <https://doi.org/10.1016/j.apenergy.2019.114471>
- Xu, Y., Li, H., Liu, H., Rodgers, M. O., & Guensler, R. L. (2017). Eco-driving for transit: An effective strategy to conserve fuel and emissions. *Applied Energy*, 194, 784–797. <https://doi.org/10.1016/j.apenergy.2016.09.101>
- Yang, H., Almutairi, F., & Rakha, H. (2020). Eco-Driving at Signalized Intersections: A Multiple Signal Optimization Approach. *IEEE Transactions on Intelligent Transportation Systems*, 1–13. <https://doi.org/10.1109/TITS.2020.2978184>
- Yuan, W., & Frey, H. C. (2020). Potential for Metro Rail Energy Savings and Emissions Reduction via Eco-driving. *Applied Energy*, 268, 114944. <https://doi.org/10.1016/j.apenergy.2020.114944>
- Yuan, W., Frey, H. C., Wei, T., Rastogi, N., VanderGriend, S., Miller, D., & Mattison, L. (2019). Comparison of real-world vehicle fuel use and tailpipe emissions for gasoline-ethanol fuel blends. *Fuel*, 249, 352–364. <https://doi.org/10.1016/j.fuel.2019.03.115>
- Zhai, H., Frey, H. C., & Roupail, N. M. (2011). Development of a modal emissions model for a hybrid electric vehicle. *Transportation Research Part D: Transport and Environment*, 16(6), 444–450. <https://doi.org/10.1016/j.trd.2011.05.001>
- Zhou, M., Jin, H., & Wang, W. (2016). A review of vehicle fuel consumption models to evaluate eco-driving and eco-routing. *Transportation Research Part D: Transport and Environment*, 49, 203–218. <https://doi.org/10.1016/j.trd.2016.09.008>